"I know x exists, but I can't tell you where to look for it"
- Hilbert

University of Alberta

DECELLULARIZED ALLOGRAFT HEART VALVES AS A SCAFFOLD FOR TISSUE-ENGINEERED VALVE PROSTHESES

by

ERIC JOSEPH LEHR ©

A thesis submitted to the Faculty of Graduate Studies and Research
in partial fulfillment of the requirements for the degree of

DOCTOR OF PHILOSOPHY
in
EXPERIMENTAL SURGERY

Department of Surgery

Edmonton, Alberta
Fall 2007

Your file Votre référence
ISBN: 978-0-494-33008-1
Our file Notre référence
ISBN: 978-0-494-33008-1

ABSTRACT

Heart valve disease is a strong contributor to morbidity and mortality. Nearly 100,000 valve procedures are performed yearly in the United States. Current prostheses are limited by the requirement for either systemic anticoagulation for mechanical valves or by structural degeneration in the case of biologic valves. Tissue engineered valves offer the potential of overcoming both of these limitations along with the capacity for growth. Decellularized allograft valves have been proposed as a scaffold for tissue engineered heart valves.

An ovine model was developed to test tissue engineered vascular patches without the requirement for cardiopulmonary bypass. An intraaortic shunt was designed and characterized. It was effective at restoring blood flow and pressure to the distal aorta during implantation in the descending thoracic aorta.

The relative allogenicity of farm sheep used to assess the host immune response to decellularized tissue was systematically assessed with one-way mixed lymphocyte reaction assay. More than one third of 160 animal pairs were too closely related to elicit an allogeneic immune response.

Decellularization prevents the donor specific cellular and humoral immune responses. There were structural changes that may be related to either cryopreservation or a foreign body inflammatory response.

Finally residual Me_2SO concentration in aortic allograft conduits after decellularization was assessed by proton nuclear magnetic resonance

spectroscopy. The levels detected were much lower than levels reported to adversely affect cell function. In addition, we discovered that Me_2SO does not reach equilibrium with the aqueous compartment of the conduits prior to cryopreservation when using accepted cryopreservation protocols and that Me_2SO washout takes substantially longer than the time given under standard surgical care.

In summary, this thesis advances the characterization of the ovine large animal model for testing tissue engineered valves and vascular constructs. We provide further evidence supporting the use of decellularized allograft scaffolds for tissue engineered heart valves. The ultimate goal is to generate a living autologous valve *in vitro*. If a tissue engineering approach is successful, the ideal valve prosthesis may be realized which would provide tremendous benefit to both adults and children with cardiac valve and outflow tract disease.

ACKNOWLEDGEMENTS

I would like to express gratitude to my advisor, Dr. David Ross who inspired me to pursue research and demonstrated that one can be a great cardiac surgeon and a scientist. I am grateful for his support, advice, encouragement and focus that he provided throughout the completion of my thesis. I extend thanks to my co-supervisor, Dr. Gregory Korbutt not only for his generosity in providing space, equipment and resources for me to complete my work, but also for his intellectual support and advice. I am indebted to Dr. Gina Rayat who was also a great source of motivation, encouragement and advice, provided guidance and taught me the fundamentals of immunology. It was a privilege to work under the direction of Dr. Ray Rajotte. I learned much from his example of professionalism and leadership and appreciate his criticisms of my work. I express gratitude to Dr. Lori West for participating in my candidacy exam and for reviewing this manuscript. Also, I express appreciation to the other members of my candidacy examining committee, Dr. Gary Lopaschuk, Dr. Marek Michalak. I am likewise grateful to my external reader, Dr. John Coles for taking time to critically review my thesis. Gratitude is owed to Dr. James Coe for providing an excellent operative facility and to Jon Timinsky for his expert assistance in working with sheep.

I express gratitude to the staff and students of the Surgical Medical Research Institute. I am grateful for the assistance of Dr. Tom Churchill, Dr.

Colin Anderson, Karen Seeberger, Alana Eshpeter, Dr. Ming Chen, Dr. Linfu Zhu, Greg Olson, Christine Cook, Geneva DeMeyer, James Lyon, Allan Muir and Dr. Lisa Tanguay. I am particularly thankful to Dawne Colwell for her assistance in preparation of figures, posters and presentations. Appreciation is expressed to all of the students at SMRI who provided assistance, and a congenial workplace. I appreciate the administrative assistance of Rosemarie Henley, Margaret Henley, Colleen Ruptash and Sam Leung.

I am grateful for the assistance of numerous collaborators across the University of Alberta Campus and Capital Health Authority including Dr. Brian Chiu (Department of Laboratory Medicine and Pathology), Dr. Locksley McGann, Alireza Abazari and Maria Cabuhat (Stem Cell Laboratory of Canadian Blood Services), Ted Pretty, Susan Coggles and Tumelo Mokoena (Capital Health Comprehensive Tissue Center), Dr. Patricia Campbell, (University of Alberta Hospital HLA lab), Dr. Ryan McKay, Deryck Webb and Bruce Lix (Canadian National High Field NMR Centre [NANUC]) and Dr. Don Raboud and Dr. Jason Carey (Department of Mechanical Engineering).

I owe special thanks to Leena Desai and Sarah Hermary, my two summer students, who were a great help and who taught me more than I gave to them.

I am particularly grateful for the mentorship of Dr. Paul Armstrong and Dr. David Bigam who played important roles in my training through Tomorrows

Research Cardiovascular Health Professionals (TORCH) and the Clinician Investigator Program (CIP) respectively.

I also recognize that this work would not have been possible without the assistance of many other people whom I have not named.

I am appreciative of the financial support from the University Hospital Foundation and the Edmonton Civic Employees' Foundation, and the Canadian Institutes of Health Research TORCH, the CIP, and the Division of Cardiac Surgery.

Finally, I am deeply indebted to my wife Anne, my children Megan and Andrew, my parents, my sister and my in-laws for their constant patience, support and encouragement.

Above all, I thank God for strength granted to complete this work.

TABLE OF CONTENTS

I. INTRODUCTION 1

GENERAL INTRODUCTION 1

THE NORMAL ARTERIAL VALVE 2
- Embryology 2
- Morphology 4
- Extracellular Matrix 4
- Heart Valve Cells 6
  - Valve Endothelial Cells 6
  - Valve Interstitial Cells 8
  - Valve Endothelial Regulation of Valve Interstitial Cells 9
- Physiology of the Normal Valve 10

THE DISEASED ARTERIAL VALVE 11
- Pathophysiology 11
  - Aortic Stenosis 11
  - Aortic Regurgitation 12
  - Pulmonary and Right Ventricular Outflow Tract Disease 12
- Current Practice 13
  - History of Surgical Interventions on the Aortic Valve 13
  - Mechanical Valves 14
  - Bioprosthetic Valves 14
  - Cryopreservation 15
- Allogeneic Response 17
  - Humoral Response 18
  - Cellular Response 19
  - Allograft Valve Antigens 20
  - Methods to Reduce the Alloresponse 20

TISSUE ENGINEERING 22
- Scaffold 23
  - Biologic 23
    - Decellularization 24
  - Synthetic 25
- Repopulation 27
  - *Ex vivo* Repopulation 27
    - Differentiated Cells 27
    - Progenitor Cells 28

Bioreactors 31
In vivo repopulation 32
In vivo Animal Studies 33
Clinical Studies of Tissue Engineered Valves 33

OBJECTIVES AND GENERAL OUTLINE OF THESIS 35

REFERENCES 41

II. AN INTRA-AORTIC SHUNT PREVENTS PARALYSIS DURING AORTIC SURGERY IN SHEEP 83

INTRODUCTION 83

MATERIALS AND METHODS 84
Experimental Animals 84
Surgical Procedure 84
Physiologic Monitoring 86
Statistical Analysis 86

RESULTS 87
Hemodynamic Effect of the Shunt 87
Clinical Results 89

CONCLUSIONS 89

REFERENCES 99

III. AN EVALUATION OF THE FUNCTIONAL ALLOGENICITY OF FARM SHEEP USED IN CARDIAC VALVE STUDIES 104

INTRODUCTION 104

MATERIALS AND METHODS 106
Experimental Animals 106
Animal Husbandry 106
Cell Collection 107
One-way Mixed Lymphocyte Reaction (MLR) 107
Statistical Analysis 109

RESULTS 109

CONCLUSIONS 111

REFERENCES 120

IV. DECELLULARIZATION REDUCES THE IMMUNOGENICITY OF SHEEP PULMONARY ARTERY VASCULAR PATCHES 126

INTRODUCTION 126

MATERIALS AND METHODS 127
- Experimental Animals 127
- Patch Procurement and Preparation 128
- Cryopreservation 129
- Implant Procedure 129
- Immunohistochemistry 131
- Electron Microscopy 132
- Determination of Humoral Response 133
- Calcification 134
- RNA isolation and reverse transcription-polymerase chain reaction 135
- Statistical Analysis 136

RESULTS 136
- Histology and Immunohistochemistry 136
- Scanning Electron Microscopy 138
- Humoral Response 138
- Cytokine Expression 139
- Calcification 140
- Clinical Results 140

CONCLUSIONS 140

REFERENCES 157

V. NMR ASSESSMENT OF ME_2SO IN DECELLULARIZED CRYOPRESERVED AORTIC VALVE CONDUITS 162

INTRODUCTION 162

MATERIALS AND METHODS 165
- Tissue Procurement 165
- Cryopreservation 166

Decellularization 167
Histology 168
Determination of Tissue Me_2SO Concentration by Quantitative ^1H-NMR Spectroscopy 168
Calculation of the Diffusion Coefficient for Me_2SO 171
Statistics 173

RESULTS 173

CONCLUSIONS 175

REFERENCES 186

VI. GENERAL DISCUSSION AND CONCLUSIONS 192

DISCUSSION 192

FUTURE DIRECTIONS 199

CONCLUSIONS 201

REFERENCES 206

LIST OF TABLES

TABLE	DESCRIPTION	PAGE
Table IV-1	Primers used for PCR amplification	156

LIST OF FIGURES

FIGURE	DESCRIPTION	PAGE
Figure I-1	Signaling network model for heart valve development and remodeling	40
Figure II-1	*In situ* placement of an intra-aortic shunt	96
Figure II-2	Opening the intra-aortic shunt effectively decompresses the proximal aorta and returns hemodynamic and flow parameters to near baseline values	98
Figure III-1	Histogram of the maximum mean proliferation as measured by counts per minute for 160 mixed lymphocyte reaction pairs	117
Figure III-2	Proliferative response of responder cells	118
Figure III-3	Tabular representation of the distribution of proliferative responses, measured as counts per minute for 160 mixed lymphocyte reaction pairs.	119
Figure IV-1	Overall experimental design for assessing the effect of decellularization on the recipient cellular and humoral immune responses	145
Figure IV-2	Experimental method for the determination of the humoral response	146
Figure IV-3	Photomicrographs of representative sections of non-decellularized and decellularized patches at time of implant	147
Figure IV-4	Overall morphology of allogeneic ovine pulmonary artery patches at 4 weeks and 6 months after implantation	149
Figure IV-5	Immunohistochemistry of decellularized and non-decellularized pulmonary artery allograft patches at 4 weeks and 6 months after implantation	150

Figure IV-6 Scanning electron microscopy of the endothelial surface of explanted non-decellularized, and decellularized pulmonary artery patches at 4 weeks post implantation 152

Figure IV-7 Flow cytometric determination of the humoral response of sheep receiving allograft pulmonary artery patches 154

Figure IV-8 Calcification of non-decellularized and decellularized pulmonary artery patches at 4 weeks and 6 months 155

Figure V-1 Experimental method for determining Me_2SO concentration in ovine aortic valve conduits during decellularization 180

Figure V-2 Representative histological sections of control and decellularized conduits 182

Figure V-3 Standard curve for ^{1}H-NMR determination of Me_2SO in H_20 183

Figure V-4 Typical 1-D ^{1}H-NMR spectra for a single set of experiments representing elution of Me_2SO from wall of an ovine aortic valve conduit over time 184

Figure V-5 Me_2SO in cryopreserved aortic valves is eluted during decellularization with a series hypotonic and hypertonic solutions with Triton-X as a detergent 185

Figure VI-1 Overview of experimental strategy for enhancing endothelial cell binding to a decellularized aortic valve allograft via functionalization with an RGD binding peptide 203

Figure VI-2 Functionalization of decellularized aortic valve allograft with an RGD binding peptide 204

LIST OF ABBREVIATIONS

^{1}H-NMR	proton nuclear magnetic resonance spectroscopy
Ac	acetylated
ANOVA	analysis of variance
Con A	concanavalin-A
CPM	counts per minute
DNA	deoxyribonucleic acid
DNase	deoxyribonuclease
DSS	2,2-dimethyl-2-silapentane-5-sulfonate
ECM	extracellular matrix
EDC	1-ethyl-3-(3-dimethylaminopropyl)carbodiimide hydrochloride
EDTA	ethylenediaminetetraacetic acid
EMCH	N-(ε-maleimidocaproic acid)hydrazide
EMEM	Eagle's modified essential medium
EPC	endothelial progenitor cell
eNOS	endothelial nitric oxide synthase
F	French
FACS	fluorescence-activated cell sorting
FBS	fetal bovine serum
FGF	fibroblast growth factor

FID	free induction decay
FITC	Fluorescein isothiocyanate
GM-CSF	granulocyte macrophage colony-stimulating factor
HBSS	Hank's balanced salt solution
HLA	human leukocyte antigen
IFN-γ	interferon gamma
IL-1β	Interleukin-1β
Me_2SO	dimethyl sulfoxide
MES	2-(N-morpholino)ethane-sulfonic acid
MHC	major histocompatibility complex
MLR	mixed lymphocyte reaction
MMP	matrix metalloproteinase
NOESY	nuclear overhauser enhancement spectroscopy
OLA	ovine leukocyte antigen
PA	pulmonary artery
PBMC	peripheral blood mononuclear cell
PBS	phosphate buffered saline
PMSF	phenylmethylsulphonylfluoride
PCR	polymerase chain reaction
PRA	panel reactive antibody
RF	radio frequency

RFLP	restriction fragment length polymorphism
RNA	ribonucleic acid
RNase	ribonuclease
RPMI	Roswell Park Memorial Institute
RT-PCR	Reverse transcriptase polymerase chain reaction
SEM	standard error of the mean
SSP	single specific primer
Sulfo-NHS	N-hydroxysulfosuccinimide
TGF	transforming growth factor
TIMP	tissue inhibitor of matrix metalloproteinase
TNF	tumor necrosis factor
USD	United States dollar
US-FDA	United States Food and Drug Administration
VEC	valve endothelial cell
VIC	valve interstitial cell
vWF	von Willebrand Factor

I

INTRODUCTION

GENERAL INTRODUCTION

Valves are fundamental to the normal function of the heart by permitting only forward flow of blood from the atria to the ventricles and out of the heart into the pulmonary and systemic circulation. Arterial valves guard the outflow tracts of the heart and prevent regurgitant blood flow back into the heart from the pulmonary artery and aorta. The arterial valves are comprised of three semilunar leaflets that open and close passively. The atrio-ventricular valves prevent regurgitant flow from the ventricles back to the atria and are comprised not only of leaflets, but also papillary muscles and chordae tendinae which connect the muscle bundles to the valves leaflets. Unlike the arterial valves, valve function is active and depends upon normal operation of the entire valve apparatus.

Abnormal valve function, either stenosis or regurgitation activates compensatory mechanisms that lead to dilation of the cardiac chambers in the case of regurgitation, or to myocardial hypertrophy in aortic stenosis. In either situation decompensation eventually ensues, resulting in heart failure and eventually death. The American Heart Association reported that heart valve disease resulted in 94,000 hospital discharges and 42,590 deaths in 2002. In 2004, approximately 99,000 operations on heart valves were performed [1] in patients

older than 15. Valve pathology also has a significant economic impact. The mean financial cost of valve procedures in 2003 in the United States was US$118,656.

Current prostheses are limited by the requirement for either systemic anticoagulation for mechanical valves or by structural degeneration in the case of biologic valves. Tissue engineered valves offer the potential of overcoming both of these limitations along with the capacity for growth. This body of research develops a large animal model to assesses tissue-engineered vascular patches. The impact of decellularization on the development of the host cellular and humoral immune responses directed against allogeneic vascular patches is then determined. Cryopreserved decellularized allograft valves may provide a suitable scaffold for repopulation with autologous valve cells, Residual Me_2SO may however interfere with repopulation. We therefore demonstrated that the Me_2SO concentration in decellularized grafts is much lower that levels reported to interfere with cell function.

THE NORMAL ARTERIAL VALVE

EMBRYOLOGY

Leaflets of the aortic and pulmonary valves arise from an undermining process of bulbar cushions 1-4 [2] through a poorly defined process [3]. In the primary heart tube, the outer layer of myocardium and the inner lining of endocardial cells are separated by the cardiac jelly, or extracellular matrix (ECM).

Following rightward looping of the heart at E9.0, a subset of endothelial cells in the region of the atrioventricular canal and ventricular outflow tracts [4] undergoes endothelial-mesenchymal transdifferentiation and invade the cardiac jelly to form the cardiac cushions. Delamination of these specialized cells then gives rise to the valve leaflets through a complex process involving differentiation, apoptosis and remodeling of the ECM [3]. Finally, aortopulmonary septation is facilitated by the migration of a population of neural crest cells from the branchial arches to the distal outflow tract [5].

Our understanding of the molecular mechanisms guiding the embryologic development of the heart are poorly characterized, but are starting to be elucidated. The major signaling pathways identified to date include those under control of the transcriptional regulators VEGF, NFATc1, Wnt/β-catenin, Notch, BMP/TGFβ, ErbB, and NF1/Ras [3] (figure I-1). Endothelium derived nitric oxide has also recently been shown to be important in cardiac valve morphogenesis, and altered nitric oxide signaling may be responsible for arterial valve malformations including bicuspid aortic valve [6].A detailed review of the molecular pathways leading to arterial valve development is beyond the scope of this work and the reader is referred to other recent reports for further details. In short, the developmental pathways depend on an intricate interplay between the myocardium, the endocardium and the ECM.

MORPHOLOGY

Heart valves are comprised of an interstitial matrix covered by a confluent layer of valvular endothelial cells. Three distinct layers including the fibrosa, spongiosa, and ventricularis comprise the extracellular matrix and contribute to the structure and function of the arterial valves [7].

EXTRACELLULAR MATRIX

Valve ECM is composed of collagen (60%), elastin (10%) and proteoglycans (10%) [8]. Type I and III collagen are predominant and occur in a ratio of 3:1. Type V collagen makes up 2 percent of the total collagen content [9]. It has been observed that type I collagen is synthesized in response to injury, but type III collagen is synthesized in areas of rapid new collagen synthesis [10]. Collagen bundles provide the majority of mechanical strength and are interconnected by elastin [11]. Hyaluronic acid, dermatan sulphate, chondroitin-4-sulphate, chondroitin-6-sulfphate and heparin sulphate are the primary glycosaminoglycan side-chains of proteoglyans found in heart valves. With water, these glycosaminoglycans form a gel wherein matrix elements are covalently cross-linked.

The ECM remains in a state of constant flux that requires careful balance of synthesis and degradation. Synthesis occurs by secretion of soluble collagen by VICs into the extracellular space where it undergoes processing by enzymes

including prolyl 4-hydroxylase, lysyl hydroxylase, prolyl 3-hydroxylase, C-terminal peptidase and lysyl oxidase. Individual subunits then undergo further modification, aggregation and finally covalent cross-linking. Although humoral agents such as serotonin and angiotensin stimulate collagen secretion [12], mechanical stretch results in a much more profound response [13]. Degradation of the ECM is effected by a variety of matrix metalloproteinases (MMPs) including collagenases (MMP-1, MMP-13) and gelatinases (MMP-2, MMP-9) as well as tissue inhibitors of matrix metalloproteinases (TIMPs) (TIMP-1, TIMP-2, TIMP-3), which are important in matrix repair and remodeling [14].

The ECM of the arterial valves is arranged into three morphologically distinct layers: the fibrosa, the spongiosa and the ventricularis [7]. Each layer is morphologically distinct and confers a specific function of the valve.

Fibrosa. Aptly named, the fibrosa is comprised primarily of sheets of collagen bundles [8] predominantly arranged in wavy bundles that are oriented in the transverse direction [15]. On the outflow surface of the arterial valves, the fibrosa provides the primary load-bearing structure of the valve, supporting the valve leaflets against systemic blood pressure [16].

Spongiosa. A loosely organized layer of connective tissue in semi-fluid ground substance is found between the structural fibrosa and the elastic ventricularis [17]. Proteoglycans are interspersed in the spongiosa with randomly

oriented collagen bundles and multiple fine layers of elastic tissue. Negatively charged glucosaminoglycan side chains on proteoglycans in this layer bind water, creating a porous gel matrix, allowing the leaflets to absorb stress [8], maintain flexibility during valve motion [18] and resist compressive forces [19].

Ventricularis. On the ventricular aspect of the arterial valve leaflets is a thin layer of elastic fibers [8]. The ventricularis provides flexibility of the valve leaflet that aids in recoil during closure [16]. These properties help the leaflets withstand repeated deformation and reformation [19] and maintain the collagen crimp [11].

HEART VALVE CELLS

Valve Endothelial Cells

A monolayer of confluent endothelial cells covers the entire surface of the arterial valves. Although vascular endothelial cells have been well studied, little is known regarding the function of VECs. Possible roles may include protection, resistance to thrombus formation and regulation of VICs. VECs also transport nutrients and are vital in the transduction of mechanical and biochemical signals [20]. Inhibition of normal VEC function in diseased states, or by glutaraldehyde fixation of commercially available bioprosthetic valves, may lead to the deposition of platelets and fibrin, valve calcification, bacterial endocarditis, and eventual deterioration of the valve [21-25].

Although no specific cell surface markers have been identified, VECs exhibit unique functional characteristics that may suggest a phenotype that varies from vascular endothelial cells. Phenotypic differences between VECs and vascular endothelial cells may arise from variations in the environment of these two cell types. VECs are exposed to strains and strain rates far greater than those experienced by vascular endothelial cells [26,27]. Like vascular endothelial cells, VECs form a confluent cobblestone covering of the valve surface. Their ultrastructure includes plasmalemmal vesicles [28], rough endoplasmic reticulum [29], gap junctions [30,31] and overlapping marginal edges [32]. Although, VECs lack Weibel-Palade bodies (rod-shaped microtubulated bodies found in endothelial cells that contain von Willebrand factor [33] and P-selectin [34]) despite expressing von Willebrand factor [35]. In static culture, both cell types are randomly oriented, but in response to shear stress, VECs align perpendicular to the direction of flow whereas vascular endothelial cells align parallel to the direction of flow [36,37]. Different cell signaling mechanisms may drive the observed difference in phenotype. Inhibition studies suggest that alignment of VECs is solely Rho-kinase dependent, but vascular endothelial cells are dependent on phosphatidylinositol 3-kinase in addition to Rho-kinase [37]. Moreover, transcriptional profiles of VECs and vascular endothelial cells indicate that VECs express more proliferation-related transcription factors [38,39] .

VECs are metabolically active. They express angiotensin converting enzyme activity, produce endothelial nitric oxide synthase (eNOS) and synthesize ECM elements including fibronectin, prostacyclin, hyaluronic acid and heparin-like glycosaminoglycans [29].

Valve Interstitial Cells

VICs are vital to the production, maintenance and repair of the valve matrix and comprise approximately 30% of the volume of mouse atrioventricular valves. They are similar in phenotype to vascular smooth muscle cells but also demonstrate characteristics consistent with fibroblasts. VICs maintain the valve ECM by producing matrix proteins and glucosaminoglycans [40]. Constant motion of valve leaflets causes continual deformations of the valvular matrix. VIC repair processes aid in maintaining valve integrity and function [40,41]. Unlike smooth muscle cells and fibroblasts which have a complete basal lamina, VICs lack a basal lamina, thus allowing direct contact with matrix elements including collagen, elastin and proteoglycans [28]. Numerous interconnecting processes coupled by communicating junctions create a cellular network across the entire valve.

In addition to secretory VICs, a subpopulation of VICs with contractile function has been identified [28,42,43]. Bundles of actin filaments are distributed through out the cell and adrenergic motor nerve endings have been identified in close relation to VICs. Cardiac and skeletal contractile proteins including α- and

β-myosin heavy chain, as well as various troponin isoforms, are expressed in VICs [44]. Stimulation with epinephrine and angiotensin II causes VIC contraction *in-vitro* [28]. Moreover, valve leaflets contract in response to a number of vasoactive agents [45-47].

Valve Endothelial Cell Regulation of Valve Interstitial Cells

Endothelial regulation of vascular smooth muscle is well established [48-51], but less is known about the interactions of VECs and VICs. Because of their direct contact with the blood stream, VECs sense circulating factors and respond to stress [52]. Communication may occur through cell junctions or by paracrine effects [53]. Butcher demonstrated that co-culture of VECs with VICs increased shear-induced total protein content but reduced α-SMA expression compared to VICs alone [54]. Inhibitory effects on α-SMA by VECs may indicate an inhibition of VIC activation [55]. Studies of VIC wound repair and valvular pathology have suggested that FGF-2 [56,57] and TGF-β1 [58,59] play a role in VIC regulation and may therefore be involved in VEC signaling. The precise mechanisms by which VECs act on VICs remain elusive.

Nitric oxide is a likely mediator between VECs and VICs. Shear stress and other mechanical factors increase eNOS expression in the vasculature [60]. Similarly, Moesgaard recently demonstrated nitric oxide release as well as eNOS mRNA expression and eNOS protein in mitral VECs, but the significance of this finding is not yet understood. The authors hypothesized that nitric oxide may

provide a protective mechanism by inhibiting platelet aggregation and leukocyte adhesion, but also suggested that VEC nitric oxide production may regulate the ECM [61]. This conclusion is reasonable because it was previously shown that inducible nitric oxide synthase enhances *in vitro* heart valve repair by promoting VIC migration [62]. Furthermore, there is some indication that endothelial derived vasoactive substances interact with VICs to promote matrix secretion in response to valve injury [54,63]. Never the less, the effect of nitric oxide on specific downstream targets in cardiac valves has not been studied.

PHYSIOLOGY OF THE NORMAL VALVE

The normal arterial valves are structures in the outflow tract of each ventricle that passively open and close in response to positive and negative pressure gradients between the ventricle and the artery. As pressure rises in the aorta or pulmonary artery at end-diastole, the arterial root increases in diameter thereby reducing the area of leaflet coaptation [64] and minimizing shear stress, flexion stress and fatigue strain [65]. Ventricular contraction raises the intraventricular pressure until it matches the arterial pressure. The valve leaflets then open and blood is ejected from the heart with minimal resistance [66]. Vortices at the sinuses of Valsalva, described first by Leonardo da Vinci [67], allow full opening of the arterial valve leaflet while leaving a space against the arterial wall. At end systole, the ventricular pressure drops reducing the arterial-

ventricular gradient. As blood flow across the valve decreases, the vortices in the sinuses of Valsalva enlarge causing the flexure point to move up the valve leaflet [68]. Equalization of the arterial and ventricular pressures effects a slight reversal of blood flow across the valve allowing the valve to close [66].

THE DISEASED ARTERIAL VALVE

PATHOPHYSIOLOGY

Aortic Stenosis

Aortic stenosis is most commonly caused by the calcification of a trileaflet or congenitally bileaflet aortic valve. Aortic valve sclerosis (calcification that does not impair blood flow across the valve) is found in 26% or the population and the prevalence of aortic valve stenosis is 2%, but increases with older age, male sex, smoking and hypertension [69]. The exact mechanisms leading to aortic valve calcification remain poorly understood, but are thought to be related to mechanical stress on the valve leaflets which results in disruption of the collagen fibers. More recently, it has been suggested that calcification is the result of an inflammatory process that is similar to the development of atherosclerosis in arteries. Additional risk factors for aortic valve calcification include dyslipidemia, uraemia, renal failure and hypercalcemia. Other clinical entities such as, diabetes mellitus, hypertension, Paget's disease and hyperparathyroidism may also lead to aortic valve calcification [70]. Leaflet motion is impeded as the calcification

progresses from the cusp to the free edge of the leaflet [71]. As the effective orifice area decreases, the left ventricle compensates for the resulting pressure overload by concentric left ventricular wall hypertrophy, which has several deleterious effects. Coronary artery blood flow is reduced and altered, leading to subendocardial ischemia and systolic and diastolic dysfunction.

Aortic Regurgitation

Aortic regurgitation occurs when the aortic valve leaflets fail to coapt during diastole, allowing previously ejected blood to flow retrograde into the ventricle, resulting in both volume and pressure overload of the ventricle. In contrast to pressure overload alone which causes concentric hypertrophy, volume overload results in eccentric hypertrophy. In chronic aortic regurgitation, the ventricle dilates, the ventricular wall thins. Consequently, wall stress increases according to the Young-Laplace Law, which states that the wall tension of a cylinder is directly proportional to the pressure and radius of the sphere and inversely proportional to the wall thickness [72,73]. Increased ventricular wall tension increases myocardial oxygen demand and concomitant reduction or even reversal in diastolic coronary blood flow, rendering the myocardium ischemic [66].

Pulmonary and Right Ventricular Outflow Tract Disease

In contrast to aortic valve disease, pulmonary valve disease is most commonly attributed to congenital malformations. A full discussion of congenital

heart disease is beyond the scope of this thesis. Suffice it to say that many congenital heart defects require complex surgical reconstruction for both palliation and cure. Often, allograft or synthetic patches and conduits are required to complete such procedures. Similar to the surgical management of acquired arterial valve disease, the optimal conduit in congenital cardiac surgery has not yet been achieved.

CURRENT PRACTICE

History of Surgical Interventions on the Aortic Valve

Heart valve prostheses have improved significantly since 1951, when Hufnagel implanted the first mechanical valve into the descending thoracic aorta [74]. Subsequently, thousands of patients have benefited from improved survival and function. In 1999, more than 50,000 aortic valve prostheses were implanted in the United States [75]. Current prostheses may be either mechanical or bioprosthetic. More than 80 prosthetic heart valves have been designed [76]. Mechanical valves comprise 55% of implants worldwide, with the remainder being biologic or tissue valves [77]. Harken described the ideal valve prosthesis in 1962. Its properties include excellent mechanical function, durability and hemodynamic performance. In addition, it should not induce an immune or inflammatory response or thrombosis and should possess the capability for growth and repair. While excellent results have been attained using current valve

prostheses, each valve has specific benefits and limitations; the creation of the ideal valve remains elusive [78].

Mechanical Valves

Mechanical valve designs include caged-ball, single-tilting-disk and bileaflet-tilting-disk [76]. Incremental design improvements over time have resulted in superior durability, with an estimated incidence of structural failure that is currently less than 0.5% per patient-year [79]. The overall freedom from reoperation is greater than 95% at 10 years and 90% at 15 years [80]. The primary limitation of mechanical valves is their risk of thromboembolism. Hence, patients with mechanical valves require systemic anticoagulation and are exposed to the risk of life-threatening hemorrhagic events [81]. Additional complications of mechanical valves include infective endocarditis, hemolysis and structural failure resulting in embolization [76].

Bioprosthetic Valves

Allograft and xenograft biologic valves are available [82], and xenograft valves may be either stented or stentless. Bovine and porcine xenograft valves are most commonly tanned with glutaraldehyde which crosslinks proteins and stabilizes the ECM and minimizes the immune response. Biological valves are less thrombogenic than mechanical valves and do not require systemic anticoagulation. A variety of factors lead to structural valve deterioration and

reoperation. Freedom from reoperation for bioprosthetic valves is 95% at 5 years, 90% at 10 years, but only 70% at 15 years.

Allograft valves offer significant advantages over mechanical and other biologic heart valve prostheses, including superior hemodynamic properties, resistance to infection, and a low incidence of thromboembolic complications [83-85]. However, their supply is limited and, like other biologic valves, their long-term durability is foreshortened. Freedom from reoperation is age-dependent, and has been reported at 15 years to be 70%, 75%, 81% and 87% for patients ages 11 – 20 years, 21 – 30 years, 31 – 40 years, and older than 40 years at age of implantation, respectively [86]. However, outcomes in younger patients are far less favourable and valve failure is accelerated with younger age. The overall freedom from reoperation in patients less than 20 years is 47% at only 10 years [85] but may be as low a 69% in the first two years of life [87]. Among other factors, ischemic injury during storage may contribute in part to the eventual structural deterioration of allograft valves. Moesgaard identified altered nitric oxide release as soon as 8 hours post-explant, suggesting VEC dysfunction only 8 hours after harvesting [61].

Cryopreservation

Techniques for cryopreserving allograft valves and blood vessels was developed in 1975 and led to the establishment of tissue banks to enhance

matching allograft supply with demand [88]. Numerous combinations of sterilization and storage techniques have been attempted, but antibiotic sterilization followed by cryopreservation has emerged as the preferred storage method allograft heart valves [89]. However, despite attempted optimization, cryopreservation of valves has also fallen short of preserving a fully viable prosthesis. Although cryopreservation does not result in a quantitative reduction of collagen, desmosine or elastin [90], cryopreserved valves show cellular changes including destruction of endothelium, loss of cellular detail, changes to cell ultrastructure and reduced viable cell numbers. Interestingly, rapid cooling rates have been suggested as a method to alter the immunogenicity of allograft valves while maintaining viability of other valve cell populations [91]. In addition to cellular injury, there is evidence that cryopreservation is associated with injury to the matrix. The region between the spongiosa and the ventricularis is fragmented and there is a loss of collagen crimp [90], as well as autolytic changes, increased collagenolysis and reduced total protein synthesis. More severe destruction of the collagen structures and elastic fibers in cryopreserved valves was recently demonstrated by laser-induced autofluorescence and multiphoton imaging, respectively. These changes were most profound in the spongiosa, where the largest ice crystals form during cryopreservation [92] and were not evident using traditional immunohistochemical methods [90]. Taken together, these results suggest that the water-rich spongiosa is most sensitive to cryoinjury. Damage

sustained by the matrix during cryopreservation may result in altered resistance to mechanical stress. Furthermore, cellular injury may inhibit repair mechanisms in the implanted graft. Injury sustained by the matrix during freezing may have significant effects on valve function given the importance of the matrix in cellular adhesion, migration, and signaling. Additional work is required to elucidate further the effects of cryopreservation and to develop methods to minimize it.

Vitrification may emerge as a solution to cryoinjury due to ice formation. A supercooled liquid that is further cooled may pass through a transition into a glassy or vitrified state instead of forming a crystal lattice. In this state, the viscosity of the solution is sufficiently great that the molecules move so slowly as to prevent crystallization [93]. Both heart valves and blood vessels have been successfully vitrified, although it is not yet known if this alternative method of preservation will enhance clinical outcomes [92,94].

ALLOGENEIC IMMUNE RESPONSE

Allograft heart valves were previously thought to be "immunologically privileged and [not to] excite a host reaction" [95,96]. Abundant data in recent years has refuted these earlier claims, demonstrating activation of allogeneic cellular and humoral immune mechanisms that are associated with destruction of the valve. Valve endothelium displays protein and carbohydrate antigens including major histocompatibility complexes (MHC) I and II on human valves

[97,98]. Although expression of α-Gal antigen on xenograft valves is less than on other types of endothelial cells, RNA transcripts were identified at the same level [99]. Consequently, both allo and xenograft valves are antigenic without treatment and may elicit cellular and humoral rejection. The allogenicity of allograft heart valves has been confirmed by studies showing the development of a secondary immune response. Rats that received allogeneic valves rejected secondary skin transplants swifter than animals receiving syngeneic grafts [100-102].

Humoral Response

Implantation of cardiac valve allografts induces the production of anti-HLA antibodies [103]. In addition, donor-specific antibodies were generated against MHC class I alloantigens when allograft valves were implanted in rats [102,104]. These studies did not mention if there was destruction of the allograft valves. Prospective cohort studies of both in-house prepared and the Cryolife® cryopreserved allograft valves demonstrated mean PRA values greater that 60% at one year in pediatric patients receiving allograft valves compared to less than 6% for pediatric patients undergoing other complex congenital cardiac surgery. In several cases, HLA-directed antibodies were identified that exhibited specificity against donor HLA [105-107]. The clinical significance of the humoral immune response is still not fully understood. However, one group of investigators demonstrated an association between the development of anti-HLA class II

antibodies and structural degeneration of the valve allograft [108]. Further analysis by the same group revealed that those patients with donor-specific anti-class II DR antibodies had significantly more structural degeneration than patients who did not develop a humoral immune response [109]. Other investigators have also associated the development of class-I HLA-directed antibodies with early valve destruction [110]. Despite these findings, the precise mechanism of humoral rejection of allograft valves remains to be demonstrated. In addition to the deleterious effects that the humoral response may have on the valve, the development of antibodies is a significant predictor of poor outcome in those patients who eventually require heart transplantation [111], irrespective of a negative lymphocyte crossmatch [112,113].

Cellular Response

The cellular immune response has also been shown to play a role in the destruction of allograft valves. *In-vitro* experiments by Hoekstra *et al* demonstrated a cell-mediated response to human allograft valves; cryopreserved valve leaflets effected a proliferative response in mixed lymphocyte reaction (MLR, see Chapter IV for a description of MLR) that was dependent on HLA-DR [114]. Paradoxically, our group showed that a short harvest-to-preservation time, which is known to improve allograft viability [104,115], was a significant predictor of early valve failure [116]. In a Brown-Norway to Lewis rat model of allograft valve transplantation, we subsequently demonstrated that T-cell

infiltration of allogeneic valves resulted in destruction of the valve leaflets at 28 days. This immune response was abrogated by immunosuppression with cyclosporine or administration of anti-α4/β2 integrin antibodies which interfere with T-cell adhesion [117], suggesting a role of T-cells in the rejection of allograft heart valves. Circulating donor-specific cytotoxic T cells and helper T cells have been identified in adults and children who received allograft valves and are correlated with destruction of the allograft valve [118,119].

Allograft Valve Antigens

Although it is certain that allograft valves are subject to cellular and humoral rejection, the antigens inciting these responses have not been fully identified. It is suspected that endothelial, interstitial and dendritic cells present HLA class I and II antigens that trigger the host immune response [84,120,121], however further work is required to determine what cells present antigen on allograft heart valves and whether valve-derived antigens are presented by host or donor antigen presenting cells, or by both. This is the basis behind decellularization as a method to minimize the allogeneic immune response to bioprosthetic valves (see below).

Methods to Reduce Alloresponse

Two general strategies may be used to avoid rejection of allogeneic heart valves: either the host immune response must be altered or the valve may be modified so that antigens are not displayed. Assessment of the heart valves in

explanted allogeneic hearts that failed due to allograft coronary disease [122-125] failed to demonstrate any evidence of cellular or humoral rejection even in the setting of graft arteriosclerosis or myocardial rejection. There are only sporadic case reports in the literature that describe valve failure in patients following allogeneic heart transplantation. Survival of valves in allogeneic cardiac transplantation may be attributed to short donor ischemic time, blood group typing and matching, and chronic systemic immunosuppression. Cyclosporine [126], and mycophenolic mofetil [127] are among many agents that have demonstrated efficacy in attenuating the alloimmune response in animals and humans. However, the side effects from long-term systemic immunosuppression currently outweigh the risks associated with reoperation due to allograft valve failure. Antibody blockade of cell adhesion molecules (anti-$\alpha 4/\beta 2$ integrin) has also been shown to be effective at minimizing the cellular immune response in iv vivo rat models of allograft valve transplantation [128]. Other approaches to altering the recipient are induction of tolerance [129] or accommodation [130], but these methods are not well studied in treating rejection of allogeneic heart valves. There are a few reports in the literature suggesting that intravenous immunoglobulin [131] may improve the outcomes of cardiac and renal transplantation by reducing preoperative PRA values [132,133]. However, a recent prospective cohort trial of prophylactic intravenous immunoglobulin failed

to demonstrate a reduction in PRA values in patients receiving allograft pulmonary artery patches during the Norwood procedure [134].

To avoid the complications associated with systemic immunosuppression, modifications may be made to the valve so that antigens are not displayed. These strategies may include eliminating the cellular components of the valve (see decellularization below) or modulating the host-donor interactions at the level of the valve [135].

TISSUE-ENGINEERING

Although the principles of tissue-engineering date back to 1930s [136], the current concept of tissue-engineering emerged in the 1980s. By providing an alternative to human organ donors, tissue engineering was a strategy to combat the increasing shortage of organ donors for transplantation and to provide more suitable materials for surgical reconstruction of congenital and acquired anatomical defects [137]. Fung stated that "a clear understanding of phenomena at the tissue level is prerequisite to the engineering of tissues". Fung further described the field of tissue-engineering as bridging physiology to cell biology and biochemistry [138]. Current tissue-engineering strategies populate biologic or synthetic scaffolds with cells to generate new tissue.

SCAFFOLD

Scaffolds provide a structure onto which cells may be introduced and give support to cells while they become organized and form new ECM. They may provide the initial dimensions and shape of the tissue, and in the case of heart valves may contribute to the eventual function and mechanical stability of the device. Scaffolds may be either of biologic origin or be completely synthetic. Ideally, cells in a tissue-engineered valve would be able to recognize the scaffold, migrate to their normal position and resume normal function rendering the engineered valve completely viable. The extent to which this ultimate goal can be achieved remains to be determined.

Biologic

Decellularized autologous and xenograft tissues were the first scaffolds utilized in tissue-engineering strategies and have been widely investigated for use in valve constructs since 1984 [139]. The primary benefit of biologic scaffolds is that they can potentially provide normal macro- and micro-architecture of the valve while maintaining normal biologic and mechanical properties. In the broadest sense, homovital, or non-preserved allograft valves are the most basic tissue engineered valve replacement. Without treatment, biologic scaffolds have the potential for immune mediated rejection, which is one of the foci of this thesis. As described above, it is thought that cells present the primary source of allo-antigens in

allogeneic heart valves. Therefore, decellularization should theoretically reduce or eliminate the antigenic load. Because matrix proteins are conserved within a species, it is unlikely that they would incite an allogeneic immune response. However, xenogeneic matrix proteins are antigenic and generate a marked immune response characterized by infiltration of mononuclear cells into the media and adventitia [140]. It is not clear whether the immune response against the valve matrix is by the same or different mechanisms as the MHC- or EC-directed response. Without treatment, xenograft valves are subject to proteolysis. Although cross-linking by glutaraldehyde inhibits proteolysis of the xenograft matrix, recent evidence suggests that glutaraldehyde fixation does not completely eliminate the cellular or humoral immune responses, although the reasons for this are not yet clear [140,141].

Decellularization

Decellularization of tissues has been accomplished by a variety of methods including thermal cycling [142], radiation [143], enzymatic and chemical treatments. Repeated freeze-thaw cycles is also effective at destroying cells and minimizes allogenicity [144], but the process leaves cell fragments in the tissue and injures structural proteins [145]. Irradiation has been used to decellularize nerve tissue without inducing damage to the tissue morphology [146], but has been associated with early cuspal failure when previously used to sterilize

allogeneic heart valves [147]. None of the former methods completely extract all cellular debris, leaving potential for allograft rejection and further injury to the matrix [148]. Enzymes such as trypsin, either with or without EDTA [149], are highly effective at decellularizing heart valves, but are the most damaging to the matrix [150]. The most commonly used approach involves disrupting cell membranes by osmotic lysis with hypertonic followed by hypotonic solutions. Cellular debris is then extracted with a detergent. Ionic, zwitterionic and nonionic detergents have all been used for extraction, although these agents may injure the matrix by degradation or denaturing matrix proteins, leave toxic residues, or alter the charge of the scaffold [139]. More recently, deoxycholic acid has been shown to decellularize heart valves effectively [151] without deleterious effects on structural proteins [152,153].

Synthetic

Regardless of the potential advantages of decellularized allograft matrix, it remains that allograft tissue is in short supply. Xenograft tissue is available in relatively abundant supply, but is also subject to rejection and possible transmission of zoonosis [154]. Consequently synthetic alternatives have been sought. Synthetic matrices offer the advantage of ease of commercial reproduction, regulation of properties such as pore size, stability and may be designed to degrade after a period of time. If cells are added during the formation of the matrix, it may be easier to ensure engraftment. The underlying rationale of

using a synthetic matrix is to provide a temporary support for cells while they lay down a new ECM thereby creating the tissue. However, synthetic matrices may lack natural cell binding sites and cell signaling molecules, lack complete biocompatibility, induce inflammation and inhibit normal cell function [155]. As the synthetic matrix degrades, it may leave holes that are filled with scar instead of the preferred tissue, resulting in fibrosis and distorted architecture.

A variety of polymers have been considered as bioresorbable matrices [155]. Polyglycolic acid and polylactic acid are the most widely studied bioresorbable matrices in tissue-engineering research. Polyglycolic acid, a polyester, has been commercially available since 1970 and is widely used in suture and medical implants [156]. Properties including hydrolytic degradation may be altered by modifications such as co-polymerization with polylactic acid. Polyglycolic acid and polylactic acid are poor substrates for cell growth *in-vitro* [157] and do not possess optimal mechanical properties for heart valves. Polyhydroxyalkanoate, a biopolyester exhibits superior elasticity and mechanical strength [158], but it is not clear if this material provides improved cell adhesion. Novel biomaterials that mimic ECM function are being developed [159,160] including polymers that present bioactive ligands [161]. Smart scaffolds which are capable of altering their shape [162], hydrophilicity, hydration [163,164], and cell adhesive properties depending on environmental conditions [165] are other exciting scaffolds that are under development. Despite the attractiveness of

biodegradable polymer scaffolds, poor cellular adhesion and tissue regeneration persist as significant limitations [166].

REPOPULATION

Successful tissue-engineering is highly dependent on populating the matrix with cells that attain the phenotype of native valve cells, thereby mimicking the micro and macro function of the native valve. Ideally, cells would resume their function of maintaining the ECM but would be under regulation such that thickening and stenosis of the leaflets would not occur [167]. Repopulation may proceed either *in vitro* prior to implantation using autologous, allogeneic or xenogeneic, differentiated or progenitor cells, or *in vivo* by the patient's own circulating cells. Each cell type is associated with specific benefits and limitations. Endothelial cells express MHC class I and II antigens which are primary targets for allogeneic immune response leading to graft rejection. Consequently, autologous cells will likely remain the preferred cell source. Alternatively, genetically modified cells may be engineered to remove antigens as has been done for xenotransplantation [168,169].

Ex vivo Repopulation

Differentiated cells

Initial attempts at heart valve engineering utilized differentiated cells to provide both interstitial cells and an endothelial surface. To minimize the

thrombogenicity of bare scaffolds, endothelial cells have been used to line tissue-engineered vascular constructs. Endothelial cells from saphenous vein [170], autologous carotid artery [166], femoral artery [171] and radial artery [172] have all been investigated as a source for valve endothelium. Their primary benefit is that they are fully differentiated and may be expanded in tissue culture. Likewise, aortic myofibroblasts [173] and venous myofibroblasts [174] have been used as a source for interstitial cells. The use of primary vascular endothelial cells and fibroblast cells requires excision of an intact vessel from the potential recipient. Hence other sources for interstitial cells have been investigated; dermal fibroblasts [175], foreskin fibroblasts [176] and umbilical cord myofibroblasts [177] have all been used in a variety of tissue-engineered valve settings. It should be stressed that although the latter cells were obtained from relatively primitive structures, in contrast to other reports (see below), these authors do not indicate that these umbilical cord derived cells were progenitor cells.

Progenitor cells

Autologous bone marrow-derived stem cells are a readily available cell source for tissue-engineering. Bone marrow is easily harvested and stem cells require minimal processing compared to tissue sources which require surgical excision of tissue and homogenization to obtain a pure cell suspension. Bone marrow contains several types of stem cells including endothelial progenitor cells (EPC)s, and hematopoietic and mesenchymal stem cells. In studies using tissue-

engineered blood vessels on a ι-lactide/ε-caprolactone copolymer on a polyglycolic acid mesh, the bone marrow stem cells differentiated into endothelium in 4 weeks and expressed endothelial cell lineage markers (CD34, CD31, Flk-1 and Tie-2) [178,179]. Another major benefit of using bone marrow stem cells is that a large volume of cells can be obtained directly from the recipient so that the cells do not require *ex-vivo* expansion and no vessels are injured in the harvesting [180].

EPCs can be isolated from blood [181] and bone marrow [182]. Although initially $CD34^+$ cells were considered EPCs, more recent studies concluded that CD133 (promin, a highly conserved cells surface molecue with unknown biological activity that is expressed only on hematopoietic stem cells [183]) together with VEGFR2 (Vascular endothelial growth factor receptor 2) expression represent a superior marker for EPCs. Controversy still persists in the literature as to the exact characterization of EPCs [184]. Regardless, EPCs can be differentiated *ex-vivo* into cells of an endothelial phenotype, expressing both endothelial markers (including von Willebrand factor and other markers) and function (incorporation of 1,1'-dioctadecyl-3,3,3',3'-tetramethylindocarbocyanine-labeled acetylated low density lipoprotein [DiI-Ac-LDL], nitric oxide production, and other markers of endothelial cell function).

Mesenchymal stem cells (MSC)s have been differentiated into all tissues arising from mesenchyme including bone [185], cartilage [186], muscle, adipose

tissue [187] and blood vessels [188]. In culture, MSCs display cell surface markers characteristic of VICs and exhibit spindle cell morphology of myofibroblasts [63] and after injection into infarcted myocardium, they differentiate into cardiac myocytes, endothelial cells and vascular smooth muscle cells [189]. MSCs therefore show promise for heart valve tissue-engineering.

Human umbilical cord blood (UCB) cells possess several advantages as a source for repopulating decellularized tissue scaffolds. A variety of cell types are present in UCB including $CD34^+$ stem cells and MSCs [190,191]. UCB banking is performed with increasing frequency. For a fetus with a known congenital heart anomaly, UCB could be harvested antenatally by cordocentesis [192] allowing for the preparation of a new valve prior to birth. UCB stem cells have the capacity to form a greater number of colonies and a higher cell cycle rate compared to other types of stem cells, thereby shortening the preparation time [193]. Compared with other stem cell sources, other important characteristics of UCB stem cells are their availability, shortened time to transplantation, lower risk of transmission of viral infectious diseases, reduced immunological reactivity, including lower risk of immunological rejection, and lower risk and severity of acute and chronic graft versus host diseases [194]. UCB stem cells have been used successfully to construct vascular grafts and patches that have generated ECM [195-197]. Tissue-engineered leaflets based on human UCB stem cells synthesized ECM and formed functional endothelium [198]. Most recently, chorionic villi-derived progenitor

cells have been described for fabrication of engineered valve prostheses [199]. These cells can be obtained by a minimally invasive procedure that is commonly used for genetic testing [200]. Chorionic villi-derived progenitor cells are easily expandable *in-vitro*, are similar in phenotype to VICs [201] and tolerate cryopreservation and are therefore well-suited for tissue-engineering. The primary advantage of UCB stem cells and chorionic villi-derived progenitor cells is that they are an autologous cell source that is available antenatally. Theoretically, they could therefore be used to construct a tissue-engineered valve antenatally when a congenital heart defect is diagnosed in utero.

Bioreactors

Communication between valve cells and ECM is vital to normal valve homeostasis as described above, and each contribute signals for growth, maintenance and repair of each other. Early in the development of tissue-engineered heart valves, it became quickly apparent that mechanical stimulation was required for cues to drive tissue formation, organization and function. Bioreactors that expose valves to flow [202-204] and strain [205,206] during *ex-vivo* repopulation and growth were developed. Pulsatile bioreactors mimic the mechanical stimuli provided by the heart during development. Several dynamic reseeding protocols have been proposed, differing in frequency, pressure, flow, duration of culture and cell seeding density. The optimal strategy to achieve in-

growth is still unclear, but it has become evident that application of mechanical stimuli increases the strength of the engineered valve.

***In vivo* Repopulation**

Although cryopreserved human allograft valves remain acellular after implantation [207,208], decellularized grafts become repopulated even without pre-seeding [209]. A number of investigators have attempted to exploit *in vivo* repopulation to minimize the time required to generate tissue-engineered heart valves [210,211]. The success of *in-vivo* repopulation presumes that the scaffold contains ligands that attract the appropriate cells and facilitate cell adhesion [212], migration [11,213] and stimulate normal function [214], metabolism [215] and interaction [216]. Mature or progenitor cells with the potential for differentiating into cells that can fulfill the role of VICs and VECs, capable of interacting with and adhering to valve ECM must circulate in the blood. GM-CSF is effective at stimulating bone marrow stem cells to home acutely infarcted myocardium [217]. When used to enhance *in vivo* repopulation of decellularized xenograft scaffolds, rapid valve deterioration ensued [218]. It is not clear whether this deleterious effect was a direct effect of GM-CSF or if GM-CSF upregulated xenograft rejection of cells in an incompletely decellularized scaffold [219]. The effect of GM-CSF on allograft scaffolds remains to be studied.

In vivo Animal Studies

In a study by Breuer, autologous endothelial cells were seeded to confluency onto a biodegradable substrate of polyglycolic acid mesh and 90/10 polyglycolic and polylactic acid in the form of a pulmonary valve leaflet. The engineered leaflet was implanted as the right posterior pulmonary valve leaflet in a lamb model. Despite being slightly thickened, the echocardiographic assessment demonstrated normal leaflet function without stenosis and only minimal regurgitation up to 77 days postoperatively [171].

Clinical Studies of Tissue-Engineered Valves

The successful implantation of an autologous tissue-engineered valve into a four-year-old girl with previous Fontan repair of a single right ventricle and pulmonary atresia was the culmination of world-wide efforts to generate improved valve prostheses. This valve was based on a biodegradable polycaprolactone-polylactic acid copolymer matrix that was seeded and conditioned *in-vitro* with autologous venous cells. Graft occlusion or aneurismal changes were not apparent on chest roentgenogram at 7 months postoperatively [174]. Long-term follow-up is not yet available, but will be required to determine if the outcomes of this tissue-engineered valve are superior to currently available alternatives.

Initial attempts at implanting decellularized xenograft scaffolds resulted in devastating complications. Of the 4 children receiving Synergraft™

decellularized xenogeneic valves, 3 died as a result of severe structural degeneration of the valve at 7 months and 1 year postoperatively, and of valve rupture 2 days post-implant [220]. A strong non-specific inflammatory response leading to lymphocytic infiltration was cited as the cause of failure [139,220], however it is important to note that incomplete decellularization of the xenograft was found on further assessment of pre-implantation samples [220]. In the post-presentation discussion at the 16th Annual Meeting of the European Association for Cardio-thoracic Surgery, one discussant reported more superior results with the same device, however these results remain unpublished (Monte Carlo, Monaco). A third group reported performing 50 Ross procedures in adult patients (median age 46) using the Matrix P valve, a decellularized xenograft valve. Only one patient required reoperation of the Matrix P valve and there were no other structural failures [221].

The exact mechanism of failure of the xenograft Synergraft™ valve is not clear. The failure of the xenograft Synergraft™ valve could reflect decellularization-related injury to the ECM, that the decellularization process is not as complete in non-human tissue, or that the xenograft matrix is far more immunogenic than previously considered. It is also possible that the pediatric population mounts a more aggressive response against the xenograft valve than older populations, although this has not been studied.

Results with the Synergraft™ decellularized allograft valve have also been reassuring. At a median of 10 months since implantation of the decellularized allograft valve in a cohort of 22 adult (median age 37) patients with congenital heart defects, there were no significant differences in the mean gradient, maximal gradient or effective orifice area compared to a cohort of patients who received standard cryopreserved allograft valves [222]. Further study is required to elucidate the differences between xenograft and allograft valve matricies and will likely have important significance to the field of tissue-engineering.

OBJECTIVES AND GENERAL OUTLINE OF THESIS

The primary objective of this work is to characterize the allogeneic immune response to a decellularized pulmonary artery vascular patch. Pulmonary and aortic valve conduits are commonly used in cardiac surgery for the reconstruction of lesions of arterial valves and outflow tracts, particularly in the pediatric population. Although these valves provide excellent hemodynamic and handling characteristics, their use is limited by eventual structural deterioration which is accelerated in younger patients. There is evidence reported in the literature that the cells in the valves that are presumed to confer viability to the valve may actually incite an allogeneic immune response. By this hypothesis, decellularization of the valve should therefore reduce the allogeneic immune

response. The resulting tissue may be an ideal scaffold for tissue-engineered valves or conduits.

In Chapter 2, a large animal model for implanting tissue-vascular patches is developed. The US-FDA requires preclinical testing of heart valves to be conducted in the orthotopic position of a large animal model, which necessitates the expense and morbidity of full cardiopulmonary bypass [223,224]. The eventual goal of this work is to develop a tissue engineered valve. However, by implanting a vascular patch into the descending thoracic aorta of sheep, preliminary data regarding the immunogenicity of tissue-engineered vascular constructs, their cellular repopulation, propensity for aneurysm formation and a host of other parameters can be obtained. In addition, this model is based on surgery to repair hypoplastic left heart syndrome where allograft vascular tissue is used to reconstruct the diminutive structures. Consequently pulmonary artery tissue and not aortic tissue was used for the implant experiments performed for this thesis. Lessons learned from this work may also be applied to other vascular surgery where various conduits and grafts are required.

To prevent spinal cord ischemia and subsequent paralysis during the implantation of vascular patches into the descending thoracic aorta, a simple intraaortic shunt was developed and characterized. This shunt restored blood flow and pressure to the distal aorta. It was cost-effective, simple to insert and remove and facilitated the implantation procedure.

Chapter 3 provides a systematic approach to assessing the relative allogenicity of large animals used in transplantation studies. Like other large animal models, most sheep used in laboratory research are taken from farms that raise animals for human consumption. Although often considered outbred, few authors have considered the validity of this assumption. One-way mixed lymphocyte reaction (MLR) assay was used to assess the relative allogenicity of nearly all pair-wise combinations of 19 sheep from a local farm that employs excelletnt husbandry practices. More than one third of the pairs were found to be too closely related to elicit an allogeneic immune response. These findings have important implications for all large animal transplant models that do not use inbred strains and underscores the importance of addressing the relative allogenicity of study animals.

In Chapter 4, the cellular and humoral immune response to decellularized pulmonary artery vascular patches is assessed. Evidence is clearly given that decellularization reduces or eliminates the donor-specific cellular and humoral immune responses of the host. No gross evidence of aneurysm formation was identified, although there was a profound intimal thickening in both control and decellularized allografts. It is not evident whether these changes are secondary to an immune or inflammatory process, or related to cryopreservation.

Finally, in Chapter 5, consideration is given to the potential for the confounding effects of Me_2SO, a penetrating cryoprotectant, on the cellular

repopulation of cryopreserved decellularized aortic conduit scaffolds. The literature reports a broad spectrum of effects of Me_2SO on endothelial and fibroblast cell function. In addition Me_2SO induces differentiation of some cell lines and inhibits it in others. Quantitative proton nuclear magnetic resonance spectroscopy was used to determine the residual Me_2SO concentration in cryopreserved aortic valve conduits during decellularization. The final Me_2SO concentration of the conduits after decellularization was several orders of magnitude less than concentrations reported to have significant effects on cell function and should therefore not interfere with cellular repopulation of a decellularized scaffold. In addition, we discovered that when following standard tissue bank protocols, Me_2SO does not reach equilibrium with the aqueous compartment of the conduits prior to cryopreservation and that Me_2SO washout takes substantially longer than the time given under standard surgical care. The implication of these findings is not yet known. It is possible that further optimization of cryopreservation protocols may result in superior cellular viability, but changing current protocols may never-the-less have a detrimental effect on current surgical results. Further work is required to delineate the optimal cryopreservation strategy.

In summary, this thesis advances the characterization of the ovine large animal model for testing tissue-engineered heart valves and vascular constructs. We provide further evidence supporting the use of decellularized allograft scaffold

for tissue-engineered heart valves. The ultimate goal is to generate an autologous valve *in-vitro*. If a tissue-engineering approach is successful, the ideal valve prosthesis may be realized which would provide tremendous benefit to both adults and children with cardiac valve and outflow tract disease.

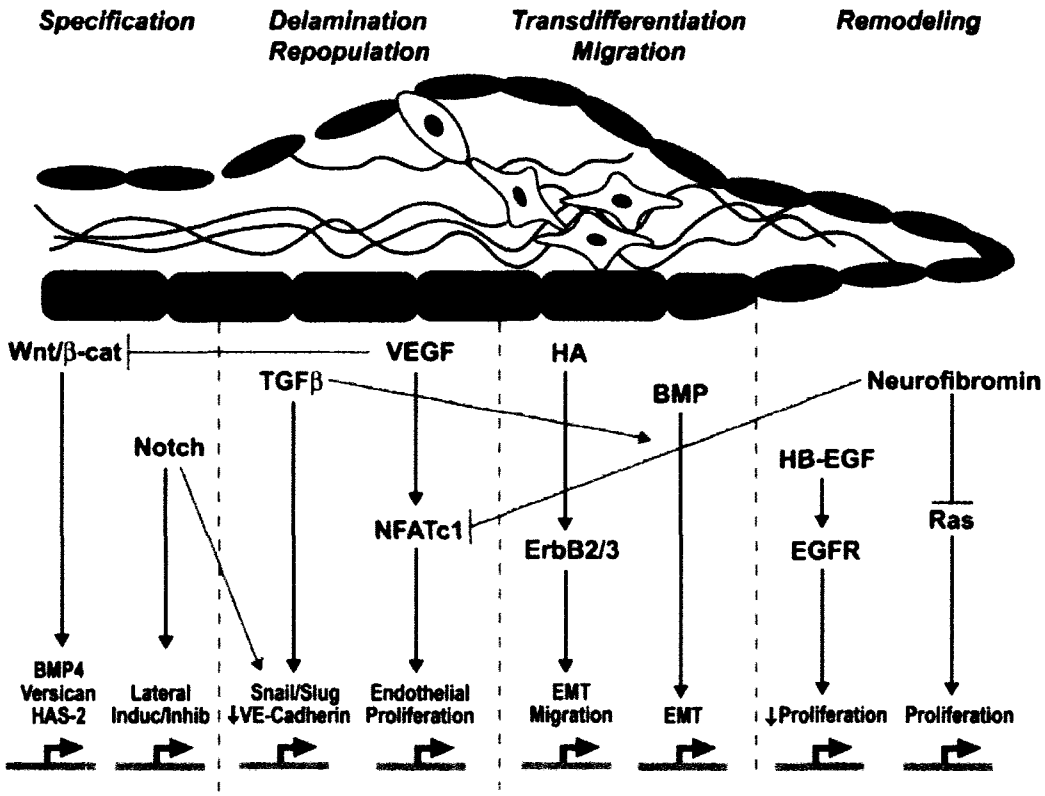

Figure I-1. Signaling network model for heart valve development and remodeling. In the signaling network model for cardiac cushion development, numerous signaling pathways and transcriptional regulators act to coordinately regulate the process of heart valve formation. Each signaling pathway is a simplified schema of the signaling events that occur. Red arrows denote positive/synergistic interactions between pathways. Blunt red arrows denote inhibitory effects between pathways. **Source**: Armstrong *et al.* [3].

REFERENCES

1. Rosamond, W., Flegal, K., Friday, G., Furie, K., Go, A., Greenlund, K., Haase, N., Ho, M., Howard, V., Kissela, B., Kittner, S., Lloyd-Jones, D., McDermott, M., Meigs, J., Moy, C., Nichol, G., O'Donnell, C. J., Roger, V., Rumsfeld, J., Sorlie, P., Steinberger, J., Thom, T., Wasserthiel-Smoller, S., Hong, Y., and for the American Heart Association Statistics Committee and Stroke Statistics Subcommittee Heart Disease and Stroke Statistics--2007 Update: A Report From the American Heart Association Statistics Committee and Stroke Statistics Subcommittee. *Circulation* **115**:e69-171, 2007.

2. Bharati, S. Embryology/pathology of the pulmonary valve in both stenosis and regurgitation. In Z. H. Hijazi, P. Bonhoeffer, T. Feldman, and C. E. Rui (Eds.), *Transcatheter Valve Repair*. Boca Raton: Taylor and Francis Group, 2006. Pp. 3-9.

3. Armstrong, E. J. and Bischoff, J. Heart valve development: endothelial cell signaling and differentiation. *Circ. Res.* **95**:459-470, 2004.

4. Anderson, R. H., Webb, S., Brown, N. A., Lamers, W., and Moorman, A. Development of the heart: (2) Septation of the atriums and ventricles. *Heart* **89**:949-958, 2003.

5. Kirby, M. L., Gale, T. F., and Stewart, D. E. Neural crest cells contribute to normal aorticopulmonary septation. *Science* **220**:1059-1061, 1983.

6. Lee, T. C., Zhao, Y. D., Courtman, D. W., and Stewart, D. J. Abnormal Aortic Valve Development in Mice Lacking Endothelial Nitric Oxide Synthase. *Circulation* **101**:2345-2348, 2000.

7. Gross, L. and Kugel, M. Topographic anatomy and histology of the valves in the human heart. *Am. J. Pathol.* **7**:445-456, 1931.

8. Kunzelman, K. S., Cochran, R. P., Murphree, S. S., Ring, W. S., Verrier, E. D., and Eberhart, R. C. Differential collagen distribution in the mitral valve and its influence on biomechanical behaviour. *J. Heart Valve Dis.* **2**:236-244, 1993.

9. Cole, W. G., Chan, D., Hickey, A. J., and Wilcken, D. E. Collagen composition of normal and myxomatous human mitral heart valves. *Biochem. J.* **219**:451-460, 1984.

10. Dawes, K. E., Cambrey, A. D., Campa, J. S., Bishop, J. E., McAnulty, R. J., Peacock, A. J., and Laurent, G. J. Changes in collagen metabolism in response to endothelin-1: evidence for fibroblast heterogeneity. *Int. J. Biochem. Cell Biol.* **28**:229-238, 1996.

11. Scott, M. and Vesely, I. Aortic valve cusp microstructure: the role of elastin. *Ann Thorac. Surg.* **60**:S391-S394, 1995.

12. Hafizi, S., Taylor, P. M., Chester, A. H., Allen, S. P., and Yacoub, M. H. Mitogenic and secretory responses of human valve interstitial cells to vasoactive agents. *J. Heart Valve Dis.* **9**:454-458, 2000.

13. Ku, C. H., Johnson, P. H., Batten, P., Sarathchandra, P., Chambers, R. C., Taylor, P. M., Yacoub, M. H., and Chester, A. H. Collagen synthesis by mesenchymal stem cells and aortic valve interstitial cells in response to mechanical stretch. *Cardiovasc. Res.* **71**:548-556, 2006.

14. Dreger, S. A., Taylor, P. M., Allen, S. P., and Yacoub, M. H. Profile and localization of matrix metalloproteinases (MMPs) and their tissue inhibitors (TIMPs) in human heart valves. *J. Heart Valve Dis.* **11**:875-880, 2002.

15. Missirlis, Y. F. and Armeniades, C. D. Ultrastructure of the human aortic valve. *Acta Anat. (Basel)* **98**:199-205, 1977.

16. Christov, A. M., Liu, L., Lowe, S., Icton, C., Dunmore-Buyze, J., Boughner, D. R., Dai, E., and Lucas, A. Laser-induced fluorescence (LIF) recognition of the structural composition of porcine heart valves. *Photochem. Photobiol.* **69**:382-389, 1999.

17. Walmsley, R. Anatomy of human mitral valve in adult cadaver and comparative anatomy of the valve. *Br. Heart J.* **40**:351-366, 1978.

18. Murata, K. and Yokoyama, Y. Acidic glycosaminoglycans in human coronary arteries, with special reference to the presence of heparin or related glucosaminoglycan. *Experientia* **37**:1139-1141, 1981.

19. Culav, E. M., Clark, C. H., and Merrilees, M. J. Connective tissues: matrix composition and its relevance to physical therapy. *Phys. Ther.* **79**:308-319, 1999.

20. Davies, P. F., Barbee, K. A., Volin, M. V., Robotewskyj, A., Chen, J., Joseph, L., Griem, M. L., Wernick, M. N., Jacobs, E., Polacek, D. C., dePaola, N., and Barakat, A. I. Spatial relationships in early signaling events of flow-mediated endothelial mechanotransduction. *Annu. Rev. Physiol* **59**:527-549, 1997.

21. Frater, R. W., Gong, G., Hoffman, D., and Liao, K. Endothelial covering of biological artificial heart valves. *Ann Thorac. Surg.* **53**:371-372, 1992.

22. Lehner, G., Fischlein, T., Baretton, G., Murphy, J. G., and Reichart, B. Endothelialized biological heart valve prostheses in the non-human primate model. *Eur. J. Cardiothorac. Surg.* **11**:498-504, 1997.

23. Cooper, M. D., Jeffery, C., Gall, D. L., and Anderson, A. S. Scanning electron microscopy studies of staphylococcal adherence to heart valve endothelial cells in organ culture: an in vitro model of acute endocarditis. *Scan Electron Microsc.*1231-1237, 1985.

24. Drake, T. A. and Pang, M. Effects of interleukin-1, lipopolysaccharide, and streptococci on procoagulant activity of cultured human cardiac valve endothelial and stromal cells. *Infect. Immun.* **57**:507-512, 1989.

25. Campbell, K. M. and Johnson, C. M. Identification of Staphylococcus aureus binding proteins on isolated porcine cardiac valve cells. *J. Lab Clin. Med.* **115**:217-223, 1990.

26. Thubrikar, M., Piepgrass, W. C., Deck, J. D., and Nolan, S. P. Stresses of natural versus prosthetic aortic valve leaflets in vivo. *Ann Thorac. Surg.* **30**:230-239, 1980.

27. Brewer, R. J., Mentzer, R. M., Jr., Deck, J. D., Ritter, R. C., Trefil, J. S., and Nolan, S. P. An in vivo study of the dimensional changes of the aortic valve leaflets during the cardiac cycle. *J. Thorac. Cardiovasc. Surg.* **74**:645-650, 1977.

28. Filip, D. A., Radu, A., and Simionescu, M. Interstitial cells of the heart valves possess characteristics similar to smooth muscle cells. *Circ. Res.* **59**:310-320, 1986.

29. Manduteanu, I., Popov, D., Radu, A., and Simionescu, M. Calf cardiac valvular endothelial cells in culture: production of glycosaminoglycans, prostacyclin and fibronectin. *J. Mol. Cell Cardiol.* **20**:103-118, 1988.

30. Lupu, F. and Simionescu, M. Organization of the intercellular junctions in the endothelium of cardiac valves. *J. Submicrosc. Cytol.* **17**:119-132, 1985.

31. Rajamannan, N. M., Springett, M. J., Pederson, L. G., and Carmichael, S. W. Localization of caveolin 1 in aortic valve endothelial cells using antigen retrieval. *J. Histochem. Cytochem.* **50**:617-628, 2002.

32. Harasaki, H., Suzuki, I., Tanaka, J., Hanano, H., and Torisu, M. Ultrastructure research of the endocardial endothelium of monkeys. *Arch. Histol. Jpn.* **38**:71-84, 1975.

33. Wagner, D. D., Olmsted, J. B., and Marder, V. J. Immunolocalization of von Willebrand protein in Weibel-Palade bodies of human endothelial cells. *J Cell Biol.* **95**:355-360, 1982.

34. Bonfanti, R., Furie, B. C., Furie, B., and Wagner, D. D. PADGEM (GMP140) is a component of Weibel-Palade bodies of human endothelial cells. *Blood* **73**:1109-1112, 1989.

35. Lester, W. M., Damji, A. A., Gedeon, I., and Tanaka, M. Interstitial cells from the atrial and ventricular sides of the bovine mitral valve respond differently to denuding endocardial injury. *In Vitro Cell Dev. Biol.* **29A**:41-50, 1993.

36. Deck, J. D. Endothelial cell orientation on aortic valve leaflets. *Cardiovasc. Res.* **20**:760-767, 1986.

37. Butcher, J. T., Penrod, A. M., Garcia, A. J., and Nerem, R. M. Unique morphology and focal adhesion development of valvular endothelial cells in static and fluid flow environments. *Arterioscler. Thromb. Vasc. Biol.* **24**:1429-1434, 2004.

38. Farivar, R. S., Cohn, L. H., Soltesz, E. G., Mihaljevic, T., Rawn, J. D., and Byrne, J. G. Transcriptional profiling and growth kinetics of endothelium reveals differences between cells derived from porcine aorta versus aortic valve. *Eur. J. Cardiothorac. Surg.* **24**:527-534, 2003.

39. Butcher, J. T., Tressel, S., Johnson, T., Turner, D., Sorescu, G., Jo, H., and Nerem, R. M. Transcriptional profiles of valvular and vascular endothelial

cells reveal phenotypic differences: influence of shear stress. *Arterioscler. Thromb. Vasc. Biol.* **26**:69-77, 2006.

40. Schneider, P. J. and Deck, J. D. Tissue and cell renewal in the natural aortic valve of rats: an autoradiographic study. *Cardiovasc. Res.* **15**:181-189, 1981.

41. Henney, A. M., Parker, D. J., and Davies, M. J. Collagen biosynthesis in normal and abnormal human heart valves. *Cardiovasc. Res.* **16**:624-630, 1982.

42. Lester, W., Rosenthal, A., Granton, B., and Gotlieb, A. I. Porcine mitral valve interstitial cells in culture. *Lab Invest* **59**:710-719, 1988.

43. Zacks, S., Rosenthal, A., Granton, B., Havenith, M., Opas, M., and Gotlieb, A. I. Characterization of Cobblestone mitral valve interstitial cells. *Arch. Pathol. Lab Med.* **115**:774-779, 1991.

44. Roy, A., Brand, N. J., and Yacoub, M. H. Molecular characterization of interstitial cells isolated from human heart valves. *J. Heart Valve Dis.* **9**:459-464, 2000.

45. Chester, A. H., Misfeld, M., and Yacoub, M. H. Receptor-mediated contraction of aortic valve leaflets. *J. Heart Valve Dis.* **9**:250-254, 2000.

46. Chester, A. H., Misfeld, M., Sievers, H. H., and Yacoub, M. H. Influence of 5-hydroxytryptamine on aortic valve competence in vitro. *J. Heart Valve Dis.* **10**:822-825, 2001.

47. Misfeld, M., Morrison, K., Sievers, H., Yacoub, M. H., and Chester, A. H. Localization of immunoreactive endothelin and characterization of its receptors in aortic cusps. *J. Heart Valve Dis.* **11**:472-476, 2002.

48. Harrison, D. G., Sayegh, H., Ohara, Y., Inoue, N., and Venema, R. C. Regulation of expression of the endothelial cell nitric oxide synthase. *Clin. Exp. Pharmacol. Physiol* **23**:251-255, 1996.

49. Brown, G. C. Nitric oxide as a competitive inhibitor of oxygen consumption in the mitochondrial respiratory chain. *Acta Physiol Scand.* **168**:667-674, 2000.

50. Ignarro, L. J. Endothelium-derived nitric oxide: actions and properties. *FASEB J.* **3**:31-36, 1989.

51. Bochaton-Piallat, M. L., Gabbiani, F., Redard, M., Desmouliere, A., and Gabbiani, G. Apoptosis participates in cellularity regulation during rat aortic intimal thickening. *Am. J. Pathol.* **146**:1059-1064, 1995.

52. Hill, A. D. and Folan-Curran, J. Microappendages on the atrioventricular valves of the guinea pig. *J. Anat.* **182 (Pt 3)**:425-428, 1993.

53. Mulholland, M. S. and Gotlieb, M. C. F. A. Cardiac Valve Interstitial Cells: Regulator of Valve Structure and Function. *Cardiovascular. Pathology* **6**:167-174, 1997.

54. Butcher, J. T. and Nerem, R. M. Valvular endothelial cells regulate the phenotype of interstitial cells in co-culture: effects of steady shear stress. *Tissue Eng* **12**:905-915, 2006.

55. Rabkin, E., Aikawa, M., Stone, J. R., Fukumoto, Y., Libby, P., and Schoen, F. J. Activated interstitial myofibroblasts express catabolic enzymes and mediate matrix remodeling in myxomatous heart valves. *Circulation* **104**:2525-2532, 2001.

56. Gotlieb, A. I., Rosenthal, A., and Kazemian, P. Fibroblast growth factor 2 regulation of mitral valve interstitial cell repair in vitro. *J. Thorac. Cardiovasc. Surg.* **124**:591-597, 2002.

57. Bogdan, C. Nitric oxide and the regulation of gene expression. *Trends Cell Biol.* **11**:66-75, 2001.

58. Jian, B., Narula, N., Li, Q. Y., Mohler, E. R., III, and Levy, R. J. Progression of aortic valve stenosis: TGF-beta1 is present in calcified aortic valve cusps and promotes aortic valve interstitial cell calcification via apoptosis. *Ann Thorac. Surg.* **75**:457-465, 2003.

59. Ng, C. M., Cheng, A., Myers, L. A., Martinez-Murillo, F., Jie, C., Bedja, D., Gabrielson, K. L., Hausladen, J. M., Mecham, R. P., Judge, D. P., and Dietz, H. C. TGF-beta-dependent pathogenesis of mitral valve prolapse in a mouse model of Marfan syndrome. *J. Clin. Invest* **114**:1586-1592, 2004.

60. Ziegler, T., Silacci, P., Harrison, V. J., and Hayoz, D. Nitric oxide synthase expression in endothelial cells exposed to mechanical forces. *Hypertension* **32**:351-355, 1998.

61. Moesgaard, S. G., Olsen, L. H., Aasted, B., Viuff, B. M., Pedersen, L. G., Pedersen, H. D., and Harrison, A. P. Direct measurements of nitric oxide release in relation to expression of endothelial nitric oxide synthase in isolated porcine mitral valves. *J. Vet. Med. A Physiol Pathol. Clin. Med.* **54**:156-160, 2007.

62. Durbin, A., Nadir, N. A., Rosenthal, A., and Gotlieb, A. I. Nitric oxide promotes in vitro interstitial cell heart valve repair. *Cardiovasc. Pathol.* **14**:12-18, 2005.

63. Rabkin-Aikawa, E., Farber, M., Aikawa, M., and Schoen, F. J. Dynamic and reversible changes of interstitial cell phenotype during remodeling of cardiac valves. *J. Heart Valve Dis.* **13**:841-847, 2004.

64. Gnyaneshwar, R., Kumar, R. K., and Balakrishnan, K. R. Dynamic analysis of the aortic valve using a finite element model. *Ann Thorac. Surg.* **73**:1122-1129, 2002.

65. Thubrikar, M., Harry, R., and Nolan, S. P. Normal aortic valve function in dogs. *Am. J Cardiol.* **40**:563-568, 1977.

66. Mihaljevic, T., Paul, S., Cohn, L. H., and Wechsler, A. Pathophysiology of Aortic Valve Disease. In L. H. Cohn and L. H. Edmunds Jr (Eds.), *Cardiac Surgery in the Adult.* New York: McGraw Hill, 2003. Pp. 791-810.

67. Wells, F. C. and Crowe, T. Leonardo da Vinci as a paradigm for modern clinical research. *J Thorac. Cardiovasc. Surg.* **127**:929-944, 2004.

68. Mercer, J. L. The movements of the dog's aortic valve studied by high speed cineangiography. *Br. J Radiol.* **46**:344-349, 1973.

69. Stewart, B. F., Siscovick, D., Lind, B. K., Gardin, J. M., Gottdiener, J. S., Smith, V. E., Kitzman, D. W., and Otto, C. M. Clinical factors associated with calcific aortic valve disease. Cardiovascular Health Study. *J Am. Coll. Cardiol.* **29**:630-634, 1997.

70. Mohler III, E. R. Are atherosclerotic processes involved in aortic-valve calcification? *The Lancet* **356**:524-525, 2000.

71. Bonow, R. O., Carabello, B. A., Chatterjee, K., de, L. A., Jr., Faxon, D. P., Freed, M. D., Gaasch, W. H., Lytle, B. W., Nishimura, R. A., O'Gara, P. T., O'Rourke, R. A., Otto, C. M., Shah, P. M., Shanewise, J. S., Smith, S. C., Jr., Jacobs, A. K., Adams, C. D., Anderson, J. L., Antman, E. M., Fuster, V., Halperin, J. L., Hiratzka, L. F., Hunt, S. A., Lytle, B. W., Nishimura, R., Page, R. L., and Riegel, B. ACC/AHA 2006 guidelines for the management of patients with valvular heart disease: a report of the American College of Cardiology/American Heart Association Task Force on Practice Guidelines (writing Committee to Revise the 1998 guidelines for the management of patients with valvular heart disease) developed in collaboration with the Society of Cardiovascular Anesthesiologists endorsed by the Society for Cardiovascular Angiography and Interventions and the Society of Thoracic Surgeons. *J Am. Coll. Cardiol.* **48**:e1-148, 2006.

72. Young, T. An essay on the cohesion of fluids. *Phil. Trans. R. Soc.* **95**:65-87, 1805.

73. De Leplace, P. S. *"Sure l'Action Capillarie." Supplement to Book 10, "Traite de Mecanique Celeste".* Paris: Coureier, 1806.

74. Hufnagel, C. A. Aortic plastic valvular prosthesis. *Bull. Georgetown. Univ. Med. Ctr.* **4**:128, 1951.

75. HCIA Inc.and Ernst & Young LLP *The DRG Handbook: Comparative Clinical and Financial Benchmarks*. New York: 1999.

76. Vongpatanasin, W., Hillis, L. D., and Lange, R. A. Prosthetic heart valves. *N. Engl. J Med.* **335**:407-416, 1996.

77. Butany, J., Ahluwalia, M. S., Munroe, C., Fayet, C., Ahn, C., Blit, P., Kepron, C., Cusimano, R. J., and Leask, R. L. Mechanical heart valve prostheses: identification and evaluation. *Cardiovasc. Pathol.* **12**:1-22, 2003.

78. Schoen, F. J. and Levy, R. J. Pathology of substitute heart valves: new concepts and developments. *J Card Surg.* **9**:222-227, 1994.

79. Birkmeyer, J. D., Marrin, C. A., and O'Connor, G. T. Should patients with Bjork-Shiley valves undergo prophylactic replacement? *Lancet* **340**:520-523, 1992.

80. Desai, N. D. and Christakis, G. T. Stented mechanical/bioprosthetic aortic valve replacement. In L. H. Cohn and L. H. Edmunds Jr (Eds.), *Cardiac Surgery in the Adult*. New York: McGraw-Hill, 2003. Pp. 825-855.

81. Cannegieter, S. C., Rosendaal, F. R., and Briet, E. Thromboembolic and bleeding complications in patients with mechanical heart valve prostheses. *Circulation* **89**:635-641, 1994.

82. Butany, J., Fayet, C., Ahluwalia, M. S., Blit, P., Ahn, C., Munroe, C., Israel, N., Cusimano, R. J., and Leask, R. L. Biological replacement heart valves. Identification and evaluation. *Cardiovasc. Pathol.* **12**:119-139, 2003.

83. McGiffin, D. C., O'Brien, M. F., Stafford, E. G., Gardner, M. A., and Pohlner, P. G. Long-term results of the viable cryopreserved allograft aortic valve: continuing evidence for superior valve durability. *J Card Surg.* **3**:289-296, 1988.

84. O'Brien, M. F., Stafford, E. G., Gardner, M. A., Pohlner, P. G., and McGiffin, D. C. A comparison of aortic valve replacement with viable cryopreserved and fresh allograft valves, with a note on chromosomal studies. *J Thorac. Cardiovasc. Surg.* **94**:812-823, 1987.

85. O'Brien, M. F., Harrocks, S., Stafford, E. G., Gardner, M. A., Pohlner, P. G., Tesar, P. J., and Stephens, F. The homograft aortic valve: a 29-year, 99.3% follow up of 1,022 valve replacements. *J Heart Valve Dis.* **10**:334-344, 2001.

86. Sadowski, J., Kapelak, B., Bartus, K., Podolec, P., Rudzinski, P., Myrdko, T., Wierzbicki, K., and Dziatkowiak, A. Reoperation after fresh homograft replacement: 23 years' experience with 655 patients. *Eur. J Cardiothorac. Surg.* **23**:996-1000, 2003.

87. Yankah, A. C., Alexi-Meskhishvili, V., Weng, Y., Schorn, K., Lange, P. E., and Hetzer, R. Accelerated degeneration of allografts in the first two years of life. *Ann. Thorac. Surg.* **60**:S71-S76, 1995.

88. Jashari, R., Van Hoeck, B., Tabaku, M., and Vanderkelen, A. Banking of the human heart valves and the arteries at the European homograft bank (EHB)--overview of a 14-year activity in this International Association in Brussels. *Cell Tissue Bank.* **5**:239-251, 2004.

89. O'Brien, M. F., Stafford, E. G., Gardner, M. A., Pohlner, P. G., and McGiffin, D. C. A comparison of aortic valve replacement with viable cryopreserved and fresh allograft valves, with a note on chromosomal studies. *J. Thorac. Cardiovasc. Surg.* **94**:812-823, 1987.

90. Schenke-Layland, K., Madershahian, N., Riemann, I., Starcher, B., Halbhuber, K. J., Konig, K., and Stock, U. A. Impact of cryopreservation on extracellular matrix structures of heart valve leaflets. *Ann. Thorac. Surg.* **81**:918-926, 2006.

91. Ketheesan, N., Kearney, J. N., and Ingham, E. The effect of cryopreservation on the immunogenicity of allogeneic cardiac valves. *Cryobiology* **33**:41-53, 1996.

92. Brockbank, K. G., Lightfoot, F. G., Song, Y. C., and Taylor, M. J. Interstitial ice formation in cryopreserved homografts: a possible cause of tissue deterioration and calcification in vivo. *J. Heart Valve Dis.* **9**:200-206, 2000.

93. Kauzmann, W. The Nature of the Glassy State and the Behavior of Liquids at Low Temperatures. *Chem. Rev.* **43**:219-256, 1948.

94. Brockbank, K. G. and Song, Y. C. Morphological analyses of ice-free and frozen cryopreserved heart valve explants. *J. Heart Valve Dis.* **13**:297-301, 2004.

95. Brockbank, K. G. and McNally, R. T. Developoments on Tissue Transplantation. In H. F. Kauffman (Ed.), *Pediatric Brain Death and Organ Retrieval.* New York: Plenum Press, 1988.

96. Hopkins, R. Resolution of the Conflicting Theories of Prolonged Cell Viability. 2005. Pp. 184-189.

97. Simon, A., Wilhelmi, M., Steinhoff, G., Harringer, W., Brucke, P., and Haverich, A. Cardiac valve endothelial cells: relevance in the long-term function of biologic valve prostheses. *J Thorac. Cardiovasc. Surg.* **116**:609-616, 1998.

98. Simon, A., Zavazava, N., Sievers, H. H., and Muller-Ruchholtz, W. In vitro cultivation and immunogenicity of human cardiac valve endothelium. *J Card Surg.* **8**:656-665, 1993.

99. Farivar, R. S., Filsoufi, F., and Adams, D. H. Mechanisms of Gal(alpha)1-3Gal(beta)1-4GlcNAc-R (alphaGal) expression on porcine valve endothelial cells. *J Thorac. Cardiovasc. Surg.* **125**:306-314, 2003.

100. Cochran, R. P. and Kunzelman, K. S. Cryopreservation does not alter antigenic expression of aortic allografts. *J Surg. Res.* **46**:597-599, 1989.

101. el Khatib, H. and Lupinetti, F. M. Antigenicity of fresh and cryopreserved rat valve allografts. *Transplantation* **49**:765-767, 1990.

102. Zhao, X. M., Green, M., Frazer, I. H., Hogan, P., and O'Brien, M. F. Donor-specific immune response after aortic valve allografting in the rat. *Ann Thorac. Surg.* **57**:1158-1163, 1994.

103. Smith, J. D., Ogino, H., Hunt, D., Laylor, R. M., Rose, M. L., and Yacoub, M. H. Humoral immune response to human aortic valve homografts. *Ann Thorac. Surg.* **60**:S127-S130, 1995.

104. Lupinetti, F. M., Christy, J. P., King, D. M., el Khatib, H., and Thompson, S. A. Immunogenicity, antigenicity, and endothelial viability of aortic

valves preserved at 4 degrees C in a nutrient medium. *J Card Surg.* **6**:454-461, 1991.

105. Meyer, S. R., Campbell, P. M., Rutledge, J. M., Halpin, A. M., Hawkins, L. E., Lakey, J. R., Rebeyka, I. M., and Ross, D. B. Use of an allograft patch in repair of hypoplastic left heart syndrome may complicate future transplantation. *Eur. J Cardiothorac. Surg* **27**:554-560, 2005.

106. Hawkins, J. A., Breinholt, J. P., Lambert, L. M., Fuller, T. C., Profaizer, T., McGough, E. C., and Shaddy, R. E. Class I and class II anti-HLA antibodies after implantation of cryopreserved allograft material in pediatric patients. *J. Thorac. Cardiovasc. Surg.* **119**:324-330, 2000.

107. Shaddy, R. E., Hunter, D. D., Osborn, K. A., Lambert, L. M., Minich, L. L., Hawkins, J. A., McGough, E. C., and Fuller, T. C. Prospective analysis of HLA immunogenicity of cryopreserved valved allografts used in pediatric heart surgery. *Circulation* **94**:1063-1067, 1996.

108. Dignan, R., O'Brien, M., Hogan, P., Passage, J., Stephens, F., Thornton, A., and Harrocks, S. Influence of HLA matching and associated factors on aortic valve homograft function. *J Heart Valve Dis.* **9**:504-511, 2000.

109. Dignan, R., O'Brien, M., Hogan, P., Thornton, A., Fowler, K., Byrne, D., Stephens, F., and Harrocks, S. Aortic valve allograft structural

deterioration is associated with a subset of antibodies to human leukocyte antigens. *J. Heart Valve Dis.* **12**:382-390, 2003.

110. Welters, M. J., Oei, F. B., Witvliet, M. D., Vaessen, L. M., Cromme-Dijkhuis, A. H., Bogers, A. J., Weimar, W., and Claas, F. H. A broad and strong humoral immune response to donor HLA after implantation of cryopreserved human heart valve allografts. *Hum. Immunol.* **63**:1019-1025, 2002.

111. Smith, J. D., Danskine, A. J., Laylor, R. M., Rose, M. L., and Yacoub, M. H. The effect of panel reactive antibodies and the donor specific crossmatch on graft survival after heart and heart-lung transplantation. *Transpl. Immunol.* **1**:60-65, 1993.

112. Lavee, J., Kormos, R. L., Duquesnoy, R. J., Zerbe, T. R., Armitage, J. M., Vanek, M., Hardesty, R. L., and Griffith, B. P. Influence of panel-reactive antibody and lymphocytotoxic crossmatch on survival after heart transplantation. *J Heart Lung Transplant.* **10**:921-929, 1991.

113. Loh, E., Bergin, J. D., Couper, G. S., and Mudge, G. H., Jr. Role of panel-reactive antibody cross-reactivity in predicting survival after orthotopic heart transplantation. *J Heart Lung Transplant.* **13**:194-201, 1994.

114. Hoekstra, F., Knoop, C., Jutte, N., Wassenaar, C., Mochtar, B., Bos, E., and Weimar, W. Effect of cryopreservation and HLA-DR matching on the cellular immunogenicity of human cardiac valve allografts. *J Heart Lung Transplant.* **13**:1095-1098, 1994.

115. Kumper, A., Kumper, C., Kraatz, E. G., Wottge, H. U., Dreyer, W., Yankah, A. C., and Bernhard, A. Assessment of different preservation and storage conditions on aortic valves: introduction of a quantitative measuring method of the integrity of endothelial cells. *Thorac. Cardiovasc. Surg.* **37**:294-298, 1989.

116. Baskett, R. J., Ross, D. B., Nanton, M. A., and Murphy, D. A. Factors in the early failure of cryopreserved homograft pulmonary valves in children: preserved immunogenicity? *J. Thorac. Cardiovasc. Surg.* **112**:1170-1178, 1996.

117. Legare, J. F., Lee, T. D., Creaser, K., and Ross, D. B. T lymphocytes mediate leaflet destruction and allograft aortic valve failure in rats. *Ann Thorac. Surg.* **70**:1238-1245, 2000.

118. Welters, M. J., Oei, F. B., Vaessen, L. M., Stegmann, A. P., Bogers, A. J., and Weimar, W. Increased numbers of circulating donor-specific T helper lymphocytes after human heart valve transplantation. *Clin. Exp. Immunol.* **124**:353-358, 2001.

119. Oei, F. B., Welters, M. J., Knoop, C. J., Vaessen, L. M., Stegmann, A. P., Weimar, W., and Bogers, A. J. Circulating donor-specific cytotoxic T lymphocytes with high avidity for donor human leukocyte antigens in pediatric and adult cardiac allograft valved conduit recipients. *Eur. J Cardiothorac. Surg.* **18**:466-472, 2000.

120. O'Brien, M. F., Johnston, N., Stafford, G., Gardner, M., Pohlner, P., McGiffin, D., Brosnan, A., and Duffy, P. A study of the cells in the explanted viable cryopreserved allograft valve. *J Card Surg.* **3**:279-287, 1988.

121. Yacoub, M. H., Suitters, A., Khaghani, A., and Rose, M. L. Localization of major histocompatibility complex (HLA, ABC, and DR) antigens in aortic homografts. In E. Bodnar and M. H. Yacoub (Eds.), *Biologic Bioprosthetic Valves: Proceeding of the III International Symposium.* New York: Yorke Medical Books, 1986. Pp. 65-72.

122. Rabkin-Aikawa, E., Aikawa, M., Farber, M., Kratz, J. R., Garcia-Cardena, G., Kouchoukos, N. T., Mitchell, M. B., Jonas, R. A., and Schoen, F. J. Clinical pulmonary autograft valves: pathologic evidence of adaptive remodeling in the aortic site. *J. Thorac. Cardiovasc. Surg.* **128**:552-561, 2004.

123. Bernstein, D., Kolla, S., Miner, M., Pitlick, P., Griffin, M., Starnes, V., Rowan, R., Billingham, M., and Baum, D. Cardiac growth after pediatric heart transplantation. *Circulation* **85**:1433-1439, 1992.

124. Valente, M., Faggian, G., Billingham, M. E., Talenti, E., Calabrese, F., Casula, R., Shumway, N. E., and Thiene, G. The aortic valve after heart transplantation. *Ann Thorac. Surg.* **60**:S135-S140, 1995.

125. Mitchell, R. N., Jonas, R. A., and Schoen, F. J. Pathology of explanted cryopreserved allograft heart valves: comparison with aortic valves from orthotopic heart transplants. *J Thorac. Cardiovasc. Surg.* **115**:118-127, 1998.

126. Yankah, A. C., Wottge, H. U., and Muller-Ruchholtz, W. Short-course cyclosporin A therapy for definite allograft valve survival immunosuppression in allograft valve operations. *Ann Thorac. Surg.* **60**:S146-S150, 1995.

127. Shaddy, R. E., Fuller, T. C., Anderson, J. B., Lambert, L. M., Brinkman, M. K., Profaizer, T., and Hawkins, J. A. Mycophenolic mofetil reduces the HLA antibody response of children to valved allograft implantation. *Ann Thorac. Surg.* **77**:1734-1739, 2004.

128. Legare, J. F., Ross, D. B., Issekutz, T. B., Ruigrok, W., Creaser, K., Hirsch, G. M., and Lee, T. D. Prevention of allograft heart valve failure in a rat model. *J Thorac. Cardiovasc. Surg.* **122**:310-317, 2001.

129. Billingham, R. E., Brent, L., and Medawar, P. B. Actively acquired tolerance to foreign cells. *Nature* **172**:603-606, 1953.

130. Koch, C. A., Khalpey, Z. I., and Platt, J. L. Accommodation: preventing injury in transplantation and disease. *J Immunol.* **172**:5143-5148, 2004.

131. Kazatchkine, M. D. and Kaveri, S. V. Immunomodulation of autoimmune and inflammatory diseases with intravenous immune globulin. *N. Engl. J Med.* **345**:747-755, 2001.

132. Jordan, S., Cunningham-Rundles, C., and McEwan, R. Utility of intravenous immune globulin in kidney transplantation: efficacy, safety, and cost implications. *Am. J Transplant.* **3**:653-664, 2003.

133. John, R., Lietz, K., Burke, E., Ankersmit, J., Mancini, D., Suciu-Foca, N., Edwards, N., Rose, E., Oz, M., and Itescu, S. Intravenous immunoglobulin reduces anti-HLA alloreactivity and shortens waiting time to cardiac transplantation in highly sensitized left ventricular assist device recipients. *Circulation* **100**:II229-II235, 1999.

134. Meyer, S. R. Immunology of decellularized allograft tissue used in congenital cardiac surgery. 146-176. 2005. The University of Alberta.

135. Li, Y., McCormack, A. M., Brand, N. J., and Yacoub, M. H. A strategy for inducing immune tolerance to valve endothelial cells through gene transfer. *J. Heart Valve Dis.* **9**:439-444, 2000.

136. Vincenzo, B. Uber die antineoplastische Immunitat. *Journal of Cancer Research and Clinical Oncology* **40**:122-140, 1934.

137. Fuchs, J. R., Nasseri, B. A., and Vacanti, J. P. Tissue engineering: a 21st century solution to surgical reconstruction. *Ann Thorac. Surg.* **72**:577-591, 2001.

138. Viola, J, Lal, B, and Grad, O. The Emergence of Tissue Engineering as a Research Field. 10-14-2003. The National Science Foundation.

139. Vesely, I. Heart valve tissue engineering. *Circ Res* **97**:743-755, 2005.

140. Courtman, D. W., Errett, B. F., and Wilson, G. J. The role of crosslinking in modification of the immune response elicited against xenogenic vascular acellular matrices. *Journal of Biomedical Materials Research* **55**:576-586, 2001.

141. Manji, R. A., Zhu, L. F., Nijjar, N. K., Rayner, D. C., Korbutt, G. S., Churchill, T. A., Rajotte, R. V., Koshal, A., and Ross, D. B. Glutaraldehyde-fixed bioprosthetic heart valve conduits calcify and fail from xenograft rejection. *Circulation* **114**:318-327, 2006.

142. Ide, C., Tohyama, K., Tajima, K., Endoh, K., Sano, K., Tamura, M., Mizoguchi, A., Kitada, M., Morihara, T., and Shirasu, M. Long acellular nerve transplants for allogeneic grafting and the effects of basic fibroblast growth factor on the growth of regenerating axons in dogs: a preliminary report. *Exp. Neurol.* **154**:99-112, 1998.

143. Hiles, R. W. Freeze dried irradiated nerve homograft: a preliminary report. *Hand* **4**:79-84, 1972.

144. Gulati, A. K. and Cole, G. P. Immunogenicity and regenerative potential of acellular nerve allografts to repair peripheral nerve in rats and rabbits. *Acta Neurochir. (Wien.)* **126**:158-164, 1994.

145. Hudson, T. W., Liu, S. Y., and Schmidt, C. E. Engineering an improved acellular nerve graft via optimized chemical processing. *Tissue Eng* **10**:1346-1358, 2004.

146. Marmor, L. The repair of peripheral nerves by irradiated homografts. *Clin. Orthop. Relat Res.* **34**:161-169, 1964.

147. Chambers, J. C., Somerville, J., Stone, S., and Ross, D. N. Pulmonary Autograft Procedure for Aortic Valve Disease : Long-term Results of the Pioneer Series. *Circulation* **96**:2206-2214, 1997.

148. Osawa, T., Tohyama, K., and Ide, C. Allogeneic nerve grafts in the rat, with special reference to the role of Schwann cell basal laminae in nerve regeneration. *J. Neurocytol.* **19**:833-849, 1990.

149. Steinhoff, G., Stock, U., Karim, N., Mertsching, H., Timke, A., Meliss, R. R., Pethig, K., Haverich, A., and Bader, A. Tissue engineering of pulmonary heart valves on allogenic acellular matrix conduits: in vivo restoration of valve tissue. *Circulation* **102**:III50-III55, 2000.

150. Meyer, S. R., Chiu, B., Churchill, T. A., Zhu, L., Lakey, J. R., and Ross, D. B. Comparison of aortic valve allograft decellularization techniques in the rat. *J. Biomed. Mater. Res. A* **79**:254-262, 2006.

151. Dohmen, P. M., da Costa, F., Holinski, S., Lopes, S. V., Yoshi, S., Reichert, L. H., Villani, R., Posner, S., and Konertz, W. Is there a possibility for a glutaraldehyde-free porcine heart valve to grow? *Eur. Surg. Res.* **38**:54-61, 2006.

152. Booth, C., Korossis, S. A., Wilcox, H. E., Watterson, K. G., Kearney, J. N., Fisher, J., and Ingham, E. Tissue engineering of cardiac valve

prostheses I: development and histological characterization of an acellular porcine scaffold. *J. Heart Valve Dis.* **11**:457-462, 2002.

153. Kasimir, M. T., Rieder, E., Seebacher, G., Silberhumer, G., Wolner, E., Weigel, G., and Simon, P. Comparison of different decellularization procedures of porcine heart valves. *Int. J. Artif. Organs* **26**:421-427, 2003.

154. Patience, C., Scobie, L., and Quinn, G. Porcine endogenous retrovirus--advances, issues and solutions. *Xenotransplantation.* **9**:373-375, 2002.

155. Mendelson, K. and Schoen, F. J. Heart valve tissue engineering: concepts, approaches, progress, and challenges. *Ann Biomed. Eng* **34**:1799-1819, 2006.

156. Grayson, A. C., Voskerician, G., Lynn, A., Anderson, J. M., Cima, M. J., and Langer, R. Differential degradation rates in vivo and in vitro of biocompatible poly(lactic acid) and poly(glycolic acid) homo- and co-polymers for a polymeric drug-delivery microchip. *J. Biomater. Sci. Polym. Ed* **15**:1281-1304, 2004.

157. Kohn, J., Abramson, S., and Langer, R. Bioresorbable and bioerodible materials. In B. D. Ratner, A. S. Hoffman, F. J. Schoen, and J. E. Lemons (Eds.), *Biomaterials Science: An Introduction to Materials in Medicine.* Orlando: Academic Press, 2004.

158. Sodian, R., Sperling, J. S., Martin, D. P., Egozy, A., Stock, U., Mayer, J. E., Jr., and Vacanti, J. P. Fabrication of a trileaflet heart valve scaffold from a polyhydroxyalkanoate biopolyester for use in tissue engineering. *Tissue Eng* **6**:183-188, 2000.

159. Lutolf, M. P. and Hubbell, J. A. Synthetic biomaterials as instructive extracellular microenvironments for morphogenesis in tissue engineering. *Nat. Biotechnol.* **23**:47-55, 2005.

160. Mann, B. K., Gobin, A. S., Tsai, A. T., Schmedlen, R. H., and West, J. L. Smooth muscle cell growth in photopolymerized hydrogels with cell adhesive and proteolytically degradable domains: synthetic ECM analogs for tissue engineering. *Biomaterials* **22**:3045-3051, 2001.

161. Pratt, A. B., Weber, F. E., Schmoekel, H. G., Muller, R., and Hubbell, J. A. Synthetic extracellular matrices for in situ tissue engineering. *Biotechnol. Bioeng.* **86**:27-36, 2004.

162. Lendlein, A. and Langer, R. Biodegradable, elastic shape-memory polymers for potential biomedical applications. *Science* **296**:1673-1676, 2002.

163. Lahann, J., Mitragotri, S., Tran, T. N., Kaido, H., Sundaram, J., Choi, I. S., Hoffer, S., Somorjai, G. A., and Langer, R. A reversibly switching surface. *Science* **299**:371-374, 2003.

164. Anderson, D. G., Burdick, J. A., and Langer, R. Materials science. Smart biomaterials. *Science* **305**:1923-1924, 2004.

165. Langer, R. and Tirrell, D. A. Designing materials for biology and medicine. *Nature* **428**:487-492, 2004.

166. Stock, U. A., Nagashima, M., Khalil, P. N., Nollert, G. D., Herden, T., Sperling, J. S., Moran, A., Lien, J., Martin, D. P., Schoen, F. J., Vacanti, J. P., and Mayer, J. E., Jr. Tissue-engineered valved conduits in the pulmonary circulation. *J. Thorac. Cardiovasc. Surg.* **119**:732-740, 2000.

167. Kim, B. S. and Mooney, D. J. Development of biocompatible synthetic extracellular matrices for tissue engineering. *Trends Biotechnol.* **16**:224-230, 1998.

168. Kuwaki, K., Tseng, Y. L., Dor, F. J., Shimizu, A., Houser, S. L., Sanderson, T. M., Lancos, C. J., Prabharasuth, D. D., Cheng, J., Moran, K., Hisashi, Y., Mueller, N., Yamada, K., Greenstein, J. L., Hawley, R. J., Patience, C., Awwad, M., Fishman, J. A., Robson, S. C., Schuurman, H. J., Sachs, D. H., and Cooper, D. K. Heart transplantation in baboons using

alpha1,3-galactosyltransferase gene-knockout pigs as donors: initial experience. *Nat. Med.* **11**:29-31, 2005.

169. Fodor, W. L., Williams, B. L., Matis, L. A., Madri, J. A., Rollins, S. A., Knight, J. W., Velander, W., and Squinto, S. P. Expression of a functional human complement inhibitor in a transgenic pig as a model for the prevention of xenogeneic hyperacute organ rejection. *Proc. Natl. Acad. Sci. U. S. A* **91**:11153-11157, 1994.

170. Shinoka, T., Breuer, C. K., Tanel, R. E., Zund, G., Miura, T., Ma, P. X., Langer, R., Vacanti, J. P., and Mayer, J. E., Jr. Tissue engineering heart valves: valve leaflet replacement study in a lamb model. *Ann Thorac. Surg.* **60**:S513-S516, 1995.

171. Breuer, C. K., Shin'oka, T., Tanel, R. E., Zund, G., Mooney, D. J., Ma, P. X., Miura, T., Colan, S., Langer, R., Mayer, J. E., and Vacanti, J. P. Tissue engineering lamb heart valve leaflets. *Biotechnology and Bioengineering* **50**:562-567, 1996.

172. Johnston, D. E., Boughner, D. R., Cimini, M., and Rogers, K. A. Radial artery as an autologous cell source for valvular tissue engineering efforts. *J Biomed. Mater. Res. A* **78**:383-393, 2006.

173. Ye, Q., nd, G., Jockenhoevel, S., Hoerstrup, S. P., Schoeberlein, A., Grunenfelder, J., and Turina, M. Tissue engineering in cardiovascular surgery: New approach to develop completely human autologous tissue. *European Journal of Cardio-Thoracic Surgery* **17**:449-454, 2000.

174. Shin'oka, T., Imai, Y., and Ikada, Y. Transplantation of a tissue-engineered pulmonary artery. *N. Engl. J Med.* **344**:532-533, 2001.

175. Zund, G., Breuer, C. K., Shinoka, T., Ma, P. X., Langer, R., Mayer, J. E., and Vacanti, J. P. The in vitro construction of a tissue engineered bioprosthetic heart valve. *Eur. J Cardiothorac. Surg.* **11**:493-497, 1997.

176. Zund, G., Hoerstrup, S. P., Schoeberlein, A., Lachat, M., Uhlschmid, G., Vogt, P. R., and Turina, M. Tissue engineering: a new approach in cardiovascular surgery: Seeding of human fibroblasts followed by human endothelial cells on resorbable mesh. *Eur. J Cardiothorac. Surg.* **13**:160-164, 1998.

177. Kadner, A., Hoerstrup, S. P., Tracy, J., Breymann, C., Maurus, C. F., Melnitchouk, S., Kadner, G., Zund, G., and Turina, M. Human umbilical cord cells: a new cell source for cardiovascular tissue engineering. *Ann Thorac. Surg.* **74**:S1422-S1428, 2002.

178. Watanabe, M., Shin'oka, T., Tohyama, S., Hibino, N., Konuma, T., Matsumura, G., Kosaka, Y., Ishida, T., Imai, Y., Yamakawa, M., Ikada, Y., and Morita, S. Tissue-engineered vascular autograft: inferior vena cava replacement in a dog model. *Tissue Eng* **7**:429-439, 2001.

179. Matsumura, G., Miyagawa-Tomita, S., Shin'oka, T., Ikada, Y., and Kurosawa, H. First evidence that bone marrow cells contribute to the construction of tissue-engineered vascular autografts in vivo. *Circulation* **108**:1729-1734, 2003.

180. Hibino, N., Shin'oka, T., Matsumura, G., Ikada, Y., and Kurosawa, H. The tissue-engineered vascular graft using bone marrow without culture. *J. Thorac. Cardiovasc. Surg.* **129**:1064-1070, 2005.

181. Asahara, T., Murohara, T., Sullivan, A., Silver, M., van der, Z. R., Li, T., Witzenbichler, B., Schatteman, G., and Isner, J. M. Isolation of putative progenitor endothelial cells for angiogenesis. *Science* **275**:964-967, 1997.

182. Shi, Q., Rafii, S., Wu, M. H., Wijelath, E. S., Yu, C., Ishida, A., Fujita, Y., Kothari, S., Mohle, R., Sauvage, L. R., Moore, M. A., Storb, R. F., and Hammond, W. P. Evidence for circulating bone marrow-derived endothelial cells. *Blood* **92**:362-367, 1998.

183. Handgretinger, R., Gordon, P. R., Leimig, T., Chen, X., Buhring, H. J., Niethammer, D., and Kuci, S. Biology and plasticity of CD133+ hematopoietic stem cells. *Ann N. Y. Acad. Sci.* **996**:141-151, 2003.

184. Urbich, C. and Dimmeler, S. Endothelial progenitor cells: characterization and role in vascular biology. *Circ. Res.* **95**:343-353, 2004.

185. Shin, H., Temenoff, J. S., Bowden, G. C., Zygourakis, K., Farach-Carson, M. C., Yaszemski, M. J., and Mikos, A. G. Osteogenic differentiation of rat bone marrow stromal cells cultured on Arg-Gly-Asp modified hydrogels without dexamethasone and beta-glycerol phosphate. *Biomaterials* **26**:3645-3654, 2005.

186. Betre, H., Ong, S. R., Guilak, F., Chilkoti, A., Fermor, B., and Setton, L. A. Chondrocytic differentiation of human adipose-derived adult stem cells in elastin-like polypeptide. *Biomaterials* **27**:91-99, 2006.

187. Patel, P. N., Gobin, A. S., West, J. L., and Patrick, C. W., Jr. Poly(ethylene glycol) hydrogel system supports preadipocyte viability, adhesion, and proliferation. *Tissue Eng* **11**:1498-1505, 2005.

188. Wu, X., Rabkin-Aikawa, E., Guleserian, K. J., Perry, T. E., Masuda, Y., Sutherland, F. W., Schoen, F. J., Mayer, J. E., Jr., and Bischoff, J. Tissue-engineered microvessels on three-dimensional biodegradable scaffolds

using human endothelial progenitor cells. *Am. J. Physiol Heart Circ. Physiol* **287**:H480-H487, 2004.

189. Orlic, D., Kajstura, J., Chimenti, S., Limana, F., Jakoniuk, I., Quaini, F., Nadal-Ginard, B., Bodine, D. M., Leri, A., and Anversa, P. Mobilized bone marrow cells repair the infarcted heart, improving function and survival. *Proc. Natl. Acad. Sci. U. S. A* **98**:10344-10349, 2001.

190. Zhang, L., Hum, M., Wang, M., Li, Y., Chen, H., Chu, C., and Jiang, H. Evaluation of modifying collagen matrix with RGD peptide through periodate oxidation. *J. Biomed. Mater. Res. A* **73**:468-475, 2005.

191. Sarugaser, R., Lickorish, D., Baksh, D., Hosseini, M. M., and Davies, J. E. Human umbilical cord perivascular (HUCPV) cells: a source of mesenchymal progenitors. *Stem Cells* **23**:220-229, 2005.

192. Kohl, T., Szabo, Z., Suda, K., Petrossian, E., Ko, E., Kececioglu, D., Moore, P., Silverman, N. H., Harrison, M. R., Chou, T. M., and Hanley, F. L. Fetoscopic and open transumbilical fetal cardiac catheterization in sheep. Potential approaches for human fetal cardiac intervention. *Circulation* **95**:1048-1053, 1997.

193. Chiu, B., Wan, J. Z., Abley, D., and Akabutu, J. Induction of vascular endothelial phenotype and cellular proliferation from human cord blood

stem cells cultured in simulated microgravity. *Acta Astronaut.* **56**:918-922, 2005.

194. Chiu, B. and Akabutu, J. Cord Blood Transplantation (CBT) For The Treatment of Malignant and Non-malignant Diseases - A Review. *Accepted for publication, in Proceedings of the Fourth Asia-Pacific International Academy of Pathology 2005, Monduzzi Editore International Proceedings. Indexed in Current Contents of ISI, Philadelphia, USA* 2005.

195. Schmidt, D., Mol, A., Neuenschwander, S., Breymann, C., Gossi, M., Zund, G., Turina, M., and Hoerstrup, S. P. Living patches engineered from human umbilical cord derived fibroblasts and endothelial progenitor cells. *Eur. J. Cardiothorac. Surg.* **27**:795-800, 2005.

196. Schmidt, D., Breymann, C., Weber, A., Guenter, C. I., Neuenschwander, S., Zund, G., Turina, M., and Hoerstrup, S. P. Umbilical cord blood derived endothelial progenitor cells for tissue engineering of vascular grafts. *Ann Thorac. Surg.* **78**:2094-2098, 2004.

197. Hoerstrup, S. P., Kadner, A., Breymann, C., Maurus, C. F., Guenter, C. I., Sodian, R., Visjager, J. F., Zund, G., and Turina, M. I. Living, autologous pulmonary artery conduits tissue engineered from human umbilical cord cells. *Ann Thorac. Surg.* **74**:46-52, 2002.

198. Schmidt, D., Mol, A., Odermatt, B., Neuenschwander, S., Breymann, C., Gossi, M., Genoni, M., Zund, G., and Hoerstrup, S. P. Engineering of Biologically Active Living Heart Valve Leaflets Using Human Umbilical Cord-Derived Progenitor Cells. *Tissue Eng* 2006.

199. Schmidt, D., Mol, A., Breymann, C., Achermann, J., Odermatt, B., Gossi, M., Neuenschwander, S., Pretre, R., Genoni, M., Zund, G., and Hoerstrup, S. P. Living autologous heart valves engineered from human prenatally harvested progenitors. *Circulation* **114**:I125-I131, 2006.

200. Rhoads, G. G., Jackson, L. G., Schlesselman, S. E., de la Cruz, F. F., Desnick, R. J., Golbus, M. S., Ledbetter, D. H., Lubs, H. A., Mahoney, M. J., Pergament, E., and . The safety and efficacy of chorionic villus sampling for early prenatal diagnosis of cytogenetic abnormalities. *N. Engl. J Med.* **320**:609-617, 1989.

201. Messier, R. H., Jr., Bass, B. L., Aly, H. M., Jones, J. L., Domkowski, P. W., Wallace, R. B., and Hopkins, R. A. Dual structural and functional phenotypes of the porcine aortic valve interstitial population: characteristics of the leaflet myofibroblast. *J Surg. Res.* **57**:1-21, 1994.

202. Hoerstrup, S. P., Sodian, R., Sperling, J. S., Vacanti, J. P., and Mayer, J. E., Jr. New pulsatile bioreactor for in vitro formation of tissue engineered heart valves. *Tissue Eng* **6**:75-79, 2000.

203. Narita, Y., Hata, K., Kagami, H., Usui, A., Ueda, M., and Ueda, Y. Novel pulse duplicating bioreactor system for tissue-engineered vascular construct. *Tissue Eng* **10**:1224-1233, 2004.

204. Williams, C. and Wick, T. M. Perfusion bioreactor for small diameter tissue-engineered arteries. *Tissue Eng* **10**:930-941, 2004.

205. Stegemann, J. P. and Nerem, R. M. Phenotype modulation in vascular tissue engineering using biochemical and mechanical stimulation. *Ann Biomed. Eng* **31**:391-402, 2003.

206. Niklason, L. E., Gao, J., Abbott, W. M., Hirschi, K. K., Houser, S., Marini, R., and Langer, R. Functional arteries grown in vitro. *Science* **284**:489-493, 1999.

207. Mayer, J. E. In search of the ideal valve replacement device. *Journal of Thoracic and Cardiovascular Surgery* **125**:S14-S15, 2003.

208. Yankah, A. C., Wottge, H. U., Muller-Hermelink, H. K., Feller, A. C., Lange, P., Wessel, U., Dreyer, H., Bernhard, A., and ller-Ruchholtz, W. Transplantation of aortic and pulmonary allografts, enhanced viability of endothelial cells by cryopreservation, importance of histocompatibility. *Journal of cardiac surgery* **2**:209-220, 1987.

209. Erdbrugger, W., Konertz, W., Dohmen, P. M., Posner, S., Ellerbrok, H., Brodde, O. E., Robenek, H., Modersohn, D., Pruss, A., Holinski, S., Stein-Konertz, M., and Pauli, G. Decellularized xenogenic heart valves reveal remodeling and growth potential in vivo. *Tissue Engineering* **12**:2059-2068, 2006.

210. Leyh, R. G., Wilhelmi, M., Rebe, P., Fischer, S., Kofidis, T., Haverich, A., and Mertsching, H. In vivo repopulation of xenogeneic and allogeneic acellular valve matrix conduits in the pulmonary circulation. *Ann Thorac. Surg.* **75**:1457-1463, 2003.

211. O'Brien, M. F., Goldstein, S., Walsh, S., Black, K. S., Elkins, R., and Clarke, D. The SynerGraft valve: a new acellular (nonglutaraldehyde-fixed) tissue heart valve for autologous recellularization first experimental studies before clinical implantation. *Semin. Thorac. Cardiovasc. Surg.* **11**:194-200, 1999.

212. Walluscheck, K. P., Steinhoff, G., and Haverich, A. Endothelial cell seeding of native vascular surfaces. *Eur. J. Vasc. Endovasc. Surg.* **11**:290-303, 1996.

213. Massia, S. P. and Hubbell, J. A. Immobilized amines and basic amino acids as mimetic heparin-binding domains for cell surface proteoglycan-mediated adhesion. *J. Biol. Chem.* **267**:10133-10141, 1992.

214. Thoumine, O., Nerem, R. M., and Girard, P. R. Oscillatory shear stress and hydrostatic pressure modulate cell-matrix attachment proteins in cultured endothelial cells. *In Vitro Cell Dev. Biol. Anim* **31**:45-54, 1995.

215. Meredith, J. E., Jr., Fazeli, B., and Schwartz, M. A. The extracellular matrix as a cell survival factor. *Mol. Biol. Cell* **4**:953-961, 1993.

216. Lee, R. T., Berditchevski, F., Cheng, G. C., and Hemler, M. E. Integrin-mediated collagen matrix reorganization by cultured human vascular smooth muscle cells. *Circ. Res.* **76**:209-214, 1995.

217. Powell, T. M., Paul, J. D., Hill, J. M., Thompson, M., Benjamin, M., Rodrigo, M., McCoy, J. P., Read, E. J., Khuu, H. M., Leitman, S. F., Finkel, T., and Cannon, R. O., III Granulocyte colony-stimulating factor mobilizes functional endothelial progenitor cells in patients with coronary artery disease. *Arterioscler. Thromb. Vasc. Biol.* **25**:296-301, 2005.

218. Juthier, F., Vincentelli, A., Gaudric, J., Corseaux, D., Fouquet, O., Calet, C., Le Tourneau, T., Soenen, V., Zawadzki, C., Fabre, O., Susen, S., Prat, A., and Jude, B. Decellularized heart valve as a scaffold for in vivo recellularization: deleterious effects of granulocyte colony-stimulating factor. *J. Thorac. Cardiovasc. Surg.* **131**:843-852, 2006.

219. Stamm, C. and Steinhoff, G. When less is more: Go slowly when repopulating a decellularized valve in vivo! *J Thorac Cardiovasc Surg* **132**:735-737, 2006.

220. Simon, P., Kasimir, M. T., Seebacher, G., Weigel, G., Ullrich, R., Salzer-Muhar, U., Rieder, E., and Wolner, E. Early failure of the tissue engineered porcine heart valve SYNERGRAFT in pediatric patients. *Eur. J. Cardiothorac. Surg.* **23**:1002-1006, 2003.

221. Konertz, W., Dohmen, P. M., Liu, J., Beholz, S., Dushe, S., Posner, S., Lembcke, A., and Erdbrugger, W. Hemodynamic characteristics of the Matrix P decellularized xenograft for pulmonary valve replacement during the Ross operation. *J Heart Valve Dis.* **14**:78-81, 2005.

222. Bechtel, J. F., Gellissen, J., Erasmi, A. W., Petersen, M., Hiob, A., Stierle, U., and Sievers, H. H. Mid-term findings on echocardiography and computed tomography after RVOT-reconstruction: comparison of decellularized (SynerGraft) and conventional allografts. *Eur. J Cardiothorac. Surg.* **27**:410-415, 2005.

223. Johnson, D. M. and Sapirstein, W. FDA's requirements for in-vivo performance data for prosthetic heart valves. *J. Heart Valve Dis.* **3**:350-355, 1994.

224. Draft Replacement Heart Valve Guidance. 10-14-1994. United States Food and Drug Administration, Division of Cardiovascular, Respiratory, and Neurological Devices.

II

AN INTRA-AORTIC SHUNT PREVENTS PARALYSIS DURING AORTIC SURGERY IN SHEEP

INTRODUCTION

Recent advances in tissue engineering have generated novel materials for vascular patches and heart valves that require pre-clinical *in-vivo* testing. Although many animal models are available, the United States Food and Drug Administration strongly suggests testing cardiovascular tissue in sheep [1,2] which are comparable in size to humans and provide an accelerated model of calcification [3]. Heterotopic implantation of tissue engineered materials in the descending thoracic aorta may provide important information regarding the strength and biological properties of these new tissues without the morbidity and expense of requiring cardiopulmonary bypass. However, sheep are particularly prone to spinal cord ischemia during aortic cross-clamping which is required for such aortic procedures. Sheep tolerate less than 15 minutes of ischemic time before a significant risk of paralysis. We report the use and hemodynamic effects of a simple intra-aortic shunt to facilitate the implantation of tissue engineered vascular patches in the descending thoracic aorta of sheep.

MATERIALS AND METHODS

Experimental Animals:

Seven juvenile Suffolk sheep (45 – 55 kg) were purchased from a local farm and housed in accordance with the guidelines of the Canadian Council of Animal Care [4] at the University of Alberta farm with food and water *ad libitum*. Approval for this study was obtained from the University of Alberta Animal Policy and Welfare Committee.

Surgical Procedure:

After fasting for 24 – 36 hours, general anesthesia was induced with 5% isoflurane (Halocarbon Lab, Inc., River Edge, NJ, USA) and maintained with 1 – 2% isoflurane following endotracheal intubation. Ventilation was supported with oxygen and nitrous oxide (1:1) delivered at a tidal volume of 10 mL/kg via an anesthetic machine (Ohio 30/70, Ohio Medical Products, Madison, WI, USA). The animal was then placed in the right lateral decubitus position and 8 French vascular sheaths were placed in the left external jugular vein, left carotid artery and the left femoral artery. Under fluoroscopic guidance, a Swan Ganz catheter (Edwards Life Sciences, Irvine, CA, USA) was introduced into the pulmonary artery and a 6 French pigtail catheter (Cook, Inc., Bloomington, IN, USA) was placed in the left ventricle.

A thoracotomy in the 6^{th} left intercostal space was performed. The pleura overlying the aorta was divided from the level of the 4^{th} to the 10^{th} intercostal

space and an ultrasonic flow probe (Triton Technology, Inc., San Diego, CA, USA) was placed around the aorta at the 9th intercostal space. Heparin (100 units/kg, Pharmaceutical Partners of Canada, Inc., Richwood Hill, ON, Canada) was administered. After controlling the intercostal arteries, umbilical tapes were placed around the aorta proximally and distally. A 9 cm shunt was prepared, consisting of a section of ¼ inch internal diameter phosphorylcholine (Phisio®)-coated polyvinylchloride cardiopulmonary perfusion circuit tubing (Sorin Biomedica Canada Inc., Richmond Hill, ON, Canada) with a 3-O silk ligature tied at the midpoint. The aorta was cross-clamped 1 cm proximal to the proximal tape and 1 cm distal to the distal tape with angled DeBakey vascular clamps. After occluding the proximal end of the shunt with a snap, a 6 cm aortotomy was made between the umbilical tapes and the shunt was inserted distally against the DeBakey clamp. The shunt was secured with a Rummel, the DeBakey clamp was removed and the shunt was flushed of air. The proximal end of the shunt was then placed in a similar fashion by sequentially advancing 2 snaps along the length of the shunt and the shunt was opened. Figure II-1 demonstrates the shunt *in situ* while implanting a decellularized patch into the descending thoracic aorta. After 1 hour of flow, the shunt was occluded with 2 snaps and divided between them to facilitate the removal of the shunt. The aortotomy was closed with a running 5-O polypropylene suture (Ethicon, Somerville, NJ, USA). Patches were sutured into the descending thoracic aorta with a running 5-O polypropylene suture. Just prior

to tying the suture, the last few stitches were loosened and the shunt was removed as described above.

Physiologic Monitoring:

Aortic pressure proximal and distal to the shunt as well as pulmonary artery and left ventricular pressures were measured continuously and recorded digitally (Ponemah 4.1 physiology platform, Data Sciences International, Valley View, OH, USA). Recording began 15 minutes before the insertion of the shunt to establish baseline values and continued until 15 minutes after removal of the shunt. Aortic blood flow distal to the shunt was likewise recorded. All data were averaged over 15 minute intervals with the Ponemah software. Data collected during the cross-clamp period were averaged over the duration that the vascular clamps were applied.

Statistical Analysis:

Data was exported as Microsoft Office Excel 2003 spreadsheets and analyzed with SPSS 14.0 (SPSS Inc., Chicago, USA). Continuous data was expressed as mean ± standard error of the mean (SEM) and were compared with the paired Student's t-test. Means of multiple groups were compared with analysis of variance (ANOVA) and post hoc Scheffe analysis.

RESULTS

Hemodynamic Effect of the Shunt:

Hemodynamic and flow data are shown in Figure II-2. The mean aortic pressure distal to the shunt prior to clamping the aorta was 86.4 ± 4.6 mmHg. Occlusion of the aorta reduced the distal mean aortic pressure to 1.79 ± 0.4 mmHg ($P < 0.001$). Opening the intra-aortic shunt restored the distal mean aortic pressure to 67.9 ± 7.3 mmHg ($P = 0.053$).

The proximal systolic blood pressure was 107 ± 5.7 mmHg at baseline and increased to 177 ± 9.9 mmHg ($P < 0.001$) while the aorta was cross-clamped, but returned to baseline level after the shunt was inserted (99.5 ± 7.2 mmHg, $P = 0.798$). Mean left ventricular pressure followed a similar pattern, beginning at 45.1 ± 7.8 mmHg, rising to 83.0 ± 11.0 mmHg ($P = 0.034$) with the cross-clamp applied and returning to 48.7 ± 7.4 mmHg ($P = 0.961$ compared to baseline) with the shunt open. In contrast, the distal systolic aortic pressure fell from 106 ± 4.3 mmHg to 2.3 ± 0.6 mmHg ($P < 0.001$) during the aortic cross-clamp period, but only returned to 74.3 ± 7.4 mmHg ($P = 0.001$) when the shunt was opened. There was no statistically significant change in mean pulmonary artery pressure compared to baseline (17.9 ± 2.2 mmHg) with the aorta occluded (23.9 ± 3.4 mmHg, $P = 0.357$) or with the shunt open (18.1 ± 2.9 mmHg, $P = 0.999$ compared to baseline). There was a statistically significant increase in left ventricular $-dP/dt$ from 1357 ± 214 $mmHg \cdot sec^{-1}$ to 2229 ± 140 $mmHg \cdot sec^{-1}$ ($P = 0.025$), but no

significant difference in +dP/dt upon clamping the aorta (1693 ± 445 mmHg•sec^{-1} vs 1659 ± 407 mmHg•sec^{-1}, P = 0.999). –dP/dt returned to baseline when the shunt was opened (1411 ± 213 mmHg•sec^{-1}, P = 0.981).

Flow in the distal aorta was 2.35 ± 0.37 L/minutes at baseline and was reduced to -0.01 ± 0.01 L/minutes ($p < 0.001$) with the aortic cross-clamped. Distal aortic flow returned to baseline level 2.49 ± 0.36 L/minutes ($p = 0.945$) when the clamp was opened.

The shunt was easy to insert and remove. Mean aortic cross-clamp time for insertion was 2.32 ± 0.4 minutes (range 0.7 – 3.7 minutes) and 6.0 ± 0.3 minutes (range 5.1 – 7.7 minutes) for removal of the shunt and closure of the aorta.

Early in this series, one animal died intraoperatively from an injury to the posterior wall of the aorta while removing the shunt. Placing a 3-O silk ligature around the midpoint of the shunt allowed for anterior traction to be applied to the shunt while dividing it thereby preventing further injuries to the posterior aortic wall. This ligature also facilitated placement of the shunt and helped to ensure that the shunt was placed in the midpoint of the aortotomy. There was also some tendency for the shunt to migrate distally in the aorta. Fixing the ligature to the superior portion of the thoracotomy incision prevented migration of the shunt.

Clinical Results:

Prior to instituting the use of this shunt, two of two sheep developed immediate paralysis of the hind legs following the implantation of a vascular patch in the descending thoracic aorta. This technique prevented hind leg paralysis in all 24 subsequent animals surviving the procedure. Ten animals were euthanized at 4 weeks and 13 were euthanized at 6 months without complication. A single animal died 61 days after surgery from a ruptured mycotic aneurysm.

CONCLUSIONS

Heart valve pathology is commonly treated by replacing the diseased valve with a mechanical, bioprosthetic or allograft valve. Although each of these prosthetic valves improves upon the natural history of valve pathology, the recipient is exposed to risks including thromboembolism, prosthetic valve endocarditis, pannus in growth, valve failure and reoperation. Other complex congenital and acquired lesions of the ventricular outflow tracts and great vessels may be reconstructed with cryopreserved allograft vascular tissue or synthetic grafts. None of the current prosthetic valves or vascular grafts is capable of growth or repair. Although superior to synthetic grafts in terms of handling and hemodynamics, cryopreserved allograft cardiovascular tissue elicits a strong cellular and humoral immune response in recipients [5-7]. When used to correct congenital heart defects in children, the host immune response may accelerate the

deterioration of the allograft [8] resulting in reduced freedom from reoperation [9] and may complicate future heart transplantation [10,11]. The limitations of current valve technology and vascular grafts have stimulated the development of tissue-engineered valves and conduits. Increasing data suggest that decellularizing the allograft may attenuate the host immune response [12]. Decelluarized allograft and xenograft heart valves and synthetic polymer scaffolds are being investigated as alternatives to currently available prostheses [13-15] and will require animal testing prior to widespread clinical use.

Juvenile sheep is a model preferred by the US-FDA for preclinical testing of cardiovascular tissue [1,2]. Sheep are comparable in size to humans, but provide an accelerated model of calcification. Although valves must be tested in the orthotopic position prior to human implantation, many characteristics of tissue engineered valve and vascular replacements including the host immunological response, propensity for aneurysm formation, calcification, host cell repopulation and survival of seeded cells may be tested in the heterotopic position.

Implantation of tissue in the descending thoracic aorta does not require full cardiopulmonary bypass thereby reducing the morbidity and mortality of the experimental animals and reducing the cost and time for the operative procedure. However, procedures on the descending aorta still require cross-clamping the aorta proximal and distal to the operative site to prevent exsanguination and enhance visualization.

Nearly one century ago, Alexis Carrel noted that the spinal cord can tolerate only short periods of ischemia without resulting in paralysis [16]. Hypotension in the distal aorta also renders the abdominal organs ischemic which can cause multiple systemic complications. Clamping the aorta results in proximal aortic hypertension leading to elevated left ventricular end-diastolic pressure and acute mitral valve incompetence [17].

A number of techniques have been described to reduce the left ventricular afterload and to improve blood flow and pressure in the distal aorta including. medication, internal [17-19] and external aortic shunts [20,21], left ventricular apex-to-aortic shunt [22] and left heart bypass [23].

Intra-aortic shunting was briefly described by Hufnagel in 1949 [17]. Subsequently, there have been only sporadic reports describing the use of intra-aortic shunts either clinically or experimentally. Alexander described the successful use of a Sundt heparin-bonded shunt for the repair of a coarctation of the thoracic aorta in a 4-year-old girl [18]. Zacharopoulos utilized 7 to 10 cm latex venous cannulae of various diameters as a shunts to resect and replace a portion of descending thoracic aorta. Use of this shunt reduced the incidence of paraplegia from 60% to 0% in 15 to 25 kg dogs [19]. Van Voorst used radiolabeled microspheres to study spinal cord and visceral blood flow during [24] and following [25] thoracic aortic surgery with intra-aortic shunting. In neonatal pigs, a 5 cm, 3/16 inch (internal diameter) silicone tubing with retention rings was

also effective in preventing paraplegia and was found to improve spinal and visceral blood flow. To date there has been a paucity of reports of intra-aortic shunting during thoracic aortic surgery in a large animal model. Chronic results have been limited to small series for no longer than seven days and hemodynamic studies have been limited to neonatal pigs

Herein, we described a simple intra-aortic shunt that is effective in reducing left ventricular afterload and maintaining aortic perfusion distal to the operative site. There were no shunt-related complications during the long-term follow-up (1 to 6 months) of 24 sheep.

Compared to other shunts described in the literature, our shunt is constructed from readily-available materials, requires minimal modifications and is inexpensive. Phosphorylcholine coated 1/4 inch (internal diameter) polyvinylchloride used in standard cardiopulmonary bypass equipment is supplied in 2.4 m lengths at a cost of $10 USD. Allowing for trimming at the time of surgery, 24 shunts can be made from one 2.4 m length at a cost of $0.42 USD per shunt. The 3-O silk ligature tied at the midpoint of the shunt is available at a cost of $0.60 USD for a total cost of $1.02 USD for the shunt.

Placement and removal of the shunt was easy and safe. Sequentially advancing two snaps along the shunt facilitated de-airing and efficient positioning without injuring the aorta. Early in our series, a single animal suffered an aortic

injury upon removing the shunt. A slight modification of the shunt prevented any subsequent complications when removing the shunt.

A primary benefit of intra-aortic shunts over external shunts is that additional aortotomies or ventriculotomies are not required for the placement of cannulae. Instead, the intra-aortic shunt is placed in the aorta via the same aortotomy used to implant the patch. Consequently, operative time, surgical trauma and potential for postoperative bleeding are reduced. Using an external aorto-aortic shunt, we found that the patch length may be limited by the location of the cannulae, which can be technically difficult to space widely beyond the limits of the thoracotomy. The intra-aortic shunt requires only Rommels to secure the shunt which are easier to place beyond the limits of the thoracotomy. Intra-aortic shunts do not clutter in the operative field and we also found that the intra-aortic shunt splints the aortotomy open, facilitating patch implantation. Finally, in contrast to external shunts comprised of two cannulae and a connector tube, our shunt has a very small volume (11.4 mL) which minimizes blood loss, priming volume and hemodilution.

Insertion of an intra-aortic shunt could potentially disrupt the endothelium of the aortic wall. To minimize the risk of this complication, the cut edges of the shunt were beveled. Although we did not examine the aortic wall microscopically, the region of the aorta where the shunt resided was free from gross evidence of injury at the time of patch explant. In our opinion, any potential

endothelial damage resulting from an intra-aortic shunt is minimal compared to the trauma resulting from aortotomies or ventriculotomies required for external shunts.

We report the use of an intra-aortic shunt for the implantation of a vascular patch in the thoracic aorta of sheep for testing novel tissue engineered vascular patches. This shunt was safe and effective in reducing the pressure in the proximal aorta and increasing pressure and blood flow in the aorta distal to the operative site in a large animal model. Moreover, this shunt was cost-effective, simple to insert and remove, and does not require any additional aortotomies. We found that the shunt also facilitated the implantation by splinting the aortotomy open. Using the described shunt, we implanted vascular patches into 25 sheep with no animals developing hind leg paralysis and only one intra-operative mortality.

Figure II-1. A. *In situ* placement of an intra-aortic shunt (arrow) via a 6th left intercostal thoracotomy for the implantation of a decellularized pulmonary artery vascular patch. **Inset.** Intra-aortic shunt consisting of a 9mm section of standard ¼ inch phosphorylcholine-coated polyvinylchloride cardiopulmonary perfusion circuit tubing with a 3-O silk ligature at the midpoint. **B.** A decellularized pulmonary artery patch implanted in the descending thoracic aorta of a juvenile sheep.

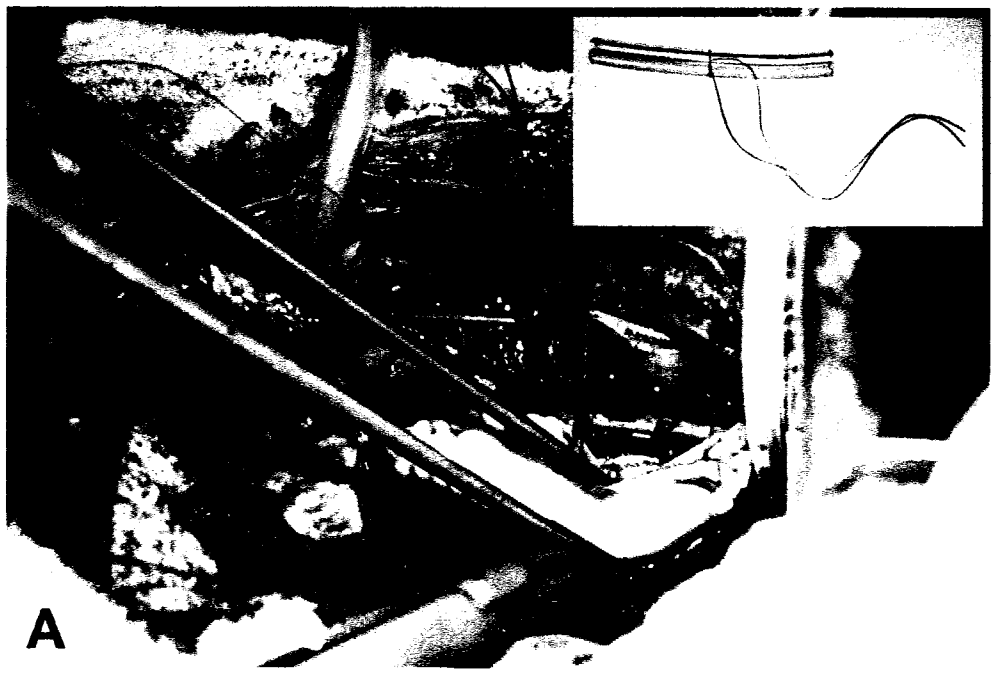

Figure II-2. Opening the intra-aortic shunt effectively decompresses the proximal aorta and returns hemodynamic and flow parameters to near baseline values. Data points represent the mean of seven experiments for each time period, as indicated. Error bars are shown except when smaller than the data points and represent the standard error of the mean. Comparison of multiple means is by ANOVA with post hoc Scheffe analysis. **A.** Systolic blood pressure proximal to the shunt and left ventricular (LV) mean pressure both increase when the aorta is clamped and then return to baseline with the shunt open (*$P < 0.001$ and **$P = 0.798$ compared to baseline; ‡$P = 0.034$ and ‡‡$P = 0.961$ compared to baseline). Distal systolic blood pressure is dramatically reduced with aortic cross-clamping and increases, but remains below baseline when the shunt is opened (†$P < 0.001$ and †† $P = 0.001$ compared to baseline). There is no statistically significant change in mean pulmonary artery (PA) pressure compared to baseline with the shunt open or closed (§$P = 0.357$ and §§ $P = 0.999$ compared to baseline). **B.** There is a statistically significant increase in left ventricular –dP/dt, but no difference in +dP/dt upon clamping the aorta. –dP/dt returns to baseline when the shunt is opened (*$P = 0.999$ and **$P = 0.998$ compared to baseline; †$P = 0.025$ and ††$P = 0.981$ compared to baseline). **C.** Blood flow in the distal aorta was 2.35 ± 0.37 L/minutes at baseline and was reduced to -0.01 ± 0.01 L/minutes (*$P < 0.001$) with the aorta cross-clamped and returned to 2.49 ± 0.36 L/minute (**$P = 0.945$) when the shunt was opened.

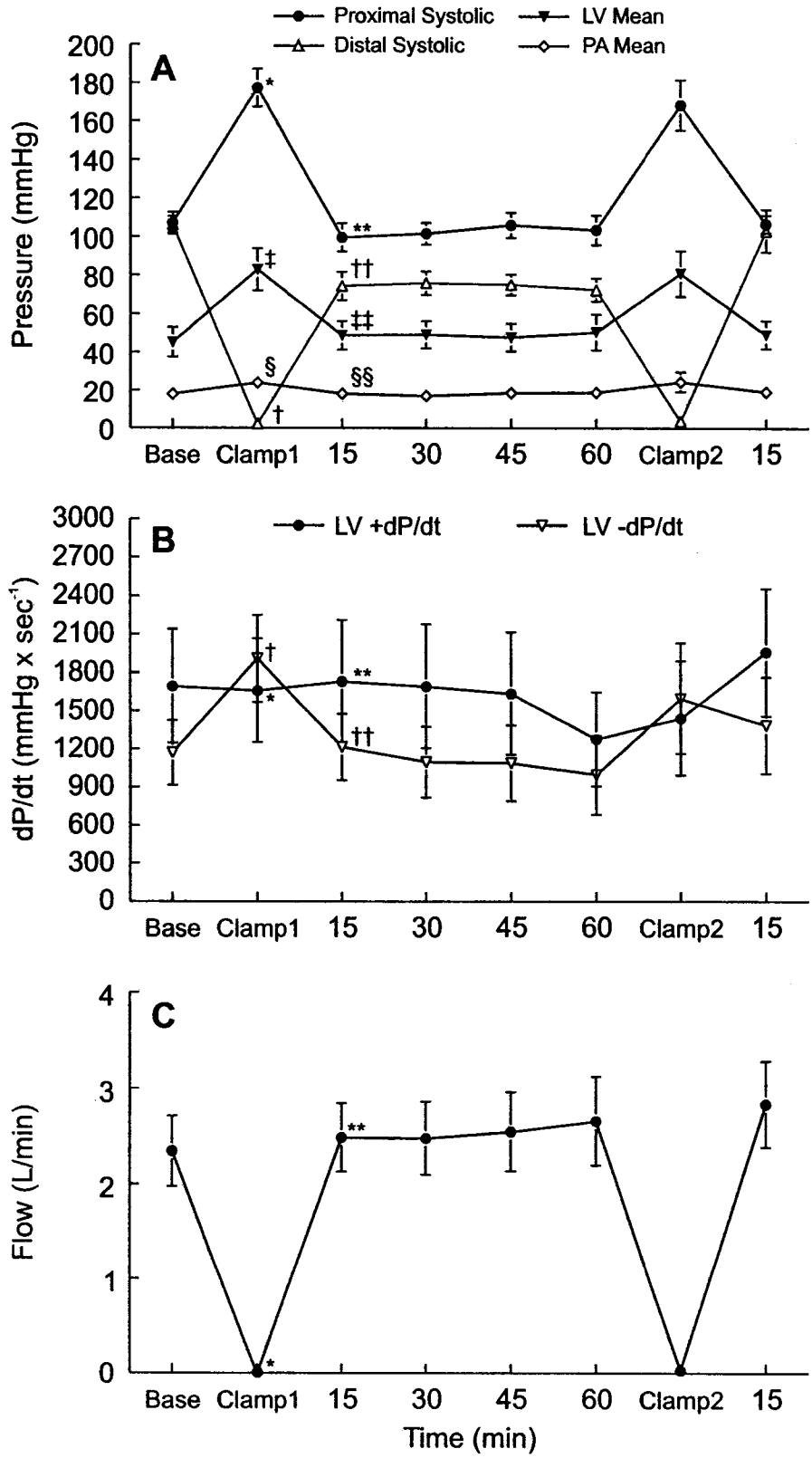

Figure II-2. Opening the intra-aortic shunt effectively decompresses the proximal aorta and returns hemodynamic and flow parameters to near baseline values. Data points represent the mean of seven experiments for each time period, as indicated. Error bars are shown except when smaller than the data points and represent the standard error of the mean. Comparison of multiple means is by ANOVA with post hoc Scheffe analysis. **A.** Systolic blood pressure proximal to the shunt and left ventricular (LV) mean pressure both increase when the aorta is clamped and then return to baseline with the shunt open (*$P < 0.001$ and **$P = 0.798$ compared to baseline; ‡$P = 0.034$ and ‡‡$P = 0.961$ compared to baseline). Distal systolic blood pressure is dramatically reduced with aortic cross-clamping and increases, but remains below baseline when the shunt is opened (†$P < 0.001$ and †† $P = 0.001$ compared to baseline). There is no statistically significant change in mean pulmonary artery (PA) pressure compared to baseline with the shunt open or closed (§$P = 0.357$ and §§ $P = 0.999$ compared to baseline). **B.** There is a statistically significant increase in left ventricular –dP/dt, but no difference in +dP/dt upon clamping the aorta. –dP/dt returns to baseline when the shunt is opened (*$P = 0.999$ and **$P = 0.998$ compared to baseline; †$P = 0.025$ and ††$P = 0.981$ compared to baseline). **C.** Blood flow in the distal aorta was 2.35 ± 0.37 L/minutes at baseline and was reduced to -0.01 ± 0.01 L/minutes (*$P < 0.001$) with the aorta cross-clamped and returned to 2.49 ± 0.36 L/minute (**$P = 0.945$) when the shunt was opened.

REFERENCES

1. Draft Replacement Heart Valve Guidance. 10-14-1994. United States Food and Drug Administration, Division of Cardiovascular, Respiratory, and Neurological Devices.

2. Johnson, D. M. and Sapirstein, W. FDA's requirements for in-vivo performance data for prosthetic heart valves. *J. Heart Valve Dis.* **3**:350-355, 1994.

3. Herijgers, P., Ozaki, S., Verbeken, E., Van Lommel, A., Racz, R., Zietkiewicz, M., Perek, B., and Flameng, W. Calcification characteristics of porcine stentless valves in juvenile sheep. *European Journal of Cardio-Thoracic Surgery* **15**:134-142, 1999.

4. *Guide to the care and use of experimental animals*.Canadian Council of Animal Care, 1993.

5. Meyer, S. R., Nagendran, J., Desai, L. S., Rayat, G. R., Churchill, T. A., Anderson, C. C., Rajotte, R. V., Lakey, J. R., and Ross, D. B. Decellularization reduces the immune response to aortic valve allografts in the rat. *J. Thorac. Cardiovasc. Surg.* **130**:469-476, 2005.

6. Hogan, P., Duplock, L., Green, M., Smith, S., Gall, K. L., Frazer, I. H., and O'Brien, M. F. Human aortic valve allografts elicit a donor-specific immune response. *J. Thorac. Cardiovasc. Surg.* **112**:1260-1266, 1996.

7. Hoekstra, F., Witvliet, M., Knoop, C., Akkersdijk, G., Jutte, N., Bogers, A., Claas, F., and Weimar, W. Donor-specific anti-human leukocyte antigen class I antibodies after implantation of cardiac valve allografts. *J. Heart Lung Transplant.* **16**:570-572, 1997.

8. Dignan, R., O'Brien, M., Hogan, P., Thornton, A., Fowler, K., Byrne, D., Stephens, F., and Harrocks, S. Aortic valve allograft structural deterioration is associated with a subset of antibodies to human leukocyte antigens. *J. Heart Valve Dis.* **12**:382-390, 2003.

9. Yankah, A. C., Alexi-Meskhishvili, V., Weng, Y., Schorn, K., Lange, P. E., and Hetzer, R. Accelerated degeneration of allografts in the first two years of life. *Ann. Thorac. Surg.* **60**:S71-S76, 1995.

10. Meyer, S. R., Campbell, P. M., Rutledge, J. M., Halpin, A. M., Hawkins, L. E., Lakey, J. R., Rebeyka, I. M., and Ross, D. B. Use of an allograft patch in repair of hypoplastic left heart syndrome may complicate future transplantation. *Eur. J Cardiothorac. Surg* **27**:554-560, 2005.

11. Jacobs, J. P., Quintessenza, J. A., Boucek, R. J., Morell, V. O., Botero, L. M., Badhwar, V., van Gelder, H. M., Asante-Korang, A., McCormack, J., and Daicoff, G. R. Pediatric cardiac transplantation in children with high panel reactive antibody. *Ann. Thorac. Surg.* **78**:1703-1709, 2004.

12. Grauss, R. W., Hazekamp, M. G., van Vliet, S., Gittenberger-de Groot, A. C., and DeRuiter, M. C. Decellularization of rat aortic valve allografts reduces leaflet destruction and extracellular matrix remodeling. *J. Thorac. Cardiovasc. Surg.* **126**:2003-2010, 2003.

13. O'Brien, M. F., Goldstein, S., Walsh, S., Black, K. S., Elkins, R., and Clarke, D. The SynerGraft valve: a new acellular (nonglutaraldehyde-fixed) tissue heart valve for autologous recellularization first experimental studies before clinical implantation. *Semin. Thorac. Cardiovasc. Surg.* **11**:194-200, 1999.

14. Dohmen, P. M., Lembcke, A., Hotz, H., Kivelitz, D., and Konertz, W. F. Ross operation with a tissue-engineered heart valve. *Ann. Thorac. Surg.* **74**:1438-1442, 2002.

15. Hoerstrup, S. P., Sodian, R., Daebritz, S., Wang, J., Bacha, E. A., Martin, D. P., Moran, A. M., Guleserian, K. J., Sperling, J. S., Kaushal, S., Vacanti, J. P., Schoen, F. J., and Mayer, J. E., Jr. Functional living trileaflet heart valves grown in vitro. *Circulation* **102**:III44-III49, 2000.

16. Carrel, A. On the experimental surgery of the thoracic aorta and the heart. *Ann. Surg* **52**:83-95, 1910.

17. Hufnagel, C. A. Resection and grafting of the thoracic aorta with minimal interruption of the circulation. *Bull. Am. Coll. Surg* **34**:38, 1949.

18. Alexander, J. C., Jr. Maintenance of distal aortic perfusion by a heparin-bonded shunt during repair of coarctation of the aorta with minimal collateral circulation. *Ann. Thorac. Surg* **32**:304-306, 1981.

19. Zacharopoulos, L. and Symbas, P. N. Internal temporary aortic shunt for managing lesions of the descending thoracic aorta. *Ann. Thorac. Surg* **35**:240-242, 1983.

20. Kouchoukos, N. T., Lell, W. A., Karp, R. B., and Samuelson, P. N. Hemodynamic effects of aortic clamping and decompression with a temporary shunt for resection of the descending thoracic aorta. *Surgery* **85**:25-30, 1979.

21. Valiathan, M. S., Weldon, C. S., Bender, H. W., Jr., Topaz, S. R., and Gott, V. L. Resection of aneurysms of the descending thoracic aorta using a GBH-coated shunt bypass. *J. Surg Res.* **8**:197-205, 1968.

22. Kuribayashi, R., Chanda, J., and Abe, T. Apico-aortic shunt: a support technique during surgery on the descending thoracic aorta. *J. Cardiovasc. Surg (Torino)* **38**:271-276, 1997.

23. Dennis, C., HALL, D. P., MORENO, J. R., and SENNING, A. Reduction of the oxygen utilization of the heart by left heart bypass. *Circ. Res.* **10**:298-305, 1962.

24. Van Voorst, S. J., Rustom, S., Pate, J. W., Maijub, A. G., and Leffler, C. W. Intraluminal shunt for the thoracic aorta: spinal cord and visceral blood flow in acute studies. *World J. Surg.* **18**:939-943, 1994.

25. Van Voorst, S. J., Labranche, G. S., Rustom, S., Jukkola, A. F., and Leffler, C. W. Intraluminal shunt for the thoracic aorta: blood flow and function in chronic studies. *Ann. Thorac. Surg.* **63**:419-424, 1997.

III

AN EVALUATION OF THE FUNCTIONAL ALLOGENICITY OF FARM SHEEP USED IN CARDIAC VALVE STUDIES

INTRODUCTION

Cryopreserved allograft cardiovascular tissue elicits a strong cellular and humoral [1-3] immune response in recipients. When it is used to correct congenital heart defects in children, the host immune response may accelerate the deterioration of the allograft [4], resulting in reduced freedom from reoperation [5], and may complicate future heart transplantation [6,7]. Increasing data suggest that decellularizing the allograft may attenuate the host's immune response [8] post-implantation.

Inbred rodent models have been valuable in characterizing the alloreactive immune response against cryopreserved cardiovascular tissue [8,9], however preclinical work requires the use of large animal models to confirm the immunologic findings in large animals and to assess safety of the valve or tissue. The US-FDA strongly suggests testing cardiovascular tissue in sheep [10] which are comparable in size to humans and provide an accelerated model of calcification of vascular grafts [11]. Accordingly, there are several reports considering the impact of graft decellularization on the host alloresponse [12,13].

A version of chapter has been published. Lehr, Rayat, Desai, Coe, Korbutt, Ross. J Thorac Cardiov Surg 2006:132:1156-1161.

These studies assume allogenicity of the animals, but do not assess the degree of inbreeding between donor and recipient animals. Unlike rat and mouse models, sheep used for animal studies are taken from flocks raised for human consumption. Although many farmers attempt to minimize inbreeding, the degree of allogenicity within flocks has not been described. Furthermore, there are no well-characterized flocks of inbred sheep available to ensure allogenicity between donors and recipients of test models. We therefore sought to determine the level of inbreeding within a flock of local farm sheep.

Because the ovine MHC is incompletely characterized, we chose to perform a functional assay for this study. Alloresponsiveness to MHC antigens between potential transplant donors and recipients can be assessed by *in vitro* mixed lymphocyte reaction (MLR) assay. MLR primarily reflects the allogeneic proliferative immune response against class II donor specific antigens. In one-way MLR, peripheral blood mononuclear cells from two individuals are cultured together. Cells from two individuals are cultured together for a few days. Stimulator cells are non-lethally irradiated to prevent them from proliferating. Responder cells will proliferate if and take up tritiated thymidine in response to allogeneic stimulator cells. Although genotyping has largely replaced functional assays for tissue-typing donors and recipients in clinical organ transplantation, MLR has been shown recently to predict patients who are at high risk for graft failure and may be used as an adjunct to DNA methods [14]. In addition, MLR

reactivity may be disparate with results obtained by serological typing [15]. MLR remains a viable method of assessing alloresponsiveness. Therefore, we used one-way MLR assay to study the alloresponsiveness within a group of 19 juvenile sheep.

MATERIALS AND METHODS

Experimental Animals:

Nineteen random sheep were purchased from a local farm and housed in accordance with the guidelines of the Canadian Council of Animal Care [16] at the University of Alberta farm with food and water *ad libitum*. Approval for this study was obtained from the University of Alberta Animal Policy and Welfare Committee.

Animal Husbandry:

Suffolk sheep were obtained from a local farm that raises approximately 1,800 food quality lambs per year from 1,000 ewes and 50 rams. To minimize inbreeding, the rams and ewes are divided into three groups. Over a 3-year period, each group of rams is rotated through each group of ewes. Every year, five to six rams from each group are replaced with rams obtained from various farms across Alberta. Offspring are never bred with their parents or siblings.

Cell Collection:

Blood was collected from the jugular vein of each sheep and transported at room temperature. Peripheral blood mononuclear cells (PBMCs) were isolated by mixing equal portions of blood and 0.9% saline (Baxter, Toronto Canada), overlaying on 15mL Lympholyte Mammal density gradient (Cedarlane, Hornby Canada) and centrifuging for 45 minutes at 2,200rpm at room temperature. The layer of PBMCs was carefully aspirated and the contaminating red blood cells were lysed with red blood cell lysis buffer (pH 7.3). PBMCs were washed twice in 0.9% saline and stimulator PBMCs were frozen at a concentration of $2.5x10^7$/mL in 10% dimethyl sulfoxide and fetal bovine serum (FBS) at -80°C until needed. Responder cells were freshly isolated and were used immediately upon isolation.

One-way MLR:

Alloresponsiveness between sheep was tested using one-way MLR assay as previously described [17]. Briefly, stimulator cells were thawed in 40mL of Hank's balanced salt solution (HBSS; Invitrogen, Burlington, Canada) supplemented with 5% FBS and 1mg/L deoxyribonuclease (Roche, Laval, Canada) and then incubated at 37°C for 40 minutes. PBMCs were suspended in 10mL HBSS and irradiated with 2,500 Rad on a Cobalt 60 irradiator (MDS Nordion, Vancouver, Canada). After irradiation, cells were washed in HBSS and suspended in Eagle's Modified Essential Medium (EMEM) supplemented with

10% FBS, 1.0 x 10^{-5} mol/L 2-mercaptoethanol, and 1% penicillin-streptomycin. Responder cells were harvested on the day of experimentation, isolated as previously described and suspended in supplemented EMEM. Stimulator cells (3.0 x 10^5) and responder cells (5.0 x 10^5) were co-cultured in 96-well flat-bottom tissue culture-treated plates (Falcon, Franklin Lakes, USA) in a total volume of 0.2 mL/well. Positive control consisted of responder cells treated with 0.1 g/L Con A (Sigma, Oakville, Canada) and negative controls consisted of stimulator and responder cells alone as well as double-irradiated stimulator and responder cultures. Cell cultures were performed in triplicate and incubated at 37°C in a humidified atmosphere of 5% CO_2 for 4, 5, 6 and 7 days. After culture, plates were pulsed with 1μCi of [^{3}H] thymidine (Amersham Biosciences Corp, Piscataway, USA) per well and incubated again at 37°C for 24hrs.

Radiolabeled cells were harvested with a Tomtec Harvester 96 (Tomtec Inc., Hamden, USA) onto glass filtermats (Wallac Oy, Turku, Finland) and scintillator sheets (Wallac Oy, Turku, Finland) were melted onto the filtermats. Responder cell proliferation was measured as counts per minute (CPM) on a scintillation counter (Perkin Elmer, Wellesley, USA). The greatest daily mean proliferation during the four days of culture represents the maximum proliferation of each MLR pair. The day where highest proliferation was observed was considered the day on which the maximum response occurred.

Statistical Analysis:

Continuous data are expressed as mean ± standard error of the mean (SEM). Means of multiple groups were compared by one-way analysis of variance with Scheffe post hoc analysis to compare individual groups using SPSS 13.0 (SPSS Inc., Chicago, USA).

RESULTS

To determine the relative alloresponsiveness of animals within the study population, one-way MLR assay was performed on all but 11 combinations of 19 animals taken in pairs; this allowed for analysis of 160 potential donor and recipient combinations. A wide variation in the proliferation of responder cells after stimulation was observed, with CPM ranging from 63 to 158,169 (35,019 ± 2,884). Figure III-1 demonstrates a bar graph of the number of MLR pairs that attained a given proliferative response. A large number of MLR pairs had a proliferative response of less than 10,000 CPM, which represents a weak allogeneic response. The remainder of the group demonstrated a strong response. Based on these findings, a negative allogeneic response was defined as CPM < 10,000 and a positive response as CPM ≥ 10,000.

MLR kinetics varied depending on the pair of stimulator and responder cells. The distribution of time to maximum proliferation for negative control and mixed cultures was evenly distributed, with a slight preponderance towards days 6

and 7 (data not shown). Therefore, alloresponsiveness was assessed as the maximum mean proliferation of triplicate experiments from days 4 to 7. Maximum proliferation in Con A treated responder cells occurred on day 4 in 81% of cultures and on day 5 for the remaining groups (data not shown).

Analysis of variance (ANOVA) of the proliferative responses of experimental and control groups was performed ($p<0.001$; Figure III-2). Scheffe post hoc analysis demonstrated that proliferative responses of the strong responder pairs (53,934 ± 3,351) were significantly greater than the response of either stimulator cells alone (648 ± 92, $p = 0.002$) or responder cells alone (6,731 ± 1,987, $p = 0.011$). No statistically significant difference in response was identified between the weak allogeneic group (2,640 ± 305) and each negative control group ($p = 0.999$ for responder cells alone and $p > 0.999$ for stimulator cells alone). Con A treated responder cells had a significantly higher proliferation than any of the other groups (263,197 ± 30,252; $p \leq 0.001$ for all groups), as expected. Con A cross-links cell surface receptors and generates a non-specific response that is more intense than the allogeneic response. Responder cells treated with Con A were used as a positive control to ensure their viability and proliferative capacity.

The MLR results from all 160 combinations tested are summarized in Figure III-3. MLRs were categorized as demonstrating either a strong or weak allogeneic response as described above. Fifty-nine (36.9%) of 160 pairs

demonstrated a weak allogeneic response whereas 101 (63.1%) of 160 pairs demonstrated a strong allogeneic response.

CONCLUSIONS

Increasing evidence suggests that allograft heart valves incite a cellular and humoral immune response in the recipient that sensitizes the recipient and may play a role in the early failure of these valves [1-4]. Early studies in allogeneic rodent models have shown that decellularization removes the cellular components of the allograft valve and attenuates this destructive immune process [1]. Inbred lines of sheep are not readily available as are rodent strains, and most sheep used for laboratory animals are raised on farms for food and may be inbred to some degree. Sheep are a preferred large animal model for preclinical testing of vascular tissue and in particular, heart valves. Studies assessing the impact of decellularization of allograft heart valves on the immune response in large animal models generally assume that donor and recipient animals are allogeneic, but do not formally test or report the degree of inbreeding. Laboratory grade tissue suppliers often receive animals from slaughterhouses in a single geographical area and cannot provide information regarding the lines of animals from which they receive tissue. Recently, Ketchedjian and associates conceded that the variability of panel reactive antibody response in animals receiving non-processed implants

may result from leukocyte antigen similarities arising from inbreeding within supplier flocks of sheep [12].

Results from this study suggest that more than one third of randomly chosen sheep from a single farm maintaining excellent breeding practices may be too closely related to mount an immune response against donor tissue. Even within the group of strong responders, a wide variation of proliferative responses was observed and only a few MLR pairs showed a very strong response. This finding may reflect a loss of variability of MHC polymorphisms or alleles between animals as a result of inbreeding.

In our study, cells from 5 of 14 animals mounted a uniformly strong proliferative allogeneic response when tested against cells from 7 or more animals (Figure III-3). It is unlikely that these responder cells are responding to exogenous factors, as cultures from these animals were prepared on different days. Responder cells may proliferate in response to serum used in the culture medium. However, only one of the 8 homogeneous responders demonstrated a high proliferation when cultured alone. Animals such as these that mount a uniformly strong allogeneic response are the ideal donor animals for allogeneic transplant studies.

Understanding the degree of allogenicity of experimental animals is fundamental to the correct interpretation of results from transplant models based on allogeneic animals when inbred strains are not available. To minimize costs,

farm sheep, as with many other large animals, may be bred from a limited number of rams thereby increasing a flock's inbreeding coefficient. This practice increases the probability of randomly selecting related animals for transplantation. Donor and recipient animals that are considered allogeneic may therefore be less disparate which will reduce the recipient's immune response against donor tissue. In this situation, a reduced alloimmune response may be falsely attributed to the treatment, when in fact the perceived result is simply a factor of the immunologic similarity between the donor and recipient. When assessing the immune response in large animal transplant models, it is critical to assess the level of allogenicity between donor and recipient animals to interpret the results correctly.

Rotational breeding with partially isolated sire lines effectively reduces inbreeding of commercial female animals and their offspring. Migration between lines may inflate the inbreeding of the females although maintaining 4 to 5 sire lines may minimize this inflation [18]. These findings clearly demonstrate that even farm sheep bred with a rotational breeding strategy gives rise to a 37% probability that 2 allogeneic sheep randomly chosen for transplantation are too closely related for their lymphocytes to elicit an *in vitro* immune response. These results further demonstrate the importance of assessing allogenicity prior to performing transplantation studies.

Several reasons for the inflated level of inbreeding within our flock of sheep exist. Our supplier of sheep maintains 3 breeding lines of rams whereas 4

or 5 sire lines are required to minimize inbreeding [18]. However, by rotating rams off the farm over a 3 year period our supplier can potentially reduce the coefficient of inbreeding within his flocks of sheep. The effectiveness of this practice to reduce inbreeding however is dependent upon the genetic dissimilarity of the immigrating rams to the existing flock. Given that sheep are not an endogenous species in Alberta, it is possible that the entire population of sheep in Alberta arose from a limited number of individuals and that the flocks in Alberta are relatively closed, thus further increasing the inbreeding coefficient. The estimated inbreeding coefficient in some closed herds may be as high as 0.514 [19].

The MHC of vertebrates is a group of cell-surface glycoproteins encoded by a group of closely-linked, highly polymorphic set of genes. This bichain complex binds and presents antigenic peptides to T cells. Whereas the MHC is relatively conserved across mammalian species [20], the ovine lymphocyte antigen has yet to be well characterized. Indeed, controversy remains whether two or three loci encode ovine class I genes [21,22]. Inbreeding may reduce the number of MHC polymorphisms, thereby increasing the probability that foreign donor tissue will be seen as self, thus attenuating the allogeneic immune response [23]. A variety of methods for MHC typing have been developed including serological testing [24] and DNA genotyping. Despite the incomplete characterization of the ovine MHC, some authors have successfully assessed

MHC variation in sheep using DNA genotyping, include polymerase chain reaction – restriction fragment length polymorphism (PCR-RFLP) [25] and sequence-specific primer-polymerase chain reaction (SSP-PCR) [26].

In this chapter MLR pairs were set up using splenocytes from proposed donor animals as stimulator cells and splenocytes from proposed recipient animals as responder cells. Ideally, the reverse combinations would also have been used, but limited resources precluded performing additional experiments. We could have also further optimized our experimental conditions by testing other stimulator to responder ratios, or by testing other lymphocytes. However, we had limited numbers of PBMCs available and given the labor involved in this assay, it was not feasible to perform additional tests. It is possible that some responder cells may have a reduced proliferative response to some donor cells despite being allogeneic. In this circumstance an increased number of proliferative pairs of animals could have been identified thereby reducing the number of animal pairs that we classified as non-disparate. An *in vivo* functional test may be used to confirm the the MHC disparity between animals. Split thickness skin grafts are an excellent *in vivo* method to assess functional allogenicity, but this method immunologically contaminates the recipient against further studies. Because we planned to perform additional transplant experiments on our animals, we chose not to perform skin graft experiments.

Given the relative importance of the sheep model for cardiovascular immunology research, it may be valuable to develop inbred strains of allogeneic sheep. Such inbred strains would allow further assessment of the immunology of allograft heart valves in a large animal model. Unfortunately, developing such strains requires a long time commitment, as a minimum of 20 generations of inbreeding would likely be required. It may therefore require over 20 years of work to develop such strains [19]. Ideally, several lines of inbred sheep would be available.

In conclusion, we found that more than one third of sheep purchased from a farm utilizing husbandry practices to reduce inbreeding were too closely related to elicit a response in a MLR assay. These findings demonstrate the importance of determining the degree of allogenicity of sheep in transplantation studies that use allogeneic sheep models. Other methods of measuring allogenicity are available and include serotyping and genotyping. At a minimum, donor and recipient animals should be purchased from separate farms that do not share breeding animals. Well-characterized inbred strains of sheep may be ideal for such studies, although reduced ovine leukocyte antigen (OLA) polymorphisms may make these animals prone to infection and they may be less representative of the human clinical setting, where donors and recipients are outbred and have a diverse repertoire of HLA polymorphisms.

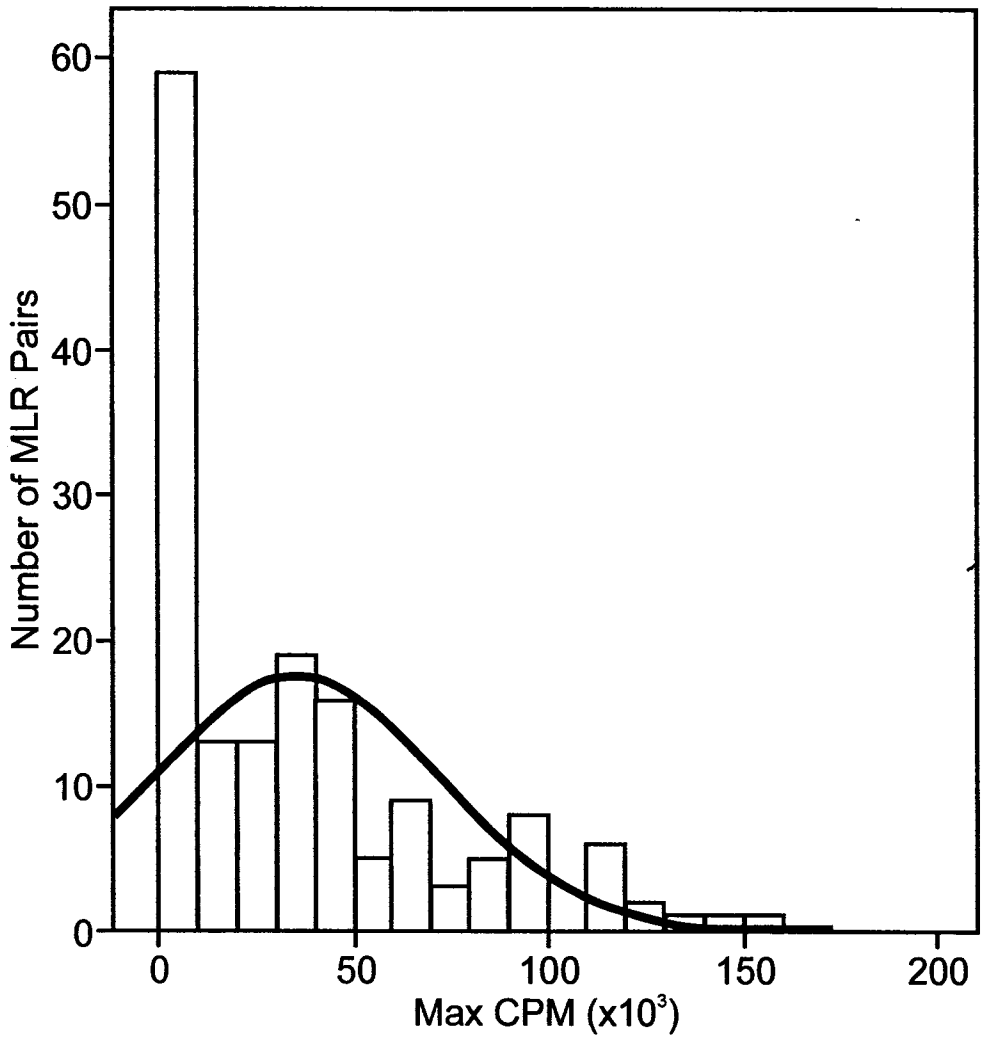

Figure III-1. Histogram of the maximum mean proliferation as measured by counts per minute (CPM) for 160 mixed lymphocyte reaction (MLR) pairs performed in triplicate. The overall mean proliferation was 35,019 +/- 2884 CPM. On the basis of the distribution of the allogeneic response, MLR pairs were categorized into strong (CPM ≥10,000) and weak (CPM <10,000) groups.

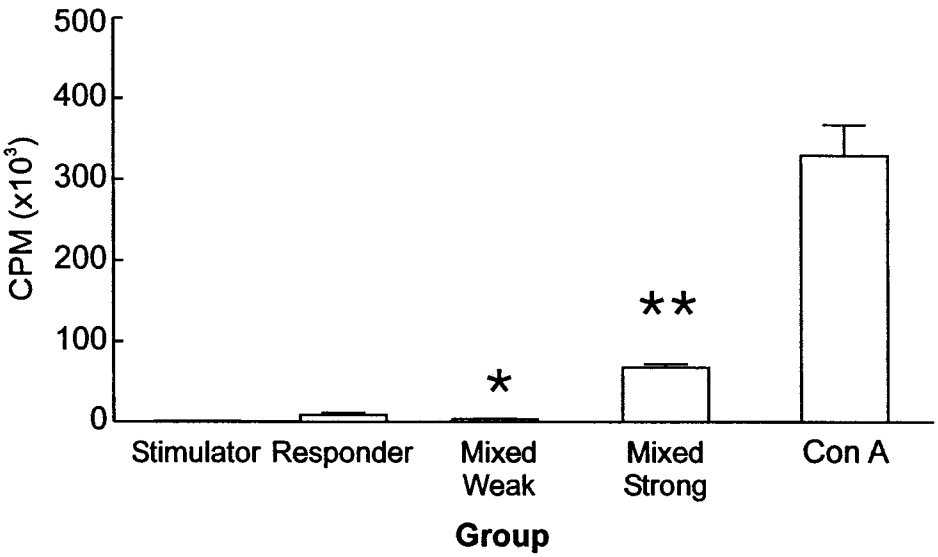

Figure III-2. Proliferative response of responder cells. Data are shown as mean counts per minute (CPM) for experimental groups (weak allogeneic response; CPM < 10,000, strong allogeneic response; CPM ≥ 10,000), negative control groups (stimulator cells alone and responder cells alone), and positive control group (concanavalin-A [Con A]-treated responder cells) and compared by analysis of variance. * $p > 0.999$ versus stimulator and responder. ** $p < 0.01$ versus stimulator, responder and mixed weak groups.

Responders

Stimulators	2	3	4	5	6	7	8	9	10	11	12	13	14	15	16	17	18	19
1	S	S	S	W	S	W	S	S	S	W	S	S	W	S	S	W	W	S
2		S	S	W	S	W	S	S	W	W	S	S	W	S	S	W	W	S
3			S	W	S	W	S	S	W	W	S	S	W	S	W	W	W	S
4				W	S	W	S	S	W	W	S	S	W	S	S	W	W	S
5					S	W	S	S	W	W	S	S	S	S	S	W	S	S
6						W	S	S	S	W	S	S	W	S	S	W	W	S
7							S	S	S	W	W	S	S	S	W	W	S	S
8								S	S	W	W	N	S	S	W	W	S	S
9									S	W	W	N	S	S	S	W	S	S
10										N	W	N	S	S	W	W	S	S
11											W	N	S	S	W	W	S	S
12												N	S	S	W	W	S	S
13													N	S	S	S	S	S
14														N	N	N	W	N
15															S	W	S	S
16																W	S	S
17																	S	S
18																		S

Figure III-3. Tabular representation of the distribution of proliferative responses, measured as counts per minute for 160 mixed lymphocyte reaction pairs. S, strong (n =101); W, weak (n = 59); N, not done.

REFERENCES

1. Meyer, S. R., Nagendran, J., Desai, L. S., Rayat, G. R., Churchill, T. A., Anderson, C. C., Rajotte, R. V., Lakey, J. R., and Ross, D. B. Decellularization reduces the immune response to aortic valve allografts in the rat. *J. Thorac. Cardiovasc. Surg.* **130**:469-476, 2005.

2. Hogan, P., Duplock, L., Green, M., Smith, S., Gall, K. L., Frazer, I. H., and O'Brien, M. F. Human aortic valve allografts elicit a donor-specific immune response. *J. Thorac. Cardiovasc. Surg.* **112**:1260-1266, 1996.

3. Hoekstra, F., Witvliet, M., Knoop, C., Akkersdijk, G., Jutte, N., Bogers, A., Claas, F., and Weimar, W. Donor-specific anti-human leukocyte antigen class I antibodies after implantation of cardiac valve allografts. *J. Heart Lung Transplant.* **16**:570-572, 1997.

4. Dignan, R., O'Brien, M., Hogan, P., Thornton, A., Fowler, K., Byrne, D., Stephens, F., and Harrocks, S. Aortic valve allograft structural deterioration is associated with a subset of antibodies to human leukocyte antigens. *J. Heart Valve Dis.* **12**:382-390, 2003.

5. Yankah, A. C., Alexi-Meskhishvili, V., Weng, Y., Schorn, K., Lange, P. E., and Hetzer, R. Accelerated degeneration of allografts in the first two years of life. *Ann. Thorac. Surg.* **60**:S71-S76, 1995.

6. Meyer, S. R., Campbell, P. M., Rutledge, J. M., Halpin, A. M., Hawkins, L. E., Lakey, J. R., Rebeyka, I. M., and Ross, D. B. Use of an allograft patch in repair of hypoplastic left heart syndrome may complicate future transplantation. *Eur. J Cardiothorac. Surg* **27**:554-560, 2005.

7. Jacobs, J. P., Quintessenza, J. A., Boucek, R. J., Morell, V. O., Botero, L. M., Badhwar, V., van Gelder, H. M., Asante-Korang, A., McCormack, J., and Daicoff, G. R. Pediatric cardiac transplantation in children with high panel reactive antibody. *Ann. Thorac. Surg.* **78**:1703-1709, 2004.

8. Grauss, R. W., Hazekamp, M. G., van Vliet, S., Gittenberger-de Groot, A. C., and DeRuiter, M. C. Decellularization of rat aortic valve allografts reduces leaflet destruction and extracellular matrix remodeling. *J. Thorac. Cardiovasc. Surg.* **126**:2003-2010, 2003.

9. Zhao, X. M., Green, M., Frazer, I. H., Hogan, P., and O'Brien, M. F. Donor-specific immune response after aortic valve allografting in the rat. *Ann. Thorac. Surg.* **57**:1158-1163, 1994.

10. Draft Replacement Heart Valve Guidance. 10-14-1994. United States Food and Drug Administration, Division of Cardiovascular, Respiratory, and Neurological Devices.

11. Herijgers, P., Ozaki, S., Verbeken, E., Van Lommel, A., Racz, R., Zietkiewicz, M., Perek, B., and Flameng, W. Calcification characteristics of porcine stentless valves in juvenile sheep. *European Journal of Cardio-Thoracic Surgery* **15**:134-142, 1999.

12. Ketchedjian, A., Kreuger, P., Lukoff, H., Robinson, E., Linthurst-Jones, A., Crouch, K., Wolfinbarger, L., and Hopkins, R. Ovine panel reactive antibody assay of HLA responsivity to allograft bioengineered vascular scaffolds. *J Thorac Cardiovasc Surg* **129**:159-166, 2005.

13. Hawkins, J. A., Hillman, N. D., Lambert, L. M., Jones, J., Di Russo, G. B., Profaizer, T., Fuller, T. C., Minich, L. L., Williams, R. V., and Shaddy, R. E. Immunogenicity of decellularized cryopreserved allografts in pediatric cardiac surgery: comparison with standard cryopreserved allografts. *J. Thorac. Cardiovasc. Surg.* **126**:247-252, 2003.

14. El Agroudy, A. E., Ismail, A. M., El Chenawy, F. A., Shehab El-Din, A. B., and Ghoneim, M. A. Pretransplant mixed lymphocyte culture still has an impact on graft survival. *Am. J. Nephrol.* **24**:296-300, 2004.

15. Smith, R. A. and Belcher, R. Disparity in HLA-DR typing and mixed lymphocyte culture reactivity. *Ann. Clin. Lab Sci.* **17**:318-323, 1987.

16. *Guide to the care and use of experimental animals*.Canadian Council of Animal Care, 1993.

17. Rayat, G. R., Johnson, Z. A., Beilke, J. N., Korbutt, G. S., Rajotte, R. V., and Gill, R. G. The degree of phylogenetic disparity of islet grafts dictates the reliance on indirect CD4 T-cell antigen recognition for rejection. *Diabetes* **52**:1433-1440, 2003.

18. Honda, T., Nomura, T., and Mukai, F. Prediction of inbreeding in commercial females maintained by rotational mating with partially isolated sire lines. *Journal of Animal Breeding and Genetics* **122**:340-348, 2005.

19. O'Connell, P. J., Hawthorne, W. J., Simond, D., Chapman, J. R., Chen, Y., Patel, A. T., Walters, S. N., Burgess, J., Weston, L., Stokes, R. A., Moran, C., and Allen, R. Genetic and functional evaluation of the level of inbreeding of the Westran pig: a herd with potential for use in xenotransplantation. *Xenotransplantation.* **12**:308-315, 2005.

20. Chardon, P., Kirszenbaum, M., Cullen, P. R., Geffrotin, C., Auffray, C., Strominger, J. L., Cohen, D., and Vaiman, M. Analysis of the sheep MHC using HLA class I, II, and C4 cDNA probes. *Immunogenetics* **22**:349-358, 1985.

21. Jugo, B. M., Joosten, I., Grosfeld-Stulemeyer, M., Amorena, B., and Hensen, E. J. Immunoprecipitation and isoelectric focusing of sheep MHC class I antigens reveal higher complexity than serology. *Eur. J. Immunogenet.* **29**:391-399, 2002.

22. Grossberger, D., Hein, W., and Marcuz, A. Class I major histocompatibility complex cDNA clones from sheep thymus: alternative splicing could make a long cytoplasmic tail. *Immunogenetics* **32**:77-87, 1990.

23. Smulders, M. J. M., Snoek, L. B., Booy, G., and Vosman, B. Complete loss of MHC genetic diversity in the Common Hamster (Cricetus cricetus) population in The Netherlands. Consequences for conservation strategies. *Conservation Genetics* **4**:441-451, 2003.

24. Lewin, H. A. Genetic organization, polymorphism and function of the Bovine Major Histocompatibility Complex. *The major histocompatibility complex of domestic animal species*. Boca Raton: CRC Press, 1996.

25. Amills, M., Francino, O., and Sanchez, A. A PCR-RFLP typing method for the caprine Mhc class II DRB gene. *Vet. Immunol. Immunopathol.* **55**:255-260, 1996.

26. Miltiadou, D., Ballingall, K. T., Ellis, S. A., Russell, G. C., and McKeever, D. J. Haplotype characterization of transcribed ovine major histocompatibility complex (MHC) class I genes. *Immunogenetics* **57**:499-509, 2005.

IV

DECELLULARIZATION REDUCES THE IMMUNOGENICITY OF SHEEP PULMONARY ARTERY VASCULAR PATCHES

INTRODUCTION

Since 1956 allograft cardiovascular tissue has been used for the reconstruction of congenital and acquired lesions of the heart and great vessels in pediatric and adult populations [1]. Cryopreserved allograft vascular tissue has excellent handling characteristics, provides an excellent hemodynamic profile and does not require anti-coagulation. Despite these advantages, cryopreserved allograft vascular tissue elicits a strong cellular and humoral [2-4] immune response in recipients. In the pediatric population, Hawkins demonstrated that when used to correct congenital heart defects in children, allograft valve conduits incite the development of anti-HLA class I and II antibodies [5] that remain detectable even 8 years following implantation [6]. Although the significance of the humoral immune response against allograft heart valves is debated [7], there is evidence that a strong humoral immune response is associated with structural valve failure [8,9]. Increasing data also suggest that the cellular elements in the valve may be primarily responsible for the allogeneic immune response [10]. The host immune response may accelerate the deterioration of the allograft [9] resulting in reduced freedom from re-operation [11] and may complicate future

A version of this chapter has been submitted for publication. Lehr, Rayat, Chiu, Churchill, Eshpeter, McGann, Coe, Korbutt, Ross. J Thorac Cariov Surg..

heart transplantation [12,13]. The host immune response is more profound in younger populations and may accelerate the destruction of the allograft in this population [11]. Thus, one attractive approach in minimizing the allogeneic immune response is to modify the valve. The other approach is to treat the recipients with immunosuppressive agents; however, chronic use of immunosuppressive agents may be associated with severe side effects. Decellularizing the allograft may attenuate the host's immune response [14] by decreasing the expression of MHC antigens on the valve. A number of studies have considered the immunological effect of decellularization of vascular tissue in large animal models; however, none has measured the development of anti-donor antibodies. The aim of this study was to assess the long-term impact of decellularization of vascular tissue on the cellular and humoral immune responses in the ovine large animal model.

MATERIALS AND METHODS

Experimental Animals:

Suffolk sheep were purchased from a local farm and housed in accordance with the guidelines of the Canadian Council of Animal Care [15] at the University of Alberta farm with food and water *ad libitum*. Approval for this study was obtained from the University of Alberta Animal Policy and Welfare Committee. The overall experimental plan is illustrated in Figure IV-1.

Patch Procurement and Preparation:

Following induction with halothane, donor animals were intubated, shaved and aseptically prepped and draped. The left hemithorax was opened widely and the animal was exsanguinated. The pulmonary artery was dissected from the heart to the level of the bifurcation, and transported in RPMI (Gibco, Grand Island, NY, USA) at 4°C. Pulmonary arteries were then decellularized in a series of hypotonic and hypertonic Tris buffers with detergent as previously described [2]. All steps were performed at 4°C in 100mL of solution unless otherwise noted. Briefly, cryopreserved aortic valve conduits were thawed in a 37°C water bath for 20 minutes. The tissue was placed in 100mL of hypotonic Tris buffered solution (10 mM, pH 8.0, 0.1 mM PMSF, 5 mM EDTA) for 48 hours. The solution was replaced with 0.5% octylphenoxy polyethoxyethonal (Triton X-100, Labchem Inc, Pittsburgh, PA, USA) in a hypertonic Tris-buffered solution (50 mM, pH 8.0, 1.5 M KCl, 5 mM EDTA) for an additional 48 hours. Allografts were then bathed in Sorensen's buffer with DNase (25 g/mL, Roche, Laval, QC, Canada), RNase (10 g/mL, Roche, Laval, QC, Canada), and $MgCl_2$ (10 mmol/L) for 5 hours at 37°C. The tissue was then soaked in 0.5% TritonX-100 in Tris buffer (50mmol/L, pH 9.0) for 48 hours and then washed in PBS for 24 hours. Control tissues were prepared as described, but were not decellularized prior to cryopreservation.

Cryopreservation:

Following the protocol of our local tissue bank, decellularized and control tissues were sterilized in antibiotic solution (Colistimethate [75,000 μg/mL, Sterimax Inc, Mississauga, ON, Canada], Vancomycin Hydrochloride [50 μg/mL, Pharmascience Inc., Montreal, QC, Canada], Lincomycin [120 μg/mL, Pharmacia, Kirkland, QC, Canada] and Cefoxitin Sodium [240 μg/mL, Novopharm, Toronto, ON, Canada]) for 24 hours. Valve conduits were rinsed 3 times in 4°C Ringer's Lactate solution (Baxter, Toronto Canada)and transferred into 100 mL 7.5% Me_2SO (Fisher Scientific, Fair Lawn, NJ, USA) in X-Vivo (Cambrex Bio Science, Walkersville, MD, USA) at 4°C for 30 minutes. After packaging in a 3-bag system, the tissue was frozen in a Cryomed 1010 programmable rate-controlled freezer (Cryomed, Mount Clements, MI, USA). The freezing protocol consisted of 5 phases. Tissues were cooled from ambient temperature to 4°C and then supercooled to -2°C. Seeding was accomplished by a burst of cold nitrogen to initiate ice formation in the supercooled sample. Cooling then proceeded at a rate of 1°C/min to -50°C and then at a rate of 7°C/min until the allograft reached -100°C. Conduits were stored in vapor phase liquid nitrogen until required.

Implant Procedure:

Patch material was thawed at 37°C in a water bath and was cut into a diamond shaped patch using a 2x4cm template. Recipient animals were induced with 5% halothane which was reduced to 1% – 2% with 50% nitrous oxide to

maintain a surgical plane. Following oral-tracheal intubation with a 6F endotracheal tube, intravenous access was established and ampicillin (1g, Novopharm, Toronto, ON, Canada), gentamycin (1g, Sandoz, Princeton, NJ, USA) and rocuronium (50mg, Organon Canada Ltd., Toronto, ON, Canada) were administered intravenously. The animal was shaved, prepped and draped aseptically and an incision was made in the fifth left intercostal space. The pleura overlying the aorta was opened and suspended with 3-0 polyprolene suture, (Ethicon, Inc., Somerville, NJ, USA). After controlling the intercostal arteries from the 4^{th} to the 6^{th} interspace, the aorta was encircled with umbilical tapes and secured with snares. Between clamps above and below the 4^{th} and 6^{th} intercostal arteries, the aorta was opened with an 11 blade and the aortotomy extended proximally and distally. A 9 cm long phosphorylcholine coated 1/4 inch (internal diameter) polyvinylchloride tube was then inserted as previously described into the aorta via the aortotomy so as to create an intra-aortic shunt to prevent spinal cord ischemia [16]. Using a continuous 5-O polypropylene suture (Ethicon), the patch was sewn in place. Just prior to tying the suture, the last few stitches were loosened and the shunt was removed while re-applying DeBakey vascular clamps. Once the aortoplasty was complete, the clamps were removed. After obtaining hemostasis, the thoracotomy was closed in layers and anesthesia was concluded.

Immunohistochemistry:

Sections of explanted grafts were fixed overnight in Z-fix (Anatech Ltd, Battle Creek, MI, USA), then processed and embedded in paraffin, after which 3μm sections were cut and placed on histobond slides (Marienfeld, Germany). After rehydration, endogenous peroxidases in tissue sections were quenched by a solution of 10% hydrogen peroxide in methanol for 6 minutes. Microwave antigen retrieval was performed when required for 15 minutes at 80% power using either 10mM sodium citrate solution (pH 6) or 10mM Tris 1mM EDTA (pH 9), followed by a cool down period of 15 minutes. Blocking was performed with 20% normal goat serum (Jackson ImmunoResearch Laboratories, West Grove, PA, USA) for 15 minutes at room temperature. Tissue sections were stained with primary antibodies against interstitial cells (mouse anti-vimentin, 1:50, Dako Cytomation, Missisauga, Canada), endothelial cells (anti-CD31, 1:50 (MCA1812, Serotec, Kidlington, UK; anti-von Willebrand factor, 1:100 AB7356, Chemicon International, Temecula, CA, USA); B-cells, mouse anti-CD79αcy, 1:200 M7051, Dako) and TGFβ (anti-human TGFβ, 1:100 MCA797, AbD Serotec, Kidlington, UK). We attempted staining for T-cells and T-cell subpopulations, but suitable antibodies were not available for sheep. The primary antibody incubation was 60 minutes followed by three washes in PBS for 5 minutes. Biotinylated goat anti-mouse IgG secondary antibody (Jackson Immuno Research Laboratories, Inc, West Grove, PA, USA) at 1:200 dilution was applied to tissue sections for 20

minutes at room temperature. After three washes in PBS, sections were incubated with the avidin-biotin-enzyme complex (ABC) for 40 minutes at room temperature (Vector Laboratories, Burlingame, CA, USA), washed three times in PBS, and developed using diaminobenzidine as chromagen (Signet Laboratories Inc., Dedham, MA, USA). The sections were then counterstained with Harris' Hematoxylin (Electron Microscopy Sciences, Hattlefield, PA, USA), and coverslipped using Entellan mounting media. Paraffin-embedded sections were also stained with hematoxylin and eosin and Movat's pentachrome as per standard technique.

Electron Microscopy:

Sections of explanted patches were prefixed in 2.5% glutaraldehyde in Millonig's buffer (pH 7.2) at room temperature for 1 hour. Samples were then washed in the same buffer three times for 10 minutes each and then placed in 1% OsO_4 at room temperature for 1 hour. After a brief wash in distilled water, samples were dehydrated in a series of ethanol (50% - 90%) washes for 10 minutes each followed by three additional washes in absolute ethanol for 10 minutes each. Samples were then dried in a CO_2 critical-point dryer (Seevac Inc. Pittsburgh, PA, USA) at 31°C for 10 minutes. All samples were mounted on aluminum stubs and sputter coated with gold (Edwards Sputter Coater, S150B, UK). Digital micrographs of samples were taken with a Hitachi Scanning Electron Microscope S2500 (Hitachi, Tokyo, Japan) as previously described [17].

Determination of Humoral Response:

Sheep anti-sheep IgG antibodies in recipient serum were measured by flow cytometry as previously described [18] and as outlined in Figure IV-2. Briefly, splenocytes were isolated from donor animals by mincing portions of spleen between sterile glass microscope slides in 10mL normal saline (Baxter, Toronto, Ontario, Canada). The resulting mixture was washed twice in normal saline. Contaminating red blood cells were lysed using red blood cell lysis buffer (0.15M NH_4Cl, 1.0mM $KHCO_3$, 0.1nM Na_2EDTA, pH 7.3). Splenocytes were then washed twice in 0.9% saline and frozen at a concentration of $2.5x10^7$/mL in 10% dimethyl sulfoxide and fetal bovine serum (FBS) at -86°C until needed. Blood (10 mL) was collected from recipient animals at time of implantation, weekly for 4 weeks and then monthly until the end of the experimental period. Clotted blood was centrifuged at 1500 rpm for 5 minutes. Serum was aspirated, aliquoted into 1.5 mL Eppendorf tubes and frozen at -86°C until required.

Splenocytes were thawed in 40mL of HBSS (Invitrogen, Burlington, Canada) supplemented with DNase (1mg/L, Roche, Laval, Canada) then incubated at 37°C for 40 minutes. Cells were centrifuged (1500 rpm for 5 minutes) and resuspended (2.5×10^6 cells/mL) in FACS buffer (PBS, 1% fetal bovine serum, Sigma, Oakville, Canada) and aliquoted (5×10^5 cells per well) onto a 96-well v-bottom plate (Nalge Nunc International, Rochester, NY, USA). After centrifugation at 1200 rpm for 2 minutes, the supernatant was aspirated and

the donor splenocytes were resuspended in 50 μL of recipient serum (1:8 dilution; in FACS buffer) and incubated at 37°C in a humidified atmosphere of 95% air and 5% CO_2 for 1 hour. Splenocytes were washed twice in 100 μL FACS buffer and incubated with 50 μL Fluorescein isothyocyanate (FITC)-conjugated AffiniPure rabbit anti-sheep IgG, Fc fragment specific antibody (313-095-046, 1:200; FACS buffer, Jackson ImmunoResearch Laboratories, Inc, West Grove, PA, USA) in the dark for 30 minutes at 4°C. After washing twice in FACS buffer, splenocytes were resuspended in 200 μL FACS buffer and transferred into 5 polystyrene round bottom tubes (BD Falcon, Bedford, MA, USA) in a total volume of 500 μL. The percentage of cells bound to antibody was detected from single parameter fluorescence histograms on a flow cytometer (FACSCalibur, BD Biosciences, Ontario, Canada) after gating on viable spleen cells. Controls for this experiment included serum taken at baseline, unstained donor splenocytes, and donor splenocytes with secondary antibody without recipient serum.

Calcification:

Calcium concentration in the explanted samples was determined according to the methods described by Sarkar and Chauhan[19] and expressed as mg calcium per mg protein, measured as described by Lowry et al [20].

RNA Isolation and Reverse Transcription-Polymerase Chain Reaction (RT-PCR) For Expression of Cytokines:

Samples were crushed in liquid nitrogen, dissolved in 1 mL of Trizol reagent (Invitrogen) and RNA extracted according to the manufacture's protocol. cDNA was constructed from 1 μg of total RNA using MultiScribe Reverse Transcriptase (Applied Biosystems, Foster City, CA, USA) according to the manufacture's protocol and 1 μL of cDNA was amplified using AmpliTaq Gold (Applied Biosystems). The PCR conditions were as follows: 95°C for 9 minutes, followed by 40 cycles of 95°C for 30 seconds and 60°C for 30 seconds with a final extension of 72°C for 12 minutes utilizing primer pairs that span at least one intron. PCR products were separated on an ethidium bromide (Sigma, Oakville, Canada) stained agarose gel (1.5%) and images captured with Alpha Digidoc software (Perkin-Elmer, Boston, MA). Bands of the expected size were ligated in the pCR5-TOPO vector (TOPO TA Cloning Kit for Sequencing, Invitrogen Canada Inc, Burlington, ON, Canada), sequenced (University of Alberta DNA Core Lab, Edmonton, AB, Canada) and compared with known GenBank sequences. Positive control consisted of sheep spleen cDNA, while the negative control consisted of water in place of experimental cDNA and GAPDH (housekeeping gene) ensured cDNA integrity.

Statistical Analysis:

Continuous data were expressed as mean ± standard error of the mean (SEM). Means of multiple groups were compared by one-way analysis of variance with Scheffe post hoc analysis to compare individual groups using SPSS 13.0 (SPSS Inc., Chicago, USA).

RESULTS

Histology and Immunohistochemistry:

Histological assessment of the tissue prior to implantation confirmed effective decellularization (Figure IV-3). Hematoxylin and eosin staining showed an acellular matrix. In contrast to non-decellularized grafts, no endothelium was present and only ghosts of cells were present. The internal and external elastic lamina were preserved as was the vasovasorum. The pale pink color of decellularized sections suggests a reduction in cytoplasm compared to control sections.

Four weeks after implant, non-decellularized patches demonstrated a number of findings in all layers of the graft that are consistent with immune rejection (Figure IV-4). There was profound cellular neointimal hyperplasia that appears to be arising from metabolically active myofibroblastic cells, and the media was edematous and very cellular. A patchy infiltrate of lymphocytes emerging from nearby vasculature was seen primarily near the border of the

external elastic lamina. The nuclei of stromal cells were fragmented and pyknotic and there was myofibroblastic proliferation within the media with neovascualrization (H&E). Movat's penachrome staining demonstrated fragmentation of the internal and external elastic lamina. Smooth muscle cell proliferation in the media was evident as indicated by vimentin staining. In addition, there was increased vascularity of the adventitia with thickened blood vessels as shown by CD31 and Von Willebrand Factor staining but none of the cells in the infiltrate stained positive for CD79 (Figure IV-5).

Similar findings were seen in control patches at 6 months (Figures IV-4 and IV-5). Specifically, the media remained edematous. The patchy immune cell infiltrate persisted and there was now evidence of karyorexis. Mononuclear cells were identified just under the endothelium. Increased myofibroblasts appear near the medial-adventitial and medial-intimal junction leading to increased periadventitial fibrosis. Smooth muscle cell proliferation and macrophages were evident in the media and CD79 positive cells were associated with blood vessels in the periadventitial region (Figure IV-5).

Compared to non-decellularized patches, decellularized grafts demonstrated fewer features consistent with immune rejection although evidence of inflammation remained (Figures IV-4 and IV-5). Myofibroblastic cells in the media were still active, there was focal thickening of the endothelial layer and the external elastic lamina remained fragmented. In distinct contrast to the control

patches, there was minimal lymphocyte infiltrate in the decellularized graft at 4 weeks and at 6 months. There was less vasculature in the adventitia of decellularized patches and the endothelial layer of the vaso vasorum was much thinner compared to control patches. There were no CD79 positive cells identified in decellularized patches at 4 weeks and at 6 months (Figure IV-5).

TGF-β was strongly expressed, particularly at the medial-adventitial junction at 4 weeks and 6 months in control patches, but only in occasional spindle cells in decellularized patches at 4 weeks but not at 6 months (Figure IV-5).

Scanning Electron Microscopy:

Scanning electron microscopy of explanted grafts demonstrate white blood cells on the surface of non-decellularized grafts at 4 weeks. White blood cells were not seen on the endothelial surface of decellularized grafts. At 4 weeks after implant, the intimal surface was fully re-endothelialized (Figure IV-6).

Humoral Response:

We next examined the effect of decellularization on the production of recipient anti-donor antibodies and found that *in-vivo* production of donor-specific antibodies was inhibited by decellularization (Figure IV-7). When donor sheep cells were incubated with recipient sheep sera, a trend towards reduced binding of alloreactive ovine IgG antibodies to donor splenocytes was identified at 4 weeks (2.92 ± 0.63 decellularized vs. 24.08 ± 10.53 non-decellularized, $p = 0.115$,

independent samples t test, equal variance not assumed). Antibody production peaked at 3 to 4 months post surgery at which point a significant difference was identified between groups (9.82± 3.25 decellularized, 57.77± 13.70, non decellularized, $p = 0.010$).

Cytokine Expression:

mRNA transcripts for interferon gamma (IFN-γ, type 1 cytokine), interleukin 10 (IL-10, type 2 cytokine), and transforming growth factor beta 1 (TGF-β1, regulatory cytokine) were identified by RT-PCR in all non-decellularized grafts at 4 weeks. Decellularization reduced the number of grafts expressing IL-10 (67%) and IFN-γ (67%) at 4 weeks, but TGF-β1 was expressed in all grafts at 4 weeks (data not shown). mRNA transcripts for interleukin 4 (IL-4) were found in two of four non-decellularized grafts at 4 weeks but were not detected in any of the decellularized grafts. Fifty percent of both decellularized and non-decellularized grafts expressed tumor necrosis factor α (TNF-α). Seventy-five percent of non-decellularized grafts expressed IL-2 at 4 weeks whereas IL-2 was expressed in only fifty percent of decellularized grafts. Taken together, these results show that all cytokines examined were detected in non-decellularized control allografts at 4 weeks but not at 6 months after transplantation indicating that there was complete cellular and humoral rejection of the graft at this time. In addition, decellularization reduced both type 1 and type 2 cytokines.

Calcification:

A trend towards a reduction in calcification was observed in the decellularized group (7.6 ± 4.3 mg calcium/mg protein vs. 36.9 ± 15.9, p = 0.107) (Figure IV-8).

Clinical Results:

A single animal receiving a decellularized patch died at 61 days after implant from a ruptured patch in the setting of a large abscess. On explantation, all decellularized patches appeared to be well healed by four weeks without evidence of aneurismal dilation or major tissue failure by gross examination.

CONCLUSIONS

Since Hufnagel developed the first mechanical heart valve, significant improvements have been made in the design and in surgical techniques which have resulted in an excellent safety profile for existing prostheses. Moreover, allograft valves have become important in the pediatric population. However, all of the currently available prostheses fall short of being the ideal valve replacement that would not require anticoagulation, provide normal hemodynamic function, last the life of the patient, non-immunogenic, non-thrombogenic and resist infection. Currently available biological valves, both allograft and xenograft have been shown to induce a recipient immune response that may lead to the structural deterioration of the valve.

In this study, we provide evidence that decellularization reduces the cellular and donor-specific humoral immune responses of the recipients. Histological analysis of non-decellularized control patches demonstrated patchy infiltration of mononuclear immune cells at 4 weeks after implantation that persisted at 6 months and was confirmed by electron microscopy. At 4 weeks, B cells (CD79-positive) were absent in the graft, but at 6 months, there was a population of B cells amoung the infiltrating immune cells. Decellularization was effective at reducing the cellular infiltrate as no immune cells were identified in the decellularized patches at either 4 weeks or 6 months after implant.

We also found a profound humoral immune response in animals that received the non-decellularized control patches, as measured by flow cytometry. The humoral response in these animals peaked between 3 and 4 months and then began to decrease as expected when the primary response subsides. In contrast, animals that received decellularized patches failed to generate any detectable anti-donor antibodies. The complete lack of antibodies in recipients of decellularized grafts as well as the lack of B cells in the grafts of these animals indicates a complete prevention of the development of the donor-specific humoral response against the grafts.

The mechanisms of cellular immunity following implantation of allograft or decellularized allografts have not been elucidated. Our results provide initial insights into two putative pathways that may be active. By RT-PCR analysis, we

demonstrated that decellularization reduced the number of grafts expressing type 1 cytokines (IFN-γ), and type 2 cytokines (IL-10) but there was no change in the number of grafts expressing TGF-β1. These further suggest that rejection of the allograft vascular patch is mediated by both cellular and humoral immune responses and that decellularization attenuates both of these response mechanisms. In contrast, upregulation of TGF-β1 may be a generalized response to the surgery or represent a non-antigen dependent generalized response to vascular injury. Although TGF-β1 protein was not identified in the decellularized patches, mRNA transcripts for this cytokine were identified at 4 weeks. Schulick et al demonstrated that local upregulation of TGF-β1 results in cartilaginous metaplasia of the arterial wall and intimal growth [21]. This ongoing signal by TGF-β1 may be the stimulus for the profound endothelial hyperplasia seen in both control and decellularized patches. At six months, IFN-γ and IL-10 were no longer expressed in non-decellulalrized control patches suggesting that the graft was completely rejected at this time. Similarly, at six months, TGF-β1 was not detected on tissue sections or in RT-PCR analysis further suggesting that the non-antigen dependent response had subsided. Additional work is required to delineate further the cytokine pathways involved in allograft rejection and in the surgical procedure response. Future work may lead to adjunctive treatments that may be beneficial in extending the durability of allograft and tissue engineered valve replacements. Although the observed cellular response and in-graft cytokine production may be

representative of a general inflammatory reaction against the implanted tissue, the humoral response confirms anti-donor specific reactivity.

We observed a trend towards reduced calcification in decellularized grafts. This trend however, did not reach statistical significance perhaps due to the large variation in calcification in the non-decellularized control group. It is not clear at this time why some animals had a high degree of graft calcification while others did not.

Evidence for structural changes in both control and decellularized patches after implant was also identified. The mechanism of these changes is not evident by this work, but it is unlikely that these changes are an antigen-directed immune response, or related to the decellularization process given the lack of antibody production and immune cell infiltrate. Moreover, similar changes were identified in control and experimental patches. It is possible that the cryopreservation method created an injury that was not apparent by histology, but manifests post-implant, or that cryopreservation causes injury leading to a generalized tissue-directed host inflammatory response. It remains to be determined whether decellularized valves are structurally weaker than standard cryopreserved valves. Decellularized porcine valves implanted in the pediatric population elicited a profound inflammatory response resulting in rapid degeneration of the valve wall and leaflets [22]. The mechanisms resulting in failure of these decellularized xenograft valves have not been fully elucidated, but may be related to incomplete

decellularization, the decellularization process or a xenogeneic immune response [23]. We did not observe any structural failures or aneurysm formation in either control or decellularized valves. In addition, implanted decellularized patches showed myofibroblastic repopulation of the matrix although at this point their potential for contribution towards growth and repair is not clear.

In conclusion, we demonstrated that osmotic lysis with octylphenoxy polyethoxyethonal effectively decellularized ovine pulmonary artery patches. This decellularization process attenuates both the cellular and humoral allogeneic immune response in sheep although some microscopic deterioration in structure was identified in both non-decellularized and decellularized grafts.

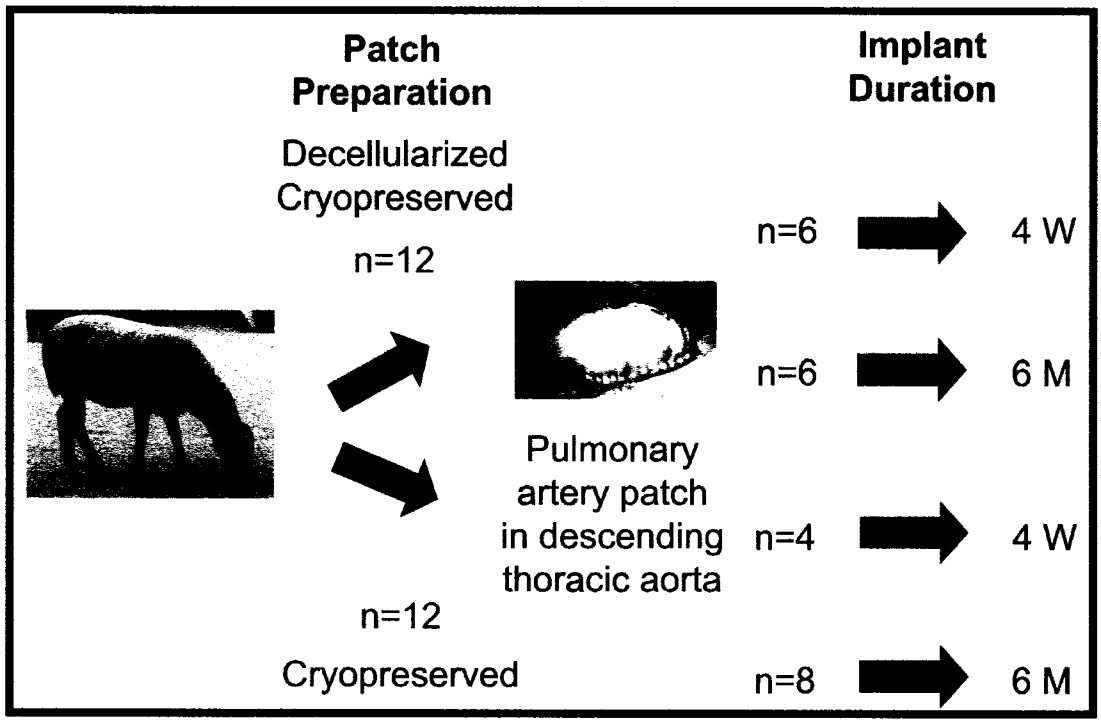

Figure IV-1. Overall experimental design for assessing the effect of decellularization on the recipient cellular and humoral immune responses.

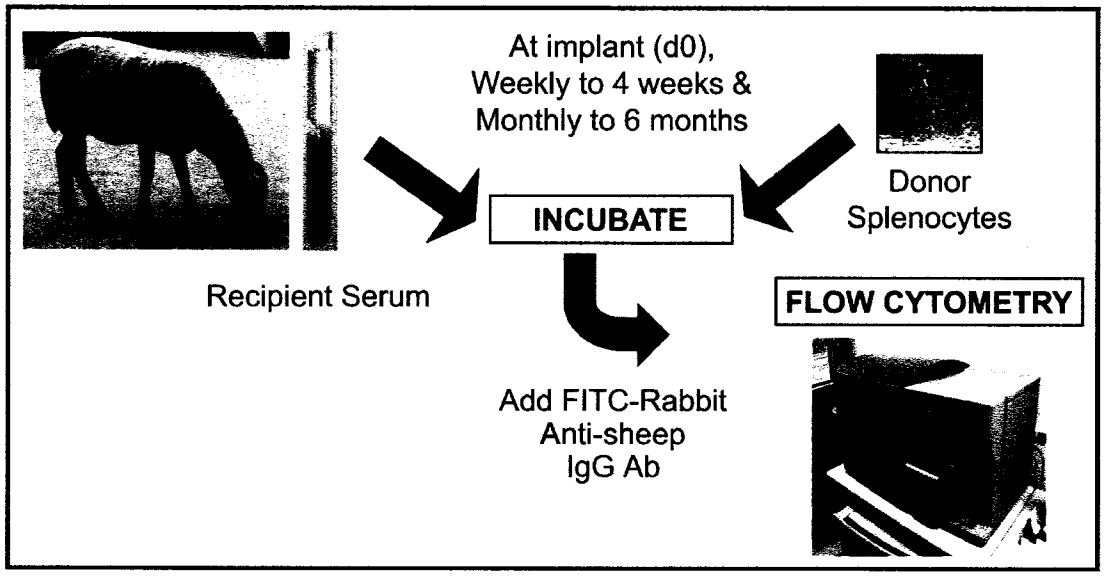

Figure IV-2. Experimental method for the determination of the recipient's donor-specific humoral immune response.

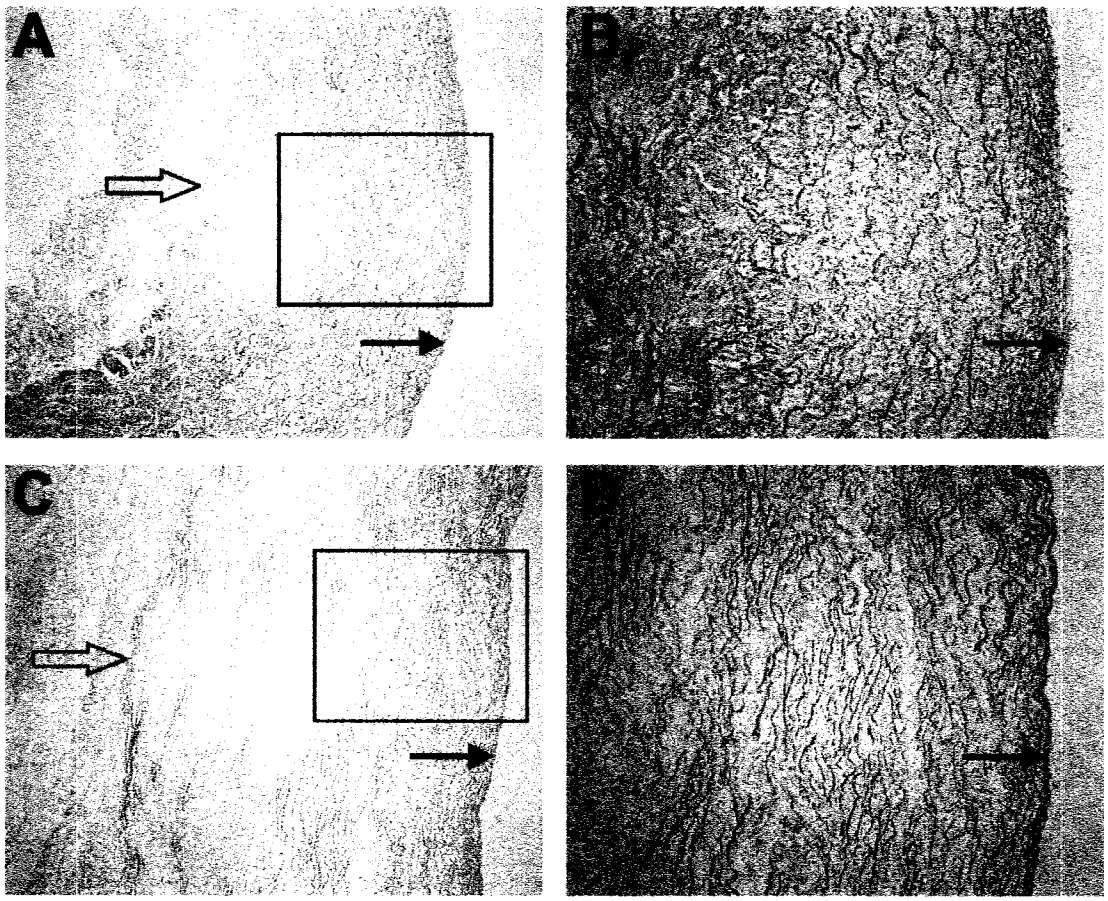

Figure IV-3. Photomicrographs of representative sections of non-decellularized and decellularized patches at time of implant. Samples were fixed in formaldehyde, embedded in paraffin, sectioned at 5 μm and stained with hematoxylin and eosin. Solid arrows and outline arrows indicate the external and internal lamina respectively. Photomicrographs A and C, represent 40X magnification of non-decellularized and decellularized grafts, respectively, B and

D are the same images but at high power magnification (100X) from the region indicated by boxes in A and C, respectively.

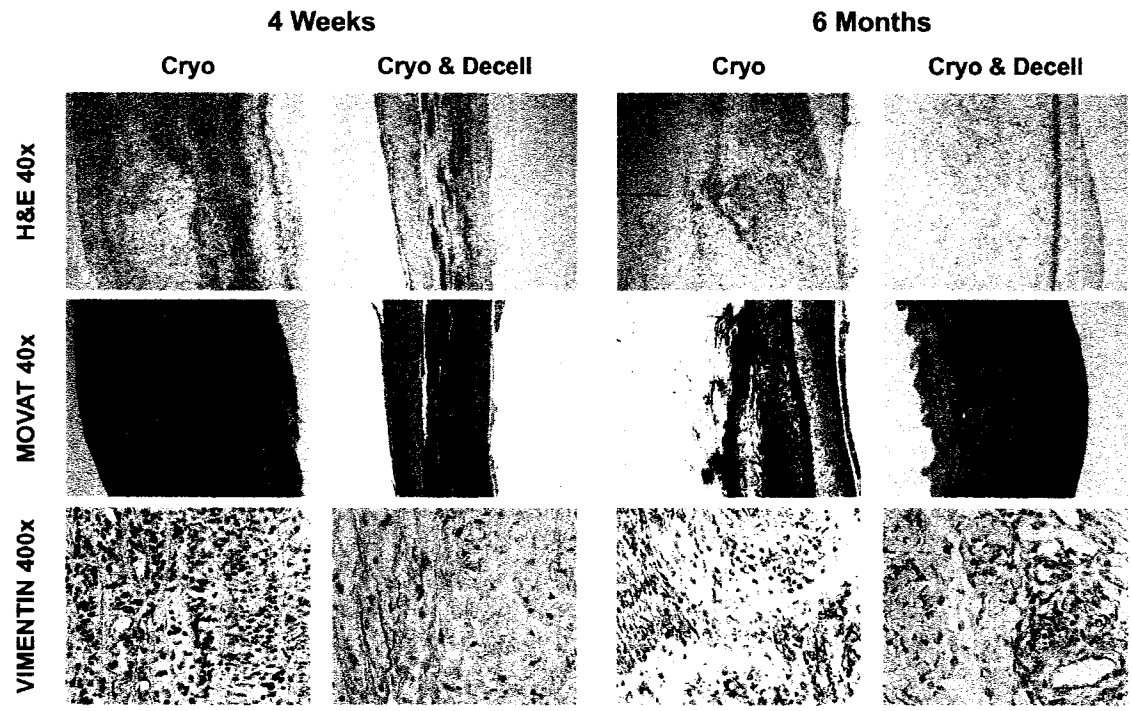

Figure IV-4. Overall morphology of allogeneic ovine pulmonary artery patches at 4 weeks and 6 months after implantation. Both decellularized and non-decellularized grafts show thickening of the intima and adventitia as well as disruption of the external elastic lamina with myofibroblastic proliferation (Movat's pentachrome stain). The media of non-decellularized patches is edematous.

:

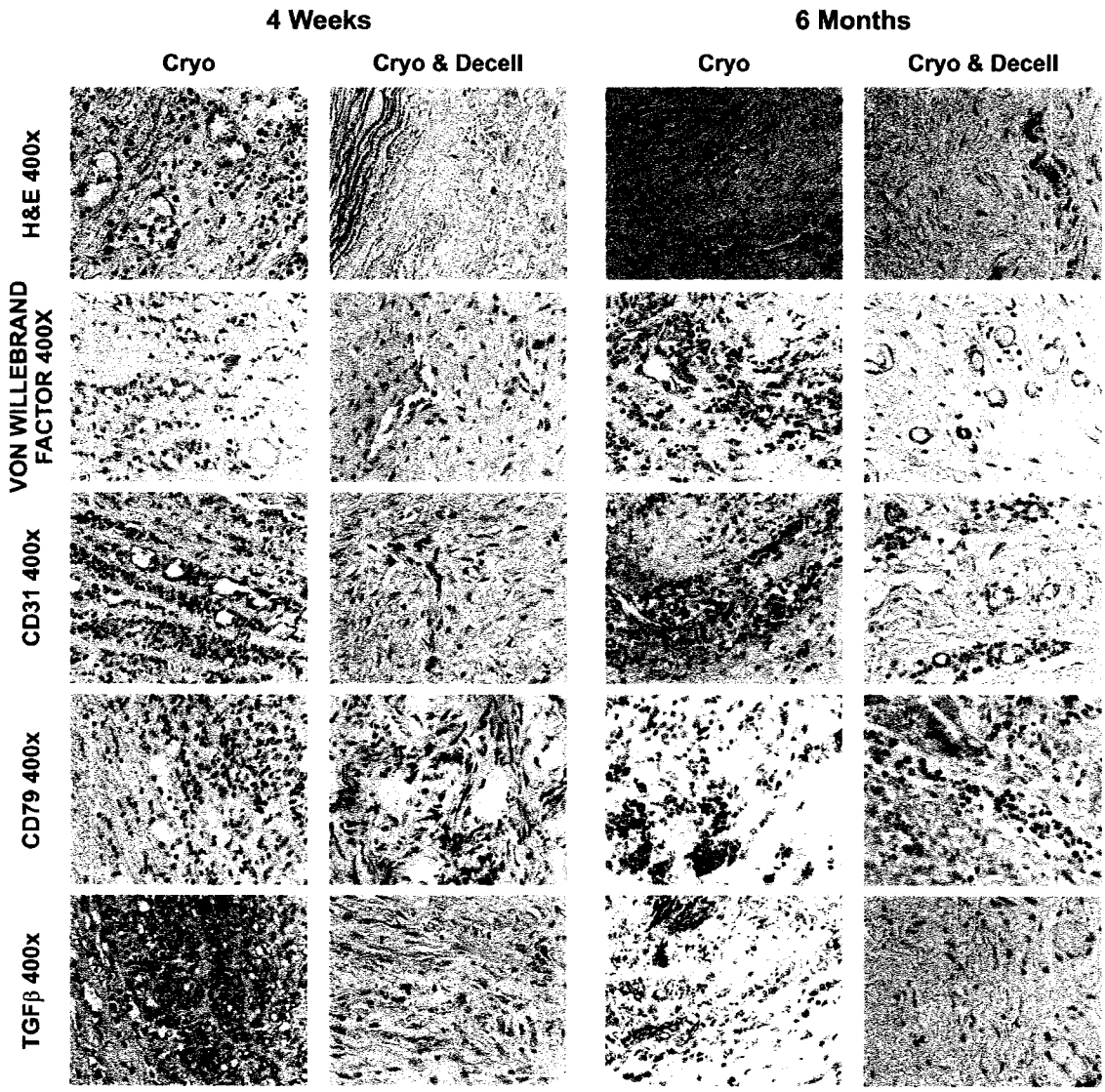

Figure IV-5. Immunohistochemistry of decellularized and non-decellularized pulmonary artery allograft patches at 4 weeks and 6 months after implant. Non-decellularized grafts have early and intense inflammatory cell infiltrate (H&E). Neovascularization of the adventitia and media with thickened vessels ($CD31^+$

and vWF) were also detected. B cells ($CD79^+$) were identified in the perivascular regions at the medial-adventitial junction in non-decellularized grafts at 6 months and TGF-ß was detected predominantly in the non-decellularized grafts at both time points. In contrast, decellularization of the graft attenuates the allogeneic immune response. Magnification is at 400x

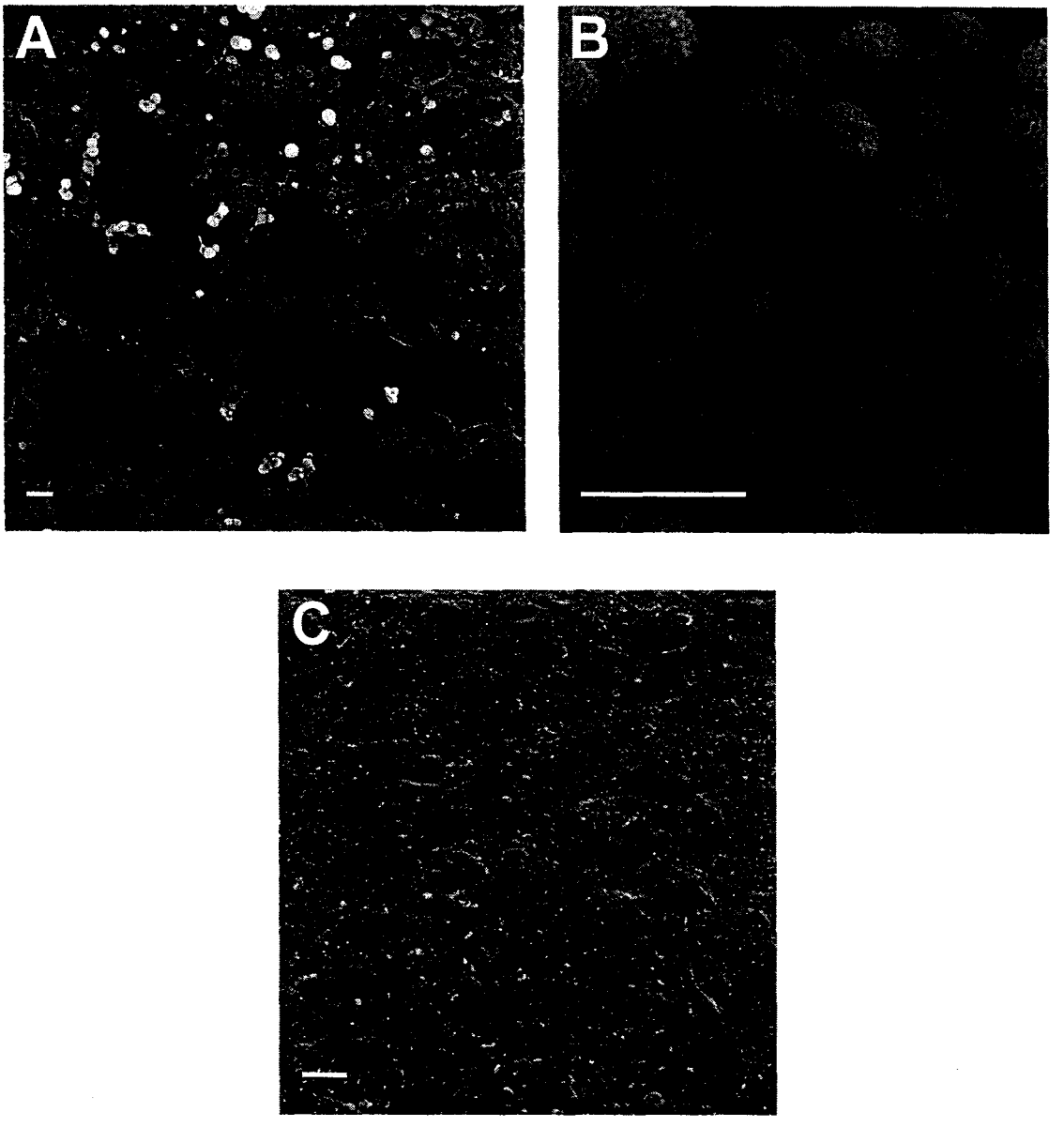

Figure IV-6. Scanning electron microscopy of the endothelial surface of explanted non-decellularized (A & B), and decellularized (C) pulmonary artery

patches at 4 weeks. Both non-decellularized and decellularized patches show re-endothelialization, but white blood cell infiltrate is identified only on non-decellularized grafts. Bar indicates 10 μm in all electronmicrographs.

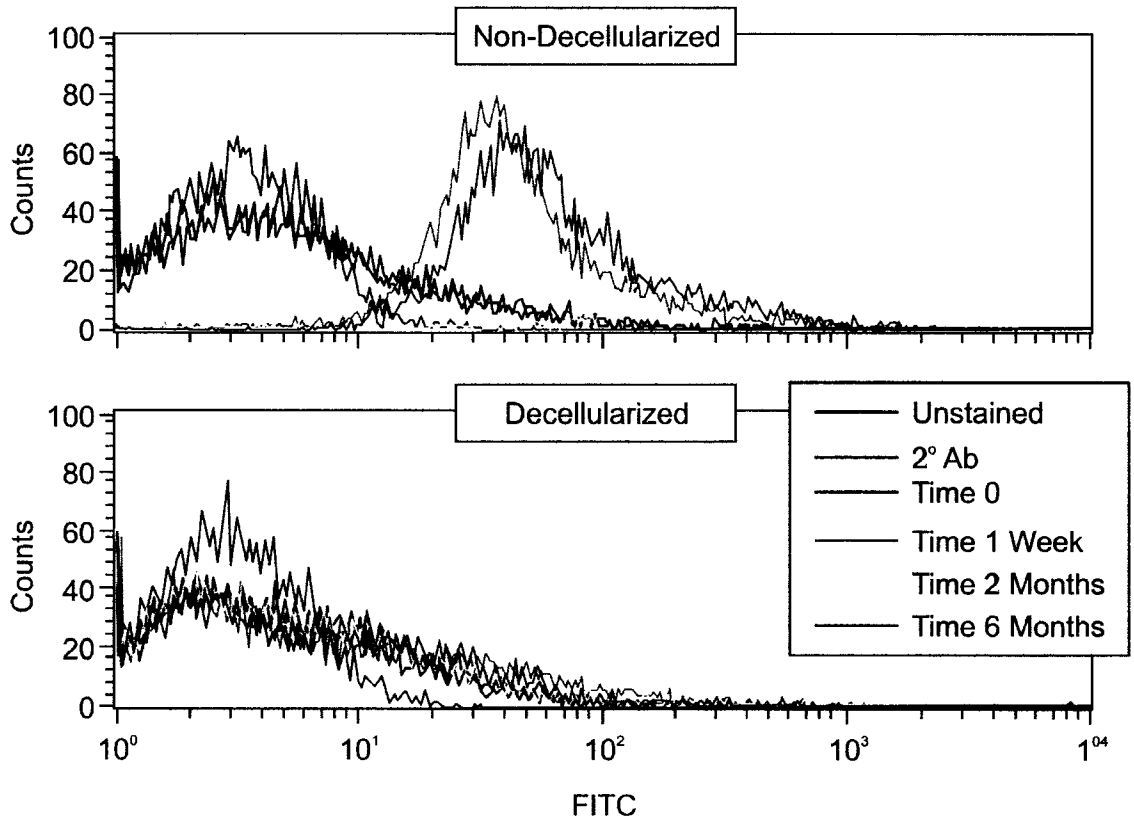

Figure IV-7. Flow cytometric determination of the humoral response of sheep receiving allograft pulmonary artery patches. Recipient generation of anti-donor IgG peaks at 2 months post implant. Decellularization of donor pulmonary artery patches eliminates the development of the recipient humoral immune response. 2^{o} Ab, Secondary antibody alone.

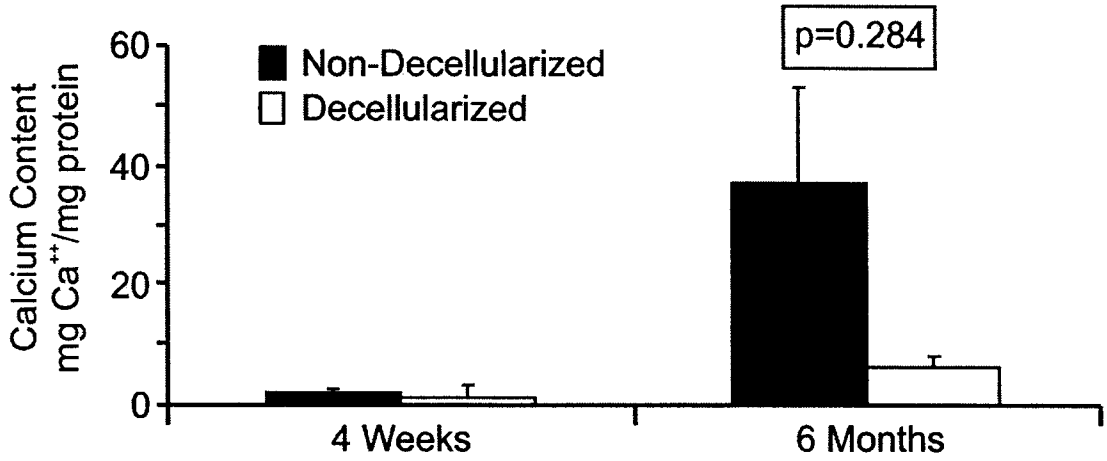

Figure IV-8. Calcification of non-decellularized and decellularized pulmonary artery patches at 4 weeks and 6 months. There is a wide variation in the degree of calcification of non-decellularized grafts. An overall trend towards reduced calcification is seen in the decellularized grafts compared to the non-decellularized grafts.

Table IV-1. Primers used for PCR amplification

Gene	Size (bp)	Strand	Sequence 5'-3'	GenBank
IL-2	214	F	ATG CCC AAG GTT AAC GCT AC	AF287479
		R	CAG CCT TTA CTG TCG CAT CA	
IL-4	206	F	GTA CCA GCC ACT TCG TCC AT	NM_001009313
		R	GCA CAT GTG GCT CCT GTA GA	
IL-10	201	F	TGT TGA CCC AGT CTC TGC TG	NM_001009327
		R	AGG GCA GAA AAC GAT GAC AG	
IFN-γ	236	F	TAA GGG TGG GCC TCT TTT CT	NM_001009803
		R	CAT CCA CCG GAA TTT GAA TC	
TNF-α	335	F	GGC TCT CCT GTC TCC CGT	NM_001024860
		R	ATT GAT GGC TTT GCG CTG	
TGF-β1	157	F	CAC GTG GAG CTG TAC CAG AA	NM_001009400
		R	GGC GAA AGC CTT CTA TTT CC	
GAPDH	310	F	AAT CCC ATC ACC ATC TTC CA	NM_008084
		R	GGC AGT GAT GGC ATG GAC TG	

REFERENCES

1. MURRAY, G. Homologous aortic-valve-segment transplants as surgical treatment for aortic and mitral insufficiency. *Angiology* **7**:466-471, 1956.

2. Meyer, S. R., Nagendran, J., Desai, L. S., Rayat, G. R., Churchill, T. A., Anderson, C. C., Rajotte, R. V., Lakey, J. R., and Ross, D. B. Decellularization reduces the immune response to aortic valve allografts in the rat. *J. Thorac. Cardiovasc. Surg.* **130**:469-476, 2005.

3. Hogan, P., Duplock, L., Green, M., Smith, S., Gall, K. L., Frazer, I. H., and O'Brien, M. F. Human aortic valve allografts elicit a donor-specific immune response. *J. Thorac. Cardiovasc. Surg.* **112**:1260-1266, 1996.

4. Hoekstra, F., Witvliet, M., Knoop, C., Akkersdijk, G., Jutte, N., Bogers, A., Claas, F., and Weimar, W. Donor-specific anti-human leukocyte antigen class I antibodies after implantation of cardiac valve allografts. *J. Heart Lung Transplant.* **16**:570-572, 1997.

5. Hawkins, J. A., Breinholt, J. P., Lambert, L. M., Fuller, T. C., Profaizer, T., McGough, E. C., and Shaddy, R. E. Class I and class II anti-HLA antibodies after implantation of cryopreserved allograft material in pediatric patients. *J. Thorac. Cardiovasc. Surg.* **119**:324-330, 2000.

6. Hooper, D. K., Hawkins, J. A., Fuller, T. C., Profaizer, T., and Shaddy, R. E. Panel-reactive antibodies late after allograft implantation in children. *Ann. Thorac. Surg.* **79**:641-644, 2005.

7. Yap, C. H., Skillington, P. D., Matalanis, G., Davis, B. B., Tait, B. D., Hudson, F., Ireland, L., Nixon, I., and Yiil, M. Anti-HLA antibodies after cryopreserved allograft valve implantation does not predict valve dysfunction at three-year follow up. *J. Heart Valve Dis.* **15**:540-544, 2006.

8. Pompilio, G., Polvani, G., Piccolo, G., Guarino, A., Nocco, A., Innocente, A., Porqueddu, M., Dainese, L., Veglia, F., Sala, A., and Biglioli, P. Six-year monitoring of the donor-specific immune response to cryopreserved aortic allograft valves: implications with valve dysfunction. *Ann. Thorac. Surg.* **78**:557-563, 2004.

9. Dignan, R., O'Brien, M., Hogan, P., Thornton, A., Fowler, K., Byrne, D., Stephens, F., and Harrocks, S. Aortic valve allograft structural deterioration is associated with a subset of antibodies to human leukocyte antigens. *J. Heart Valve Dis.* **12**:382-390, 2003.

10. Johnson, D. L., Rose, M. L., and Yacoub, M. H. Immunogenicity of human heart valve endothelial cells and fibroblasts. *Transplant. Proc.* **29**:984-985, 1997.

11. Yankah, A. C., Alexi-Meskhishvili, V., Weng, Y., Schorn, K., Lange, P. E., and Hetzer, R. Accelerated degeneration of allografts in the first two years of life. *Ann. Thorac. Surg.* **60**:S71-S76, 1995.

12. Meyer, S. R., Campbell, P. M., Rutledge, J. M., Halpin, A. M., Hawkins, L. E., Lakey, J. R., Rebeyka, I. M., and Ross, D. B. Use of an allograft patch in repair of hypoplastic left heart syndrome may complicate future transplantation. *Eur. J Cardiothorac. Surg* **27**:554-560, 2005.

13. Jacobs, J. P., Quintessenza, J. A., Boucek, R. J., Morell, V. O., Botero, L. M., Badhwar, V., van Gelder, H. M., Asante-Korang, A., McCormack, J., and Daicoff, G. R. Pediatric cardiac transplantation in children with high panel reactive antibody. *Ann. Thorac. Surg.* **78**:1703-1709, 2004.

14. Grauss, R. W., Hazekamp, M. G., van Vliet, S., Gittenberger-de Groot, A. C., and DeRuiter, M. C. Decellularization of rat aortic valve allografts reduces leaflet destruction and extracellular matrix remodeling. *J. Thorac. Cardiovasc. Surg.* **126**:2003-2010, 2003.

15. *Guide to the care and use of experimental animals*.Canadian Council of Animal Care, 1993.

16. Lehr, E. J., Coe, J. Y., and Ross, D. B. A simple intra-aortic shunt restores blood flow and prevents paralysis during aortic surgery in sheep. The Journal of Experimental Surgery . 2007.

17. Megyesi, J. F., Findlay, J. M., Vollrath, B., Cook, D. A., and Chen, M. H. In vivo angioplasty prevents the development of vasospasm in canine carotid arteries. Pharmacological and morphological analyses. *Stroke* **28**:1216-1224, 1997.

18. Rayat, G. R. and Gill, R. G. Indefinite survival of neonatal porcine islet xenografts by simultaneous targeting of LFA-1 and CD154 or CD45RB. *Diabetes* **54**:443-451, 2005.

19. Sarkar, B. C. and Chauhan, U. P. A new method for determining micro quantities of calcium in biological materials. *Anal. Biochem.* **20**:155-166, 1967.

20. Lowry, O. H., ROSEBROUGH, N. J., FRR, A. L., and RANDALL, R. J. Protein measurement with the Folin phenol reagent. *J. Biol. Chem.* **193**:265-275, 1951.

21. Schulick, A. H., Taylor, A. J., Zuo, W., Qiu, C. B., Dong, G., Woodward, R. N., Agah, R., Roberts, A. B., Virmani, R., and Dichek, D. A. Overexpression of transforming growth factor beta1 in arterial endothelium causes

hyperplasia, apoptosis, and cartilaginous metaplasia. *Proc. Natl. Acad. Sci. U. S. A* **95**:6983-6988, 1998.

22. Simon, P., Kasimir, M. T., Seebacher, G., Weigel, G., Ullrich, R., Salzer-Muhar, U., Rieder, E., and Wolner, E. Early failure of the tissue engineered porcine heart valve SYNERGRAFT in pediatric patients. *Eur. J. Cardiothorac. Surg.* **23**:1002-1006, 2003.

23. Rieder, E., Seebacher, G., Kasimir, M. T., Eichmair, E., Winter, B., Dekan, B., Wolner, E., Simon, P., and Weigel, G. Tissue Engineering of Heart Valves: Decellularized Porcine and Human Valve Scaffolds Differ Importantly in Residual Potential to Attract Monocytic Cells. *Circulation* **111**:2792-2797, 2005.

V

NMR ASSESSMENT OF ME_2SO IN DECELLULARIZED CRYOPRESERVED AORTIC VALVE CONDUITS

INTRODUCTION

Since Hufnagel described the transplantation of allograft vascular tissue in 1947 [1] and developed the first mechanical valve prosthesis in 1951 [2], significant advances have been made in the treatment of congenital and acquired abnormalities of the cardiac outflow tract, heart valves and great vessels. Building on Hufnagel's work, Barrett-Boyes implanted an aortic valve allograft in the orthotopic position in 1962 and Binet introduced xenogeneic valves in 1965. Meanwhile synthetic materials were developed for vascular grafts.

Despite refinements of synthetic vascular materials and prosthetic valves, the ideal vascular prosthesis that would provide normal hemodynamic function, last the life of the patient, but be non-immunogenic, non-thrombogenic and resist infection has yet to be attained. Mechanical valves have virtually achieved life-long durability [3,4], but are thrombogenic and require life-long systemic anticoagulation with its associated risk of bleeding. Tissue valves are not thrombogenic, but have limited durability and require intermittent reoperations for replacement. Despite improvements in alternative materials, allograft vascular tissue is still commonly used for the surgical repair of severe congenital and

A version of this chapter has been accepted for publication.
Lehr, Hermary, McKay, Webb, Abazari, McGann, Coe, Korbutt, Ross. J Surg Res.

acquired defects of the heart and great vessels because of its superior handling and hemodynamic properties compared to current alternatives [5].

Xenograft [6] and allograft [7] valves both induce antigen-mediated immune damage leading to calcification and destruction of the valve. The allogeneic immune response has been characterized as an intense cellular infiltration and the development of anti-donor specific antibodies [8]. This allo-sensitization of the recipient limits the likelihood of obtaining a suitable donor organ should future heart transplantation be required, and increases the risk for a poor outcome[9]. Recent evidence suggests that the cellular elements of the allograft tissue are the source of this response, and that removing these elements by decellularization attenuates the host alloreponse [10]. However, this acellular tissue lacks potential for growth or repair and is thrombogenic [11].

Cryopreservation of allograft valves and blood vessels was developed in 1975 and led to the establishment of tissue banks which enhanced matching allograft supply with demand [12]. A tissue engineering approach involving repopulating a banked decellularized allograft scaffold with autologous cells may eventually overcome the current limitations of this tissue and lead to the development of the ideal valve replacement, including the capability of growth and repair. Although other scaffolds have been described, the decellularized allograft may be superior because it is composed of the same macromolecules in

the exact configuration as the native human valve and conduit and has undergone minimal chemical alterations.

Me_2SO is a penetrating cryoprotectant to limit the development of ice within tissue during cryopreservation, but may adversely affect tissue viability and biological function [13,14]. Residual Me_2SO in thawed decellularized tissue may also inhibit repopulation by altering normal function of endothelial cells [15] and fibroblasts [16,17]. A Me_2SO concentration of 0.28M (2%) has been shown to inhibit RNA, protein and DNA synthesis during the early periods of serum-stimulated growth of mouse embryo fibroblast cells [18] through the inhibition of interleukin 6, c-myc and c-fos gene expression [19]. Me_2SO concentrations greater than 0.28M (2%) inhibit capillary tube formation by endothelial cells via suppression of matrix metalloproteinase-2 [15]. Other groups have shown that Me_2SO inhibits the differentiation of precursor cells [20,21]. While these inhibitory effects occur at relatively high Me_2SO concentrations, Crawford and Braunwald showed that even 1.4×10^{-2}M (0.1%) Me_2SO inhibited fibroblast proliferation [17]. Dagia *et al* report that treating human umbilical vein endothelial cells with 7.0×10^{-3}M (0.05%) Me_2SO had minimal effect on myeloid (HL60) cell adhesion [22]. Several studies have used Me_2SO as a solvent vehicle to study the effect of other pharmacologic agents or growth factors. Again, these studies report varied effects of Me_2SO on endothelial and fibroblast function. Fibroblast granulocyte macrophage colony-stimulating factor production was

reduced by 46% with 1.0 x 10^{-2}M (0.1%) Me_2SO [16] yet 1.4 x 10^{-2}M (0.1%) Me_2SO exerted seemingly minimal effect on fibroblast production of tumor necrosis factor - α (TNF-α) or interleukin-1β (IL-1β) [23]. It is therefore important to assess the level of Me_2SO to avoid any confounding effects that Me_2SO may have on repopulation following cryopreservation.

In this study we used high field proton nuclear magnetic resonance spectroscopy (^{1}H-NMR) to measure residual Me_2SO concentrations in aortic valve conduits and to determine the kinetics of Me_2SO elution from the aqueous compartment of ovine aortic valve conduit. ^{1}H-NMR measures the number of protons for each species and therefore allows for the direct measurement of the Me_2SO concentration in biological tissues including cornea [24], cartilage [25] and heart valve leaflets [13].

MATERIALS AND METHODS

Tissue Procurement:

Juvenile Suffolk sheep (45 – 55 kg) were purchased from a local farm and housed in accordance with the guidelines of the Canadian Council of Animal Care [26] at the University of Alberta farm with food and water *ad libitum*. Approval for this study was obtained from the University of Alberta Animal Policy and Welfare Committee. Following induction with halothane, donor animals were intubated, shaved and aseptically prepped and draped. The left hemithorax was

opened widely and the animal was exsanguinated. The aorta was dissected from the pulmonary artery and left ventricular outflow tract and transported in RPMI (Gibco, Grand Island, NY, USA) at 4°C.

Cryopreservation:

Following the protocol of our local tissue bank, tissue was sterilized in antibiotic solution (Colistimethate 75,000 μg/mL [Sterimax Inc, Mississauga, ON, Canada], Vancomycin Hydrochloride 50 μg/mL [Pharmascience Inc., Montreal, QC, Canada], Lincomycin 120 μg/mL [Pharmacia, Kirkland, QC, Canada] and Cefoxitin Sodium 240 μg/mL [Novopharm, Toronto, ON, Canada]) for 24 hours. Valve conduits were rinsed 3 times in 4°C Ringer's Lactate (Baxter, Toronto Canada) and transferred into 100 mL 7.5% Me_2SO (Fisher Scientific, Fair Lawn, NJ, USA) in X-Vivo (Cambrex Bio Science, Walkersville, MD, USA) at 4°C for 30 minutes. After packaging in a 3 bag system, the tissue was frozen in a Cryomed 1010 programmable rate-controlled freezer (Cryomed, Mount Clements, MI, USA). The freezing protocol consisted of 5 phases. Tissues were cooled from ambient temperature to 4°C and then supercooled to -2°C. Seeding was accomplished by a burst of cold nitrogen to initiate ice formation in the supercooled sample. Cooling then proceeded at a rate of 1°C/min to -50°C and then at a rate of 7°C/min until the allograft reached -100°C. Conduits were stored in vapor phase liquid nitrogen until required.

Decellularization:

Figure V-1 illustrates the overall experimental method for determining the Me_2SO concentration in aortic valve conduits during the decellularization process. Aortic roots were decellularized in a series of hypotonic and hypertonic Tris buffers with detergent as previously described [10]. We recently showed that osmotic lysis with low dose detergent is more effective at eliminating antigenic cellular elements from allograft heart valves while preserving the extracellular matrix than osmotic lysis alone or enzymatic decellularization [27].

All steps were performed at 4°C in 100 mL of solution unless otherwise noted. Briefly, cryopreserved aortic valve conduits were thawed in a 37°C water bath for 20 minutes. The tissue was rinsed three times for approximately 1 second in PBS to remove residual surface ME_2SO and then placed in 100 mL of hypotonic Tris buffered solution (10 mM, pH 8.0, 0.1 mM PMSF, 5 mM EDTA) for 48 hours. The solution was replaced with 0.5% octylphenoxy polyethoxyethonal (Triton X-100, Labchem Inc, Pittsburgh, PA, USA) in a hypertonic Tris-buffered solution (50 mM, pH 8.0, 1.5 M KCl, 5 mM EDTA) for an additional 48 hours. Allografts were then bathed in Sorensen's buffer with DNase (25 g/mL, Roche, Laval, QC, Canada), RNase (10 g/mL, Roche, Laval, QC, Canada), and $MgCl_2$ (10 mmol/L) for 5 hours at 37°C. The tissue was then soaked in 0.5% TritonX-100 in Tris buffer (50 mmol/L, pH 9.0) for 48 hours and finally washed in PBS for 24 hours.

Tissue samples were cut from the valve conduits at predetermined intervals (time 0, 15, 30, 45 minutes, 1, 2, 3, 4, 5, 6, 12, 18, 24 hours, 2, 3, 4, 5, 6, 7, 8, and 9 days) throughout the decellularization process for determination of the residual Me_2SO concentration in the conduit wall.

Histology:

Formaldehyde-fixed (Z-fix, Anatech LTD, Battlecreek, MI, USA), paraffin embedded samples of control and decellularized conduits taken at time of implant were serially sectioned (5 μm) and stained with hematoxylin and eosin.

Determination of Tissue Me_2SO Concentration by Quantitative ^{1}H-NMR Spectroscopy:

Equilibration. Tissue sections removed from the valve conduit during the decellularization process were equilibrated in 10 mL of sterile, distilled and deionized H_2O for 28 days at 4°C. ^{1}H-NMR spectroscopy was used to determine Me_2SO concentration in the aqueous compartment of the tissue as described below [13]. Each tissue sample was placed in 10 mL of 100% methanol. After 6 hours, the methanol was replaced with diethyl ether. The ether was removed after a minimum of 3 hours. Residual ether was evaporated overnight and the tissue dry weight was then measured.

NMR Sample Preparation. All NMR samples were prepared to 600 μL volumes. NMR samples consisted of 90% equilibration solution, 10% D_2O,

0.02 % w/v NaN_3, and 2,2-dimethyl-2-silapentane-5-sulfonate (0.5 mM) as an internal reference standard [28].

NMR Spectroscopy and Assignments. A standard calibration curve was performed at 25°C on a 4-channel Varian Inova 600 MHz (Oxford 14.1 Tesla magnet) using a Varian 5mm triax gradient HCN (18 mm coil length) probe. All other experiments were conducted at 25°C on a 4-channel Varian Inova 500 MHz (Oxford 11.74 Tesla magnet) spectrometer equipped with a Varian 5 mm Z-axis gradient HCN probe (16 mm radio frequency (RF) coil length). One dimensional nuclear overhauser enhancement spectroscopy (NOESY) spectra (*i.e.* presaturation - 90° pulse – mixing time - 90° pulse - acquire) were collected with 4 steady state scans, 1024 acquisitions per free induction decay (FID), a relaxation delay water presaturation period of 2 seconds (gammaB1 of ~ 150 Hz), saturation during the mixing 50 ms mixing time, a sweep width of 6000 Hz, and an acquisition time of 2 seconds.

All directly detected data sets (12k complex data points) were zero filled to ~64k complex points. The 1D-^{1}H spectra were apodized using a 0.5 Hz line broadening prior to discrete Fourier transformation. A 100 Hz suppression algorithm was applied to the residual solvent peak. All spectra were processed, analyzed, and assigned with the VNMRJ 1.1C (Varian Inc.) and the Advanced Chemistry Development (v8.17) software packages (ACD/Labs Inc.).

Me_2SO Standard Curve. A standard NMR peak intensity curve for the Me_2SO methyl resonance on the 600 MHz spectrometer was established over the concentration range of 0.1 M to 1 μM by serial concentration dilutions of a factor of 10 for each point of the curve. Peak areas were integrated over a consistent spectral width (2.50 – 2.75 ppm) using automated utilities in the ACD software suite.

Me_2SO concentration in equilibration solution determined by NMR. Me_2SO concentration of equilibration solutions for tissue from each time point was determined using the same NMR peak area integration of the Me_2SO methyl resonances as in the standard concentration curve procedures. Each determination was performed in triplicate and then averaged.

Calculation of Me_2SO concentration in tissue samples. Me_2SO content in the samples taken at each time point was calculated from the Me_2SO concentration in the tissue equilibration solution using the dilution equation for solutions (equation 1)

$$C_t V_t = C_f V_f , \qquad 1$$

where C_t and C_f are the Me_2SO concentrations in the tissue prior to equilibration and of the equilibrated solution respectively, and V_t and V_f are the tissue water volume and total equilibration volume respectively. C_f was determined from the Me_2SO NMR peak area using the standard curve (equation 2) obtained by serial dilutions of Me_2SO,

$$A_{Me_2SO} = mC_f \quad , \qquad 2$$

where A_{Me_2SO} is the NMR peak area integration of the Me_2SO methyl resonances, m is the slope of the standard curve, C_f is the final Me_2SO in the equilibrated solution.

Rearranging and combining equations 1 and 2 gives

$$C_t = \frac{(V_f)A_{Me_2SO}}{V_t m} \quad , \qquad 3$$

but $V_f = V_t$ + equilibration solution volume (V_{eq}), and V_t is the difference between the tissue wet and dry weights divided by the density of water ρ (which is 1.00 g/mL at 4°C), so

$$C_t = \frac{\left(\frac{W_{twet} - W_{tdry}}{\rho} + V_{eq}\right)\left(A_{Me_2SO}\right)}{\frac{W_{twet} - W_{tdry}}{\rho} m} \quad , \qquad 4$$

where W_{twet} and W_{tdry} are the tissue wet and dry weights respectively.

Calculation of the Diffusion Coefficient for Me_2SO:

A one dimensional Fickian diffusion model was assumed as conduits are very thin sheets and the diffusion area at the sides of the sheet is negligible in

comparison to area of the cut edges. A solution to such a problem is provided by Crank [29] as follows:

$$\frac{M_t}{M_\infty} = 1 - \sum_{n=0}^{\infty} \frac{8}{(2n+1)^2 \pi^2} \exp\left(\frac{-D(2n+1)^2 \pi^2 t}{4l^2}\right), \quad 5$$

where M_t is the amount of the solute that has left the sheet after time t, M_∞ is the equilibrium solute concentration, D is the diffusion coefficient and l is the thickness of the sheet. The valve conduits were suspended in 100ml of decellularization solution without Me_2SO, but after 48 hours, the final concentration of Me_2SO in the tissues plateaus to a non zero-value which is assumed to be sufficient time to reach equilibrium with the ambient (see Figure V-5). For this case Crank also provides a solution:

$$\frac{M_t}{M_\infty} = 1 - \sum_{n=0}^{\infty} \frac{2\alpha(1+\alpha)}{1+\alpha+\alpha^2 q_n^2} \exp\left(\frac{-Dq_n^2 t}{l^2}\right) \quad 6$$

where α is the fractional uptake or the ratio of the volumes of solution and sheet and is given by:

$$\frac{M_\infty}{2lC_0} = \frac{1}{1+1/\alpha}, \quad 7$$

And q_n's are the non-zero positive roots of $\tan q_n = -\alpha q_n$.

A custom written computing program fits the best value for D from a wide range of D values using the lease square error method.

Statistics: Continuous data from each experiment are expressed as mean ± SEM. Means of related groups with equal distribution are compared by a paired t-test using SPSS 13.0 (SPSS Inc., Chicago, USA). Differences were considered significant when $p < 0.05$.

RESULTS

Hematoxylin and eosin stained decellularized grafts prior to implant were virtually acellular (Figure V-2). No endothelium was present and only ghosts of cells are appreciable. The internal and external elastic lamina are preserved as is the vasovasorum. The pale pink color of decellularized sections suggests a reduction in cytoplasm compared to control sections.

NMR signal intensity is proportional to the number of Me_2SO molecules in the sample such that the integrated peak area (or area under the curve) of the Me_2SO methyl resonances gives a measure of the total number of Me_2SO molecules in the sample. Plotting the integrated peak area of the ^{1}H-NMR peak for Me_2SO methyl singlet on the 600 MHz spectrometer versus concentration yielded a linear curve ($R = 0.998$) with a slope of 1495 for 6 serial dilutions of Me_2SO

over the concentration range of 1 μM to 0.1 M (Figure V-3). The integrated area for the Me_2SO methyl singlet peak was then used to calibrate the assay.

Figure V-4 shows the series of ^{1}H-NMR spectra for a representative experiment. The Me_2SO methyl singlet is well resolved from other contaminants in the equilibration solution. DSS (2,2-dimethyl-2-silapentane-5-sulfonate) was used as an internal reference standard and the DSS methyl peak is also well resolved.

After thawing, the mean Me_2SO concentration in the aqueous compartment of valve conduits from triplicate experiments was 0.302 ± 0.081 M (Figure V-5). The decellularization process resulted in a stepwise reduction in the Me_2SO concentration to less than $8.56 \times 10^{-5} \pm 9 \times 10^{-5}$ M ($p = 0.02$) with each step corresponding to a change in the solution used in the decellularization process. Elution of Me_2SO from the valve conduit proceeded at the fastest rate during the first 45 minutes of the decellularization process during which time it fell to one quarter ($7.53 \times 10^{-2} \pm 1.03 \times 10^{-2}$ M) of the initial level. After 4 hours, the in-conduit Me_2SO concentration reached equilibrium with the surrounding solution. With each subsequent change in solution, the Me_2SO concentration in the conduit dropped by approximately 2 orders of magnitude, as would be expected with an approximate 1:100 dilution.

It is possible to calculate a diffusion coefficient for Me_2SO in conduits using the data from Figure V-5. Fitting the above model to the experimental data

(Equations 5-7) gives a diffusion coefficient of 2.4 x 10^{-6} cm^2/s for Me_2SO in heart valve conduits. In this model changes in volume of the tissue due to osmotic effects are not considered.

CONCLUSIONS

Toxicity is time, temperature and concentration dependent. High Me_2SO concentration (3M) is cytotoxic to porcine endothelial cells [30], but there is conflicting evidence regarding the toxicity of lower Me_2SO concentrations on fibroblast and endothelial cells that could be used to repopulate decellularized vascular tissue. Although the literature describes conflicting effects of Me_2SO on the function of various cell types, it is clear that a very low concentration of Me_2SO must be achieved to avoid potential confounding effects when utilizing cryopreserved heart valves for novel tissue-engineered constructs. We have demonstrated that the Me_2SO concentration in the aqueous compartment of cryopreserved ovine aortic valve conduits following decellularization is several orders of magnitude below even the lowest concentration of Me_2SO reported to adversely affect the survival or function of endothelial, fibroblast and stem cells.

Me_2SO elution occurred in a stepwise fashion corresponding to changes in the decellularization solutions. The decellularization process therefore represents a serial dilution of Me_2SO from the valve conduits with the tissue concentration reaching equilibrium with the surrounding solution prior to change.

Cardiac valve conduits are a complex tissue composed of both cellular and extracellular components that may be altered during decellularization. The kinetics of Me_2SO permeation into vascular tissue have been described by a number of investigators, however fewer investigators have considered the kinetics of Me_2SO elution from vascular tissue and there are no reports of Me_2SO washout during decellularization of cryopreserved vascular tissue. Hu *et al.* reported that their standard dilution removal protocol at 4°C results in a final Me_2SO concentration of 2.8×10^{-1}M [31], and that it requires more than 80 minutes to achieve this concentration. Their final Me_2SO concentration is 10 fold greater than their predicted final concentration and is greater than the concentrations reported to have inhibitory effects on cell function.

We have found that the concentration of Me_2SO immediately after thawing was low compared to the concentration of Me_2SO in the freezing solution. This finding suggests that the equilibration period for the cryoprotectant may have been too short to permit complete permeation prior to freezing even though we followed the freezing protocol of our local tissue bank. It is possible that the kinetics of Me_2SO permeation in the ovine aortic valve conduit differ from the human, however, it would seem unlikely that such a substantial difference would exist. The structure of ovine and human valve conduits are similar and consequently one would expect that the kinetics would likewise be similar. Moreover, the valve conduits tested were smaller than those from the adult human

and we allowed for a slightly lengthier period of MMM permeation than specified by the tissue bank protocol. In addition, previous work suggests that 360 minutes are required to attain greater than 90% of equilibrium diffusion in aortic valve leaflets [13] and conduits [31] respectively. These reports as well as our data presented herein demonstrate that current heart valve cryopreservation protocols may not permit adequate Me_2SO permeation for optimal tissue preservation Whether attempting to enhance MMM permeation would improve the outcomes of cryopreserved allograft valves is not clear. Certainly, good results have been obtained by utilizing the current protocol. It may be that incomplete equilibration of MMM during permeation results in suboptimal cell survival. This in turn may reduces the antigenic load of the allograft valve thereby inadvertently improving valve durability. Additional work is required to develop more effective cryopreservation methods that focus more on maintaining the integrity of the ECM rather than cell survival.

In the clinical setting, it is commonly assumed that the Me_2SO used to cryopreserve aortic and pulmonary valve allografts is washed out of the valve by three 5-minute rinses in Ringer's lactate. In contrast to the accepted procedure, we show that equilibration of Me_2SO does not occur until after 4 hours and therefore current intra-operative strategies for thawing cardiac valve allografts are insufficient for complete Me_2SO washout.

We calculated a diffusion coefficient of 2.5 x 10^{-6} cm^2/s for the washout of Me_2SO from human aortic valve conduit walls during the initial phase of decellularization. This value is larger, but similar in magnitude to the value determined by Lakey *et al* for the diffusion of Me_2SO into human aortic valve leaflets, 2.05 x 10^{-6} cm^2/s [13], but smaller than the diffusion coefficient for the diffusion of Me_2SO into human cartilage 6.1 x 10^{-6} cm^2/s [32]. The diffusion coefficient for the decellularized conduit may be greater because the decellularization process removes the endothelial layer from the inner most layer of the conduit wall and lyses the interstitial cells. As a result, one barrier to diffusion is removed and the lysed cells may create additional pathways for Me_2SO to leave the tissue.

Our findings likely apply to decellularized cryopreserved pulmonary valve conduits, although we did not formally test them. If we assume that the matrix structure is similar between the aortic and pulmonary valve conduits, then wall thickness would be the primary determinant of differences in the diffusion coefficient. Because the wall of pulmonary valve conduits is thinner than the wall of a similar sized aortic valve conduit, the diffusion coefficient for a pulmonary valve conduit would be larger resulting in increased flux of Me_2SO out of the valve. Therefore, the concentration of Me_2SO in pulmonary valve conduits undergoing the same process of decellularization should have a lower residual

Me_2SO concentration following decellularization than we demonstrated in decellularized aortic valve conduits.

Decellularized cryopreserved heart valves may become an important matrix in the development of a tissue engineered heart valve. Our data demonstrate that, based on current literature, the residual Me_2SO concentration in decellularized cryopreserved aortic valve conduits is sufficiently minimal to avoid any potential adverse effects on cellular repopulation. In addition, current cryopreservation protocols employed by tissue banks may not provide adequate Me_2SO permeation for optimal cell and matrix preservation. Finally, the current practice used in the operating theater to thaw cryopreserved heart valves is unlikely to completely remove the Me_2SO used for cryopreservation. Additional work will be required to further refine heart valve cryopreservation techniques.

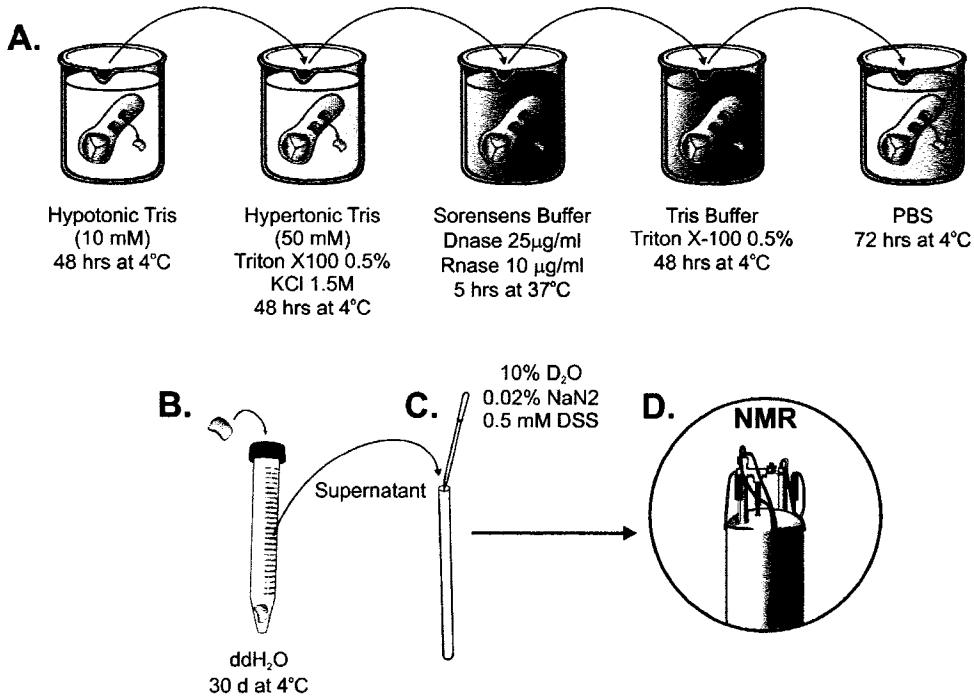

Figure V-1. Experimental method for determining Me_2SO concentration in ovine aortic valve conduits during decellularization. Ovine aortic valve conduits cryopreserved in 7.5% Me_2SO were thawed and then decellularized **(A)** by exchanging a series of hypotonic and hypertonic Tris buffered solutions with Triton-X followed by a very quick rinse (less than 2 seconds) in PBS. The decellularization process occurred over a period of 9 days. Samples were cut from the valve conduit at regular intervals (0, 15, 30, 45 minutes, 1, 2, 3, 4, 5, 6, 12, 18, 24 hours, 2, 3, 4, 5, 6, 7, 8, and 9 days) throughout the decellularization process and allowed to equilibrate in ddH_2O for 28 days **(B)**. Me_2SO concentration in the equilibration solution was determined by proton nuclear magnetic resonance

spectrometry and was used to calculate the Me_2SO concentration in the aqueous compartment of the aortic valve conduit **(C and D)**.

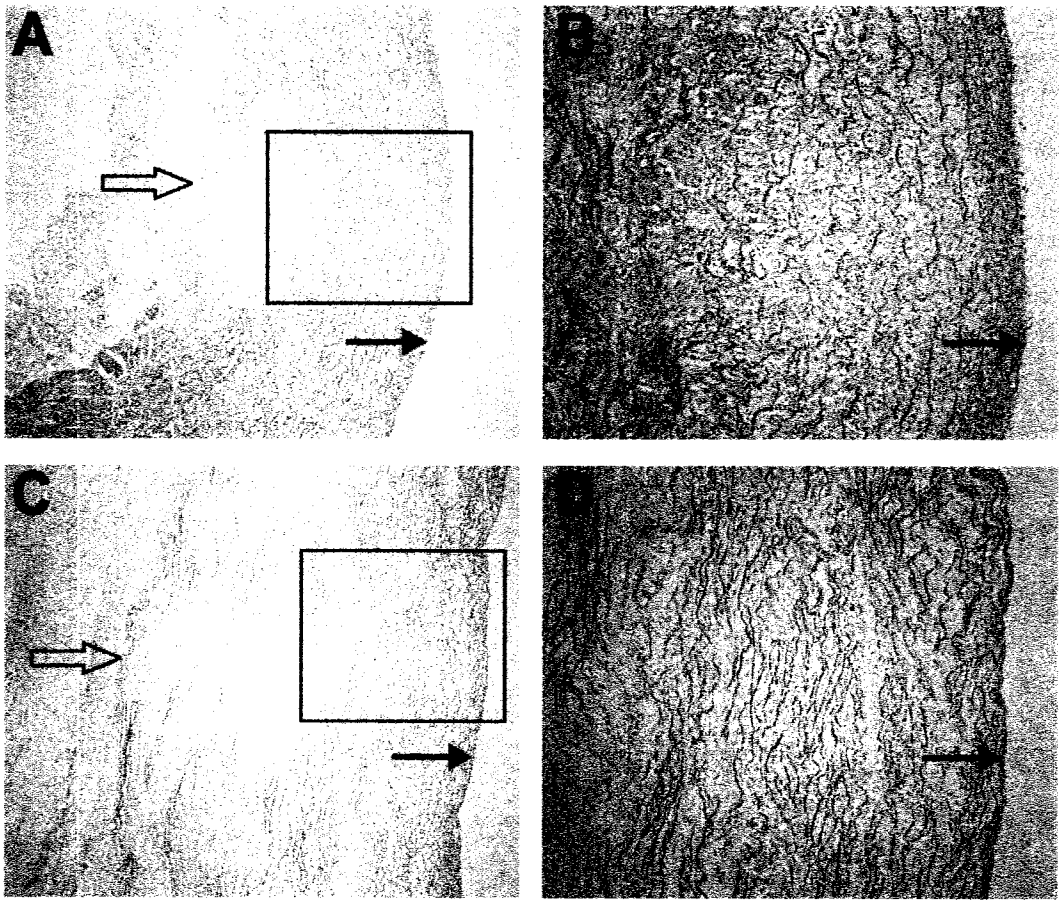

Figure V-2. Representative sections of control (A) and decellularized (C) conduits. Samples were fixed in formaldehyde, embedded in paraffin, sectioned at 5 μm and stained with hematoxylin and eosin. Solid arrows and outline arrows indicate the internal and external lamina respectively. Photomicrographs B and D are high power images (100X) from the region indicated by boxes in A and C (40X), respectively.

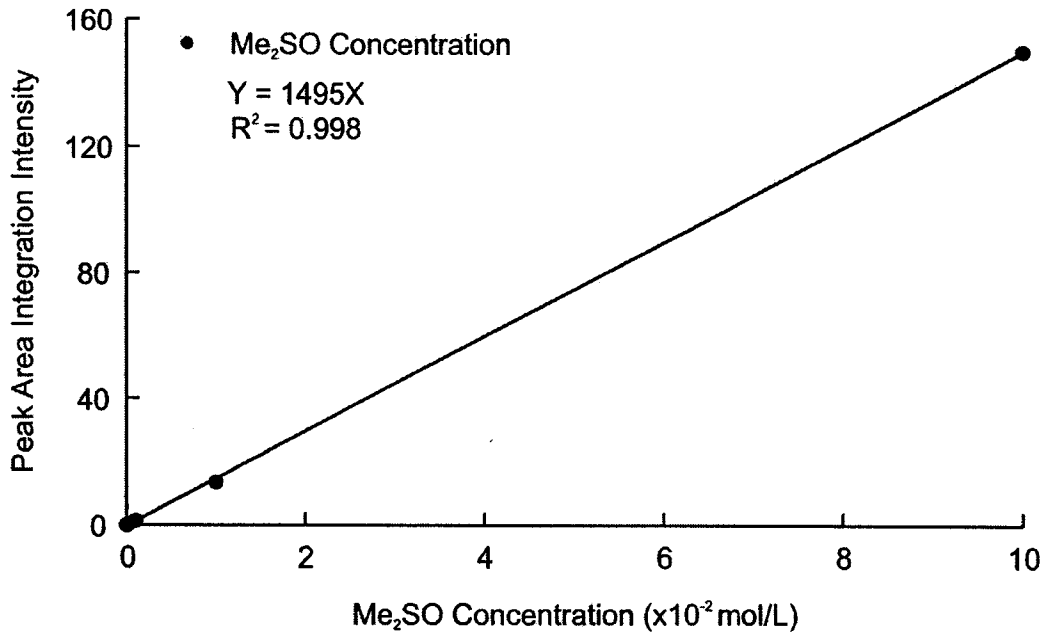

Figure V-3. Standard curve for ^{1}H-NMR determination of Me_2SO in H_20. The curve was obtained by 6 serial concentration dilutions of a factor of 10 over the concentration range of 1 μM to 0.1 M. 1D-^{1}H spectra were apodized using a 0.5 Hz line broadening prior to discrete Fourier transformation and a 100 Hz suppression algorithm was applied to the residual solvent peak. The peak for the methyl singlet (600 MHz) was then integrated and plotted against the dilution concentrations.

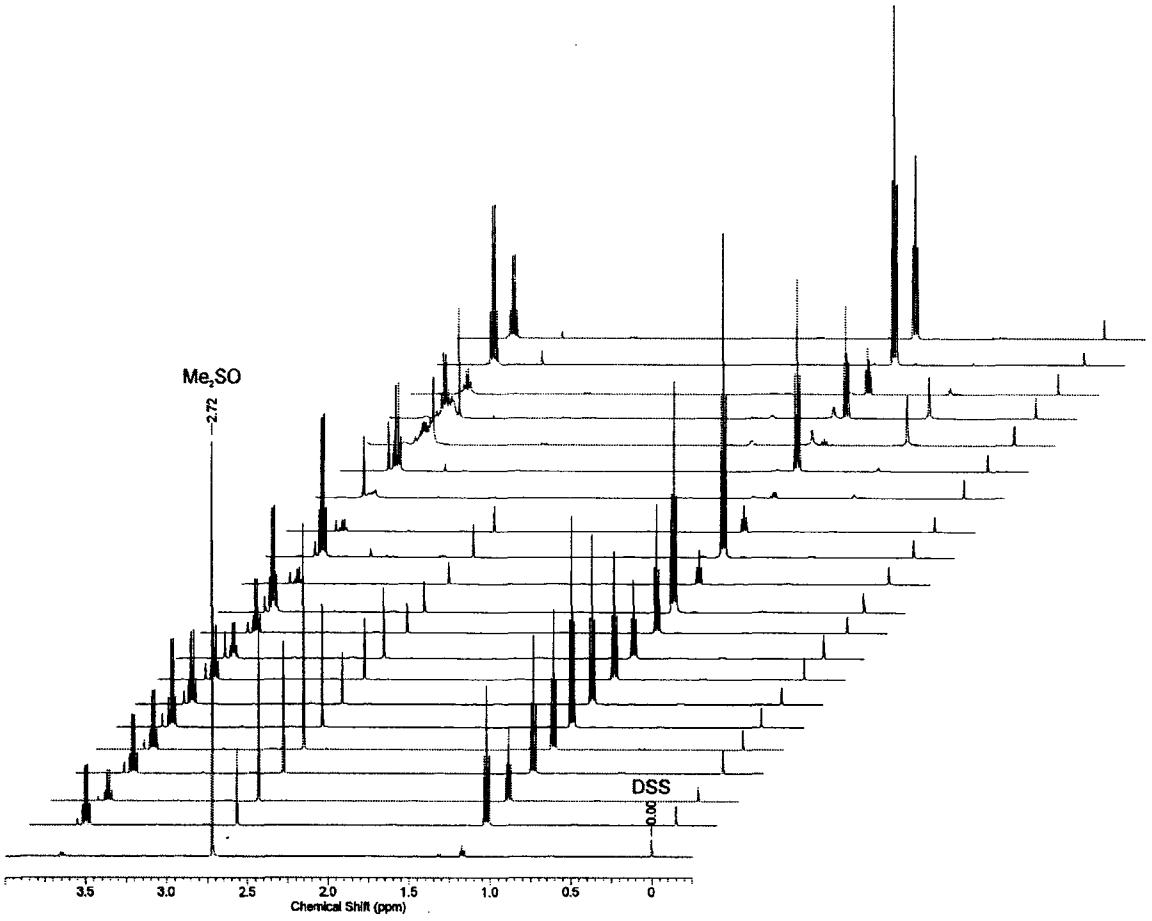

Figure V-4. Typical 1-D ^{1}H-NMR spectra for a single set of experiments representing elution of Me_2SO from wall of an ovine aortic valve conduit over time. Tissue samples were equilibrated in 10 mL of double distilled, deionized water. Peak height was later standardized to sample tissue water volume. Me_2SO and DSS peaks are indicated. The unlabeled peaks flanking the Me_2SO peaks are alcohols used to sterilize equipment used in cutting samples from the valve conduits.

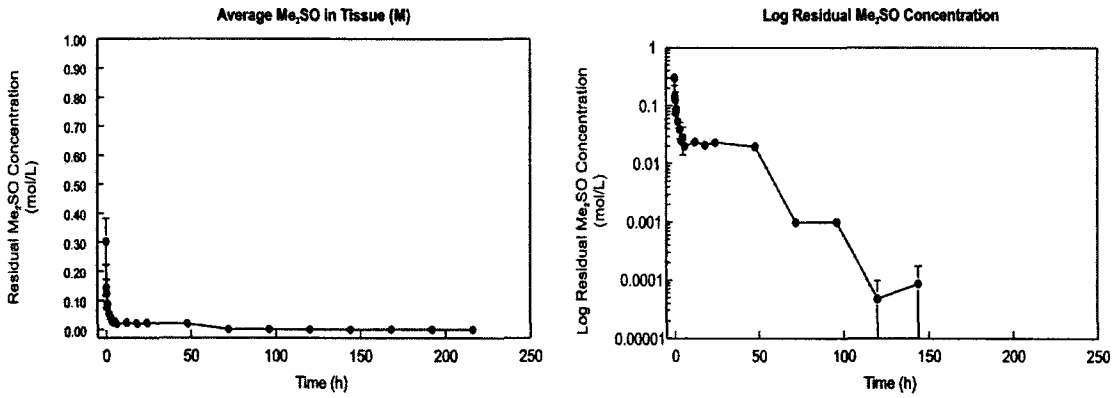

Figure V-5. Me_2SO in cryopreserved aortic valves is eluted during decellularization with a series hypotonic and hypertonic solutions with Triton-X as a detergent. Data points represent the mean ± SEM for triplicate experiments at the indicated time points throughout the decellularization process. Major steps in the curve correspond to changes in the decellularization solution. Error bars are shown except when smaller than the data points.

REFERENCES

1. Hufnagel, C. A. Preserved homologous arterial transplant. *Bull. Am. Coll. Surg* **32**:321-324, 1947.

2. Hufnagel, C. A. Aortic plastic valvular prosthesis. *Bull. Georgetown. Univ. Med. Ctr.* **4**:128, 1951.

3. Hammermeister, K. E., Sethi, G. K., Henderson, W. G., Oprian, C., Kim, T., and Rahimtoola, S. A comparison of outcomes in men 11 years after heart-valve replacement with a mechanical valve or bioprosthesis. Veterans Affairs Cooperative Study on Valvular Heart Disease. *N. Engl. J. Med.* **328**:1289-1296, 1993.

4. Lund, O., Nielsen, S. L., Arildsen, H., Ilkjaer, L. B., and Pilegaard, H. K. Standard aortic St. Jude valve at 18 years: performance profile and determinants of outcome. *Ann. Thorac. Surg* **69**:1459-1465, 2000.

5. Lupinetti, F. M., Warner, J., Jones, T. K., and Herndon, S. P. Comparison of human tissues and mechanical prostheses for aortic valve replacement in children. *Circulation* **96**:321-325, 1997.

6. Manji, R. A., Zhu, L. F., Nijjar, N. K., Rayner, D. C., Korbutt, G. S., Churchill, T. A., Rajotte, R. V., Koshal, A., and Ross, D. B. Glutaraldehyde-

fixed bioprosthetic heart valve conduits calcify and fail from xenograft rejection. *Circulation* **114**:318-327, 2006.

7. Dignan, R., O'Brien, M., Hogan, P., Thornton, A., Fowler, K., Byrne, D., Stephens, F., and Harrocks, S. Aortic valve allograft structural deterioration is associated with a subset of antibodies to human leukocyte antigens. *J. Heart Valve Dis.* **12**:382-390, 2003.

8. Hogan, P., Duplock, L., Green, M., Smith, S., Gall, K. L., Frazer, I. H., and O'Brien, M. F. Human aortic valve allografts elicit a donor-specific immune response. *J. Thorac. Cardiovasc. Surg.* **112**:1260-1266, 1996.

9. Meyer, S. R., Campbell, P. M., Rutledge, J. M., Halpin, A. M., Hawkins, L. E., Lakey, J. R., Rebeyka, I. M., and Ross, D. B. Use of an allograft patch in repair of hypoplastic left heart syndrome may complicate future transplantation. *Eur. J Cardiothorac. Surg* **27**:554-560, 2005.

10. Meyer, S. R., Nagendran, J., Desai, L. S., Rayat, G. R., Churchill, T. A., Anderson, C. C., Rajotte, R. V., Lakey, J. R., and Ross, D. B. Decellularization reduces the immune response to aortic valve allografts in the rat. *J. Thorac. Cardiovasc. Surg.* **130**:469-476, 2005.

11. Kasimir, M. T., Weigel, G., Sharma, J., Rieder, E., Seebacher, G., Wolner, E., and Simon, P. The decellularized porcine heart valve matrix in tissue

engineering: platelet adhesion and activation. *Thromb. Haemost.* **94**:562-567, 2005.

12. Jashari, R., Van Hoeck, B., Tabaku, M., and Vanderkelen, A. Banking of the human heart valves and the arteries at the European homograft bank (EHB)--overview of a 14-year activity in this International Association in Brussels. *Cell Tissue Bank.* **5**:239-251, 2004.

13. Lakey, J. R., Helms, L. M., Moser, G., Lix, B., Slupsky, C. M., Rebeyka, I. M., Sykes, B. D., and McGann, L. E. Dynamics of cryoprotectant permeation in porcine heart valve leaflets. *Cell Transplant.* **12**:123-128, 2003.

14. Fahy, G. M. The relevance of cryoprotectant "toxicity" to cryobiology. *Cryobiology* **23**:1-13, 1986.

15. Koizumi, K., Tsutsumi, Y., Yoshioka, Y., Watanabe, M., Okamoto, T., Mukai, Y., Nakagawa, S., and Mayumi, T. Anti-angiogenic effects of dimethyl sulfoxide on endothelial cells. *Biol. Pharm. Bull.* **26**:1295-1298, 2003.

16. Spoelstra, F. M., Kauffman, H. F., Hovenga, H., Noordhoek, J. A., de Monchy, J. G., and Postma, D. S. Effects of budesonide and formoterol on

eosinophil activation induced by human lung fibroblasts. *Am. J. Respir. Crit Care Med.* **162**:1229-1234, 2000.

17. Crawford, J. M. and Braunwald, N. S. Toxicity in vital fluorescence microscopy: effect of dimethylsulfoxide, rhodamine-123, and DiI-low density lipoprotein on fibroblast growth in vitro. *In Vitro Cell Dev. Biol.* **27A**:633-638, 1991.

18. Nagashunmugam, T., Srinivas, S., and Shanmugam, G. Effect of dimethyl sulfoxide on mouse embryo fibroblasts: inhibition of plasminogen activator inhibitor deposition and interference with early events of serum-stimulated growth. *Biol. Cell* **66**:307-315, 1989.

19. Srinivas, S., Sironmani, T. A., and Shanmugam, G. Dimethyl sulfoxide inhibits the expression of early growth-response genes and arrests fibroblasts at quiescence. *Exp. Cell Res.* **196**:279-286, 1991.

20. Blau, H. M. and Epstein, C. J. Manipulation of myogenesis in vitro: reversible inhibition by DMSO. *Cell* **17**:95-108, 1979.

21. Wang, H. and Scott, R. E. Inhibition of distinct steps in the adipocyte differentiation pathway in 3T3 T mesenchymal stem cells by dimethyl sulphoxide (DMSO). *Cell Prolif.* **26**:55-66, 1993.

22. Dagia, N. M. and Goetz, D. J. A proteasome inhibitor reduces concurrent, sequential, and long-term IL-1 beta- and TNF-alpha-induced ECAM expression and adhesion. *Am. J. Physiol Cell Physiol* **285**:C813-C822, 2003.

23. Cowling, R. T., Gurantz, D., Peng, J., Dillmann, W. H., and Greenberg, B. H. Transcription factor NF-kappa B is necessary for up-regulation of type 1 angiotensin II receptor mRNA in rat cardiac fibroblasts treated with tumor necrosis factor-alpha or interleukin-1 beta. *J. Biol. Chem.* **277**:5719-5724, 2002.

24. Taylor, M. J. and Busza, A. A convenient, non-invasive method for measureing the kinetics of permeation of dimethyl sulphoxide into isolated corneas using NMR spectroscopy. *Cryo-Letters* **13**:273-282, 1992.

25. Muldrew, K., Sykes, B., Schachar, N., and McGann, L. E. Permeation kinetics of dimethyl sulfoxide in articular cartilage. *Cryo-Letters* **17**:331-340, 1996.

26. *Guide to the care and use of experimental animals*.Canadian Council of Animal Care, 1993.

27. Meyer, S. R., Chiu, B., Churchill, T. A., Zhu, L., Lakey, J. R., and Ross, D. B. Comparison of aortic valve allograft decellularization techniques in the rat. *J. Biomed. Mater. Res. A* **79**:254-262, 2006.

28. Markley, J. L., Bax, A., Arata, Y., Hilbers, C. W., Kaptein, R., Sykes, B. D., Wright, P. E., and Wuthrich, K. Recommendations for the presentation of NMR structures of proteins and nucleic acids. IUPAC-IUBMB-IUPAB Inter-Union Task Group on the Standardization of Data Bases of Protein and Nucleic Acid Structures Determined by NMR Spectroscopy. *J. Biomol. NMR* **12**:1-23, 1998.

29. Crank, J. *The Mathematics of Diffusion*. Oxford: Oxford University Press, 1975.

30. Pollock, G. A., Hamlyn, L., Maguire, S. H., Stewart-Richardson, P. A., and Hardie, I. R. Effects of four cryoprotectants in combination with two vehicle solutions on cultured vascular endothelial cells. *Cryobiology* **28**:413-421, 1991.

31. Hu, J. F. and Wolfinbarger, L., Jr. Dimethyl sulfoxide concentration in fresh and cryopreserved porcine valved conduit tissues. *Cryobiology* **31**:461-467, 1994.

32. Carsi, B., Lopez-Lacomba, J. L., Sanz, J., Marco, F., and Lopez-Duran, L. Cryoprotectant permeation through human articular cartilage. *Osteoarthritis and Cartilage* **12**:787-792, 2004.

VI

GENERAL DISCUSSION AND CONCLUSIONS

DISCUSSION

Valvular heart disease is a significant contributor to morbidity and mortality in the western world. Recent estimates by the American Heart Association indicate that in 2002, 94,000 hospital discharges and 42,590 deaths were attributable to heart valve pathology. In addition, nearly 100,000 adult patients undergo operative procedures each year and a smaller number of pediatric patients have complex congenital heart lesions that required valves and conduits for reconstruction and palliation [1]. Despite major advances in valve technology, there are still significant limitations with current technology. Mechanical valves have excellent long-term durability but they require systemic anticoagulation. Alternatively, bioprosthetic valves are subject to calcification and structural degeneration, but are non-thrombogenic. Acceptable long-term freedom from reoperation has been achieved in the adult population, even with biologic valves. Lack of growth and higher failure rates make the currently available prostheses less favorable in the pediatric population [2]. Allograft valves attain the best hemodynamic properties of any valve replacement to date and are available in sizes suitable for children of all ages. However, when used to correct congenital heart defects in children, the host immune response may

accelerate the deterioration of the allograft [3] resulting in reduced freedom from reoperation [4] and the potential to complicate future heart transplantation [5,6]. Although incremental improvements to current technology are still made, a valve replacement that has normal mechanical function, durability and hemodynamic performance, but does not induce an immune or inflammatory response or thrombosis and possess the capability for growth and repair remains elusive [7]. Percutaneously placed valves may reduce the operative morbidity and possible mortality [8,9]. Novel materials [10] and valve designs [11] may be able to overcome the problem of calcification and thrombogenicity, but it is unlikely that the ideal valve replacement will ever be achieved with traditional approaches.

Although *in vivo* regeneration of a valve would be ideal, the likelihood of achieving this goal is exceptionally remote given that the regeneration would need to occur while the heart is functioning and without interfering with the normal function of the heart. Consequently, the achievable gold standard in valve replacement is *de novo in vitro* development of an autologous valve. Stem cell technology gives promise to making such a valve reality. However until an *in vitro* autologous valve is available, a tissue engineering approaches to valve manufacturing offers the best potential for attaining an ideal valve replacement in the near future.

Valves transplanted with cardiac allografts and heterotopic autologous pulmonary valves continue to grow [12]. A review of the literature found only

sporadic case reports of valve failure following cardiac transplantation. Most valve failure results from iatrogenic injury to the tricuspid valve during cardiac biopsy to monitor rejection. Reports of stenosis or regurgitation of the aortic or pulmonary valve are rare. One echocardiographic study compared hemodynamic valve parameters of 13 pediatric patients who had undergone cardiac transplantation to 93 healthy children. At a mean of 3.1 years post transplantation, right or left ventricular chamber dimensions were within normal size and demonstrated normal growth, although wall thickness was increased in 7 patients. However, there was no evidence of obstruction at the anastomotic sites [13]. These results provide proof-in-principle for the potential to successfully transplant cardiac valves that can grow and gives hope to the eventual success of a tissue engineered valve.

The US-FDA requires that novel heart valves are tested in the orthotopic position in a large animal model prior to human trials [14]. However, these trials require the use of cardiopulmonary bypass which is labor intensive, costly and puts the animals at risk of all the complications associated with this procedure. We therefore sought a model to test the immunologic aspects of decellularization in a large animal model without the requirement of cardiopulmonary bypass. Our decision to test a vascular patch was based on several considerations. First, non-valved allograft conduits are commonly used in congenital cardiac surgery. Second, we were primarily interested in assessing the effects of decellularization

on the allogeneic immune response. We presumed that because of the greater area and volume of tissue in the conduit wall, it carried a higher antigen load than the valve leaflets. Finally, we wished to avoid the potential for leaflet thrombosis in a non-functioning valve model [15] and the morbidity associated with native aortic valve insufficiency in a functioning model [16].

Several animal models described in the literature were considered, including inflow occlusion and a side-biting clamp on the pulmonary or ascending aorta. We found that implantation between two aortic cross-clamps in the descending thoracic aorta provided the best exposure and allowed a much larger patch to be implanted, thereby giving sufficient tissue for detailed analysis. Despite the attractiveness of this model, the spinal cord is very sensitive to ischemia. Various techniques have previously been described to improve distal aortic perfusion during aortic surgery. The majority of these techniques involve shunts that require either additional incisions into the vascular tree or have not been validated in a large animal model. The simple intra-aortic shunt that we describe in Chapter 2 of this thesis effectively reduced left ventricular afterload and maintained distal aortic perfusion during aortic cross clamping. It was easy to insert and aided the implantation of the patch. The shunt described is constructed at a cost of only $1.02USD from phosphorylcholine coated 1/4 inch (internal diameter) polyvinylchloride used in standard cardiopulmonary bypass equipment. This shunt was successfully utilized while implanting tissue-engineered vascular

patches into the descending thoracic aorta of 25 sheep (see Chapter 4). After implementing this shunt, no animals developed hind leg paralysis and there was only one intra-operative mortality. No animals suffered late shunt-related complications.

Cells and a scaffold are the two primary components of tissue engineered valves. Acellular allograft valves may prove be the best scaffold because they are of the precise anatomic morphology and are composed of the exact extracellular matrix as the native valve. Our primary objective was to assess the immunogenicity of decellularized allograft patches in a large animal model. Inbred rodent models are valuable in characterizing the allogeneic (and xenogeneic) immune response against transplanted valves and to assess the effect of various treatments in reducing immune mediated injury to the allograft. However, as previously described, large animal testing is required prior to clinical trials, but there are no commercially available inbred strains of sheep and the ovine MHC is incompletely characterized. We therefore used a one-way MLR assay to study the relative alloresponsiveness of sheep from a local farm that maintains husbandry practices to minimize inbreeding. We demonstrated that more than one-third of 160 pairs demonstrated a weak allogeneic response which suggests that these animals are too closely related to mount an allogeneic immune response. These results emphasize the importance of considering the relative allogeneicity of large animals when carrying out transplantation studies. Ideally,

given the importance of sheep for valve research, inbred lines would be developed. It is unlikely that such lines will be readily available because a minimum of 20 generations of animals are typically required for the generation of inbred strains.

Previous studies, by our group and others, using inbred strains of rats demonstrated that decellularization reduces the immunogenicity of allograft heart valves and the donor specific humoral immune response [15]. Another group showed a reduction in OLA antigens that was attributable to decellularization [17]. We conclusively demonstrated that decellularization with osmotic shock and detergent washout of the remaining cellular debris completely eliminates the donor-specific allogeneic humoral immune response by. There was a significant reduction in the cellular immune response as well, but this was more difficult to fully characterize because of a lack of suitable antibodies. Although there was no evidence of aneurysm formation, both decellularized and non-decellularized grafts showed evidence of non-specific inflammation and intimal hyperplasia. Recent evidence suggests that decellularization causes microscopic changes to the extracellular matrix [18]. The significance of these recent findings is as of yet undetermined but may be one reason for the non-specific inflammatory response that we identified. A more recent method of decellularization using the milder detergent deoxycholic acid appears to attenuate the generalized inflammatory response in recipients of decellularized valve xenografts [19-21].

Allograft heart valves, like other human allografts, are in short supply. To minimize allograft demand and supply mismatch, cryopreservation was established as a method to bank allograft valves until required. ME_2SO is a common cryoprotectant that is considered to be relatively non-toxic. It may however have confounding effects in tissue engineering applications. As described in Chapter 5, altered cytokine expression and endothelial cell function, have been observed across a broad range of ME_2SO concentrations that are commonly used during cryopreservation. ME_2SO has also been used to stimulate differentiation of embryonal carcinoma cells [22], but inhibits differentiation in other cell types [23]. Because repopulation is likely dependent on cell-ECM interactions, even low levels of ME_2SO may affect repopulation. Using high field ^{1}H-NMR, we determined the ME_2SO concentration while decellularizing ovine aortic valves. We demonstrated that the ME_2SO concentration following decellularization is far lower than levels reported to alter cell function. Surprisingly, we found that the cryopreservation protocols currently employed by tissue banks may not provide adequate Me_2SO permeation for optimal cell and matrix preservation. Finally, the current practice used in the operating theater to thaw cryopreserved heart valves is unlikely to completely remove the Me_2SO used for cryopreservation. The implication of residual Me_2SO is as of yet unknown, but it may have a detrimental effect on cells that repopulate the allograft early after implantation.

FUTURE DIRECTIONS

Although much progress has been made in the design of tissue-engineered heart valves, there are still significant impediments to realizing the promised benefits of this technology. Despite measured successes and even implantation of valves into animals, this field remains in its infancy. Perhaps the greatest barrier to progress of the field is the incomplete understanding of the molecular events in the embryological development of human heart valves. Until we gain a complete understanding all of the embryological events and signaling pathways we will likely never obtain full control of *in vitro* fabrication of valve or any other tissue-engineered structure. The second significant blockade on the road to tissue engineered valves is our superficial understanding of the function of cells within heart valves, the ECM, as well as cell-ECM interactions. The ECM is vital in transmitting environmental cues to the cell via integrins which then activate signaling pathways in the cell and in turn regulate gene expression and determine phenotype. The importance of cell-ECM in tissue engineered heart valves is evidenced by the use of pulsatile bioreactors when populating acellular scaffolds [24]. A detailed understanding of these complex interactions is required if we intend to recapitulate *in vitro* what nature enacts *in vivo.*

Perhaps we are also limited by our analytical methods. Most studies of decellularized and synthetic valve scaffolds consider only mechanical strength

testing and perhaps biochemical assessment of the overall ECM component content. These methods provide only a rudimentary assessment of the state of the ECM. A more rigorous assessment is required. Using more sophisticated imaging techniques ultrastructural deterioration and disintegration was identified in most collagenous structures that was not perceptible using conventional imaging techniques [18,25]. These results show that processing leads to injury, but does little to further the understanding of the nature of the mechanism of the injury.

Once armed with a complete understanding of valve embryology and signaling pathways, "smart" scaffolds could be developed for use with stem cells to allow manipulation of developmental signals during fabrication. One such strategy is to covalently link cell adhesive peptides to the matrix as shown in Figure VI-1 and VI-2. A more elegant approach is to link removable or inducible signaling molecules to the matrix in a similar fashion. A functionalized matrix would give additional levels of control that could be switched on or off as required. For example, integrins providing guidance to mobilize VICs to the interior of the matrix could be cleaved once the cells are implace. Another set of ligands can then be activated to stimulate the production of new ECM [26].

Much work is required to bridge the gap between the current state of tissue engineering and realization of its promises. Although *in vitro* autologous valves may require generations of work before they are realized, the steps along the way

will likely lead to incremental improvements that will enhance the lives of the thousands of patients who require valve surgery.

CONCLUSIONS

Significant findings of this thesis on the use of decellularized allograft valves in tissue engineering as a scaffold for repopulation include:

I. Determining that sheep tolerate less than 15 minutes of aortic cross-clamp time without a significant risk of paralysis from spinal cord ischemia

II. The development of a simple and cost-effective shunt to prevent spinal cord ischemia during aortic surgery on sheep by restoring hemodynamics

III. Approximately 1 of 3 sheep are too closely related to elicit a proliferative response in mixed lymphocyte reaction

IV. Rotational breeding strategies may not be sufficient to ensure allogenicity of farm animals

V. Measures must be taken to ensure allogenicity of outbred large animals when using them for transplantation studies

VI. Decellularization prevents the host cellular and donor-specific humoral immune response against allograft heart valves

VII. Cryopreservation results in adverse changes to the matrix of heart valves following implantation, but does not result in aneurysm formation at six months

VIII. The residual concentration of Me_2SO following decellularization of allograft valves is far below concentrations reported to impact cellular function of fibroblasts and endothelial cells

IX. Current methods to cryopreserve heart valves do not allow Me_2SO to not reach equilibrium and should therefore be further optimized

X. Me_2SO is likely not fully eluted from cryopreserved heart valves

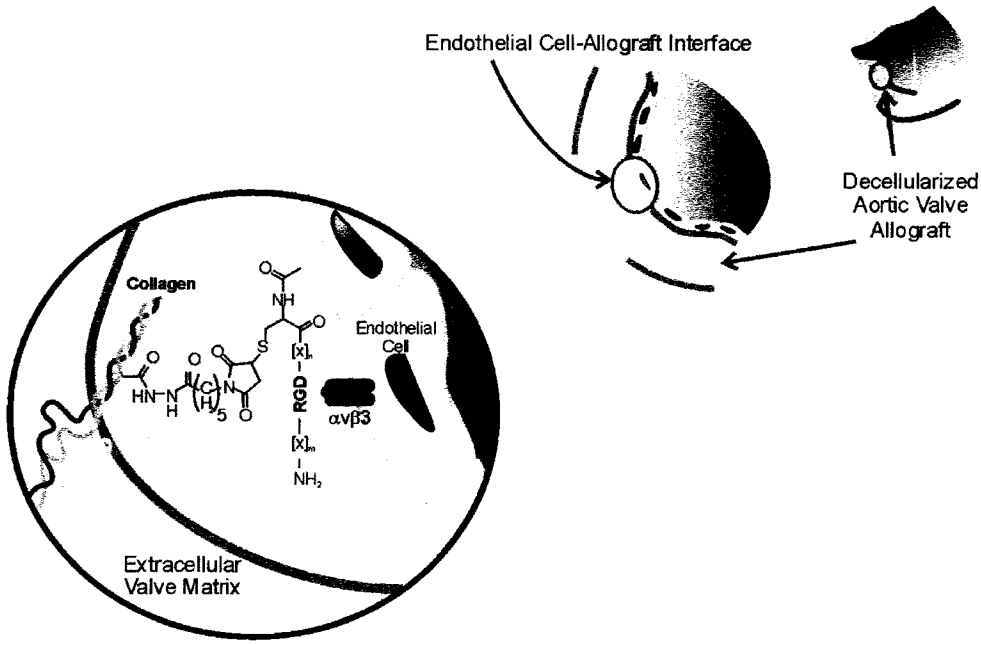

Figure VI-1. Overview of experimental strategy for enhancing endothelial cell binding to a decellularized aortic valve allograft via functionalization with RGD binding peptide. A cell adhesive peptide is covalently linked to collagen in the valve scaffold.

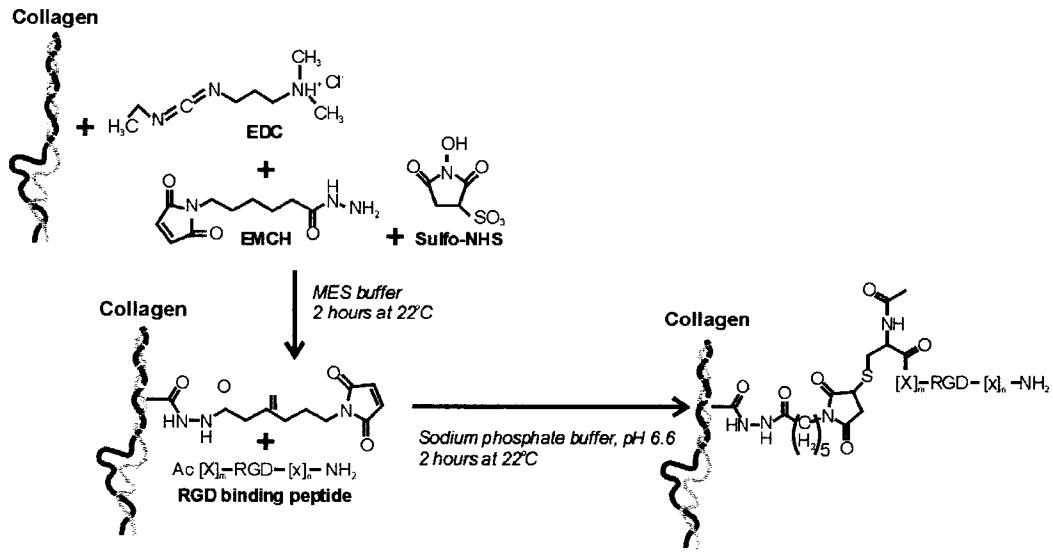

Figure VI-2. Functionalization of decellularized aortic valve allograft with RGD binding peptide. Adapted from Stile *et al.* [27]. In the first stage of binding, the decellularized allograft is bathed in a 0.1 M 2-(N-morpholino)ethane-sulfonic acid (MES) buffered solution with N-(ε-maleimidocaproic acid)hydrazide (EMCH). This bifunctional molecule has a primary amino moiety on one end that will bind to the carboxyl terminus of the collagen in the allograft scaffold, and a maleimide group on the other end that will be used to bind the RGD peptide in the second stage of the RGD peptide binding process. 1-Ethyl-3-(3-dimethylaminopropyl)carbodiimide hydrochloride (EDC), a dehydrating reagent, and N-hydroxysulfosuccinimide (Sulfo-NHS), is added to the solution to generate

a NHS-ester-activated molecule. The NHS-ester-containing molecule is then spontaneously reacted with the primary amino group of EMCH, creating a stable amine bond between the decellularized graft and EMCH. The second stage of the binding process consists of bathing the EMCH-bonded decellularized graft in a sodium phosphate buffered solution. An acetylated (Ac), aminated (NH_2), RGD-FITC binding peptide is added to the solution which binds to the maleimide moiety of EMCH.

REFERENCES

1. Rosamond, W., Flegal, K., Friday, G., Furie, K., Go, A., Greenlund, K., Haase, N., Ho, M., Howard, V., Kissela, B., Kittner, S., Lloyd-Jones, D., McDermott, M., Meigs, J., Moy, C., Nichol, G., O'Donnell, C. J., Roger, V., Rumsfeld, J., Sorlie, P., Steinberger, J., Thom, T., Wasserthiel-Smoller, S., Hong, Y., and for the American Heart Association Statistics Committee and Stroke Statistics Subcommittee Heart Disease and Stroke Statistics--2007 Update: A Report From the American Heart Association Statistics Committee and Stroke Statistics Subcommittee. *Circulation* **115**:e69-171, 2007.

2. Kanter, K. R., Budde, J. M., Parks, W. J., Tam, V. K., Sharma, S., Williams, W. H., and Fyfe, D. A. One hundred pulmonary valve replacements in children after relief of right ventricular outflow tract obstruction. *Ann Thorac. Surg.* **73**:1801-1806, 2002.

3. Dignan, R., O'Brien, M., Hogan, P., Thornton, A., Fowler, K., Byrne, D., Stephens, F., and Harrocks, S. Aortic valve allograft structural deterioration is associated with a subset of antibodies to human leukocyte antigens. *J. Heart Valve Dis.* **12**:382-390, 2003.

4. Yankah, A. C., Alexi-Meskhishvili, V., Weng, Y., Schorn, K., Lange, P. E., and Hetzer, R. Accelerated degeneration of allografts in the first two years of life. *Ann. Thorac. Surg.* **60**:S71-S76, 1995.

5. Meyer, S. R., Campbell, P. M., Rutledge, J. M., Halpin, A. M., Hawkins, L. E., Lakey, J. R., Rebeyka, I. M., and Ross, D. B. Use of an allograft patch in repair of hypoplastic left heart syndrome may complicate future transplantation. *Eur. J Cardiothorac. Surg* **27**:554-560, 2005.

6. Jacobs, J. P., Quintessenza, J. A., Boucek, R. J., Morell, V. O., Botero, L. M., Badhwar, V., van Gelder, H. M., Asante-Korang, A., McCormack, J., and Daicoff, G. R. Pediatric cardiac transplantation in children with high panel reactive antibody. *Ann. Thorac. Surg.* **78**:1703-1709, 2004.

7. Harken, D. E., TAYLOR, W. J., LEFEMINE, A. A., LUNZER, S., LOW, H. B., COHEN, M. L., and JACOBEY, J. A. Aortic valve replacement with a caged ball valve. *Am. J. Cardiol.* **9**:292-299, 1962.

8. Bonhoeffer, P., Boudjemline, Y., Qureshi, S. A., Le Bidois, J., Iserin, L., Acar, P., Merckx, J., Kachaner, J., and Sidi, D. Percutaneous insertion of the pulmonary valve. *J. Am. Coll. Cardiol.* **39**:1664-1669, 2002.

9. Cribier, A., Eltchaninoff, H., Bash, A., Borenstein, N., Tron, C., Bauer, F., Derumeaux, G., Anselme, F., Laborde, F., and Leon, M. B. Percutaneous

transcatheter implantation of an aortic valve prosthesis for calcific aortic stenosis: first human case description. *Circulation* **106**:3006-3008, 2002.

10. Palmaz, J. C., Sprague, E. A., Fuss, C, Marton, D., Wiseman, R. W., Banas, C. E., Boyle, C. T., and Bailey, S. R. Valvular prostheses having metal or pseudometallic construction and methods of manufacture. Advanced Bio Prosthetic Surfaces, Ltd. San Antonio TX. [7195641]. 3-27-2007.
11. Southart, J. A. and Low, R. L. Percutaneous valve therapies. In J. Tremmel (Ed.), *SIS 2006 Yearbook*. Seattle: 2006.
12. Rabkin-Aikawa, E., Aikawa, M., Farber, M., Kratz, J. R., Garcia-Cardena, G., Kouchoukos, N. T., Mitchell, M. B., Jonas, R. A., and Schoen, F. J. Clinical pulmonary autograft valves: pathologic evidence of adaptive remodeling in the aortic site. *J. Thorac. Cardiovasc. Surg.* **128**:552-561, 2004.
13. Bernstein, D., Kolla, S., Miner, M., Pitlick, P., Griffin, M., Starnes, V., Rowan, R., Billingham, M., and Baum, D. Cardiac growth after pediatric heart transplantation. *Circulation* **85**:1433-1439, 1992.
14. Johnson, D. M. and Sapirstein, W. FDA's requirements for in-vivo performance data for prosthetic heart valves. *J. Heart Valve Dis.* **3**:350-355, 1994.

15. Meyer, S. R., Nagendran, J., Desai, L. S., Rayat, G. R., Churchill, T. A., Anderson, C. C., Rajotte, R. V., Lakey, J. R., and Ross, D. B. Decellularization reduces the immune response to aortic valve allografts in the rat. *J. Thorac. Cardiovasc. Surg.* **130**:469-476, 2005.

16. Legare, J. F., Nanton, M. A., Bryan, P., Lee, T. D., and Ross, D. B. Aortic valve graft implantation in rats: a new functional model. *J. Thorac. Cardiovasc. Surg.* **120**:679-685, 2000.

17. Ketchedjian, A., Kreuger, P., Lukoff, H., Robinson, E., Linthurst-Jones, A., Crouch, K., Wolfinbarger, L., and Hopkins, R. Ovine panel reactive antibody assay of HLA responsivity to allograft bioengineered vascular scaffolds. *J Thorac Cardiovasc Surg* **129**:159-166, 2005.

18. Schenke-Layland, K., Vasilevski, O., Opitz, F., Konig, K., Riemann, I., Halbhuber, K. J., Wahlers, T., and Stock, U. A. Impact of decellularization of xenogeneic tissue on extracellular matrix integrity for tissue engineering of heart valves. *J Struct. Biol.* **143**:201-208, 2003.

19. Kasimir, M. T., Rieder, E., Seebacher, G., Silberhumer, G., Wolner, E., Weigel, G., and Simon, P. Comparison of different decellularization procedures of porcine heart valves. *Int. J. Artif. Organs* **26**:421-427, 2003.

20. Booth, C., Korossis, S. A., Wilcox, H. E., Watterson, K. G., Kearney, J. N., Fisher, J., and Ingham, E. Tissue engineering of cardiac valve prostheses I: development and histological characterization of an acellular porcine scaffold. *J. Heart Valve Dis.* **11**:457-462, 2002.

21. Erdbrugger, W., Konertz, W., Dohmen, P. M., Posner, S., Ellerbrok, H., Brodde, O. E., Robenek, H., Modersohn, D., Pruss, A., Holinski, S., Stein-Konertz, M., and Pauli, G. Decellularized xenogenic heart valves reveal remodeling and growth potential in vivo. *Tissue Engineering* **12**:2059-2068, 2006.

22. Edwards, M. K., Harris, J. F., and McBurney, M. W. Induced muscle differentiation in an embryonal carcinoma cell line. *Mol. Cell Biol.* **3**:2280-2286, 1983.

23. Wang, H. and Scott, R. E. Inhibition of distinct steps in the adipocyte differentiation pathway in 3T3 T mesenchymal stem cells by dimethyl sulphoxide (DMSO). *Cell Prolif.* **26**:55-66, 1993.

24. Hoerstrup, S. P., Sodian, R., Sperling, J. S., Vacanti, J. P., and Mayer, J. E., Jr. New pulsatile bioreactor for in vitro formation of tissue engineered heart valves. *Tissue Eng* **6**:75-79, 2000.

25. Schenke-Layland, K., Madershahian, N., Riemann, I., Starcher, B., Halbhuber, K. J., Konig, K., and Stock, U. A. Impact of cryopreservation on extracellular matrix structures of heart valve leaflets. *Ann. Thorac. Surg.* **81**:918-926, 2006.

26. Lutolf, M. P. and Hubbell, J. A. Synthetic biomaterials as instructive extracellular microenvironments for morphogenesis in tissue engineering. *Nat. Biotechnol.* **23**:47-55, 2005.

27. Stile, R. A., Shull, K. R., and Healy, K. E. Axisymmetric adhesion test to examine the interfacial interactions between biologically-modified networks and models of the extracellular matrix. *Langmuir* **19**:1853-1860, 2003.